Characterization of Function and Regulation of the Subtilase cytotoxin and Shiga toxin of pathogenic *Escherichia coli*

Dissertation for obtaining the Doctoral Degree of Natural Sciences (Dr. rer. nat.)

Faculty of Natural Sciences

University of Hohenheim

Institute of Food Science and Biotechnology/
Department of Food Microbiology and Hygiene

Submitted by
Laura Heinisch

from Waiblingen, Germany
2021

Dean: Prof. Dr. Uwe Beifuß

1st Reviewer: Prof. Dr. Herbert Schmidt

2nd Reviewer: Prof. Dr. Lutz Fischer

Date of submission: 09. September 2021

Date of oral examination: 19. January 2022

This work was accepted by the Faculty of Natural Sciences at the University of Hohenheim on 27. November 2021 as “Dissertation for Obtaining the Doctoral Degree of Natural Sciences”.

Contents

Eidesstattliche Versicherung über die eigenständig erbrachte Leistung gemäß § 18 Absatz 3 Satz 5 der Promotionsordnung der Universität Hohenheim für die Fakultäten Agrar-, Natur- sowie Wirtschafts- und Sozialwissenschaften

1. Bei der eingereichten Dissertation zum Thema “Characterization of Function and Regulation of the Subtilase cytotoxin and Shiga toxin of pathogenic *Escherichia coli*” handelt es sich um meine eigenständig erbrachte Leistung.

2. Ich habe nur die angegebenen Quellen und Hilfsmittel benutzt und mich keiner unzulässigen Hilfe Dritter bedient. Insbesondere habe ich wörtlich oder sinngemäß aus anderen Werken übernommene Inhalte als solche kenntlich gemacht.

3. Ich habe nicht die Hilfe einer kommerziellen Promotionsvermittlung oder -beratung in Anspruch genommen.

4. Die Bedeutung der eidesstattlichen Versicherung und der strafrechtlichen Folgen einer unrichtigen oder unvollständigen eidesstattlichen Versicherung sind mir bekannt.

Die Richtigkeit der vorstehenden Erklärung bestätige ich. Ich versichere an Eides statt, dass ich nach bestem Wissen die reine Wahrheit erklärt und nichts verschwiegen habe.

_____ _____

Ort, Datum Unterschrift

Acknowledgements

First, I would like to express my sincere thanks to Prof. Herbert Schmidt for giving me the opportunity to work on this interesting topic in his department, for his advice and support during my thesis, and the good cooperation in the last years.

I would like to thank Prof. Lutz Fischer for his advice on my work during my previous presentations and for acting as the second reviewer of this thesis.

I am very thankful to the German Research Foundation (DFG) for funding (Schm1360/11-01).

Next, I would like to express my special gratitude to Dr. Maike Krause for the advice and support throughout the last years. Her comments and thoughts on my work were very valuable to me and she always shared a sympathetic ear to me.

Furthermore, I would like to thank all members of the Department of Food Microbiology and Hygiene. I really enjoyed working with all of you and I am grateful for your support and help during my work there. Thank you for all the fun moments, I am happy that I can call some of you not only colleagues but my friends. I would like to express a special thanks to Dr. Agnes Weiß who supported my work and helped me in growing on presenting on conferences.

Additionally, I would like to thank all co-authors in contributing to my publications. A special thanks to the technical assistance from Lydia Pertschy and Markus Kranz contributing to the work.

Last, I would like to heartfully thank my family and all my friends for the moral and motivational support, and continuous encouragement throughout all the years. A special thanks to Yannik Wieler who always had faith in me and tried to follow my thoughts in the world of *E. coli*. Without you all, I couldn't have made it!

Abstract

Food-borne diseases caused by enterohemorrhagic *Escherichia coli* (EHEC) constitute a great threat to human health worldwide. Pathogenicity of EHEC strongly depends on the ability to produce virulence factors such as amongst others bacterial toxins. One of these toxins are the so-called Shiga toxins (Stx), which is why EHEC are assigned to the group of Shiga toxin-producing *Escherichia coli* (STEC).

Stx belong to the family of AB_5 protein toxins consisting of two subunits. One of them, the StxA-subunit causes depurination of the 28S rRNA in eukaryotic ribosomes by exhibiting *N*-glycosidase activity subsequently leading to inhibition of the protein biosynthesis followed by apoptosis of the host cell. The second one is the homopentameric B-subunit, which mediates binding to the host cell surface via the receptor glycolipid globotriaosylceramide (Gb_3). Besides Stx, the subtilase cytotoxin (SubAB) has been described in STEC in recent years. SubAB, also assigned to the family of AB_5 toxins, generates its cytotoxic activity via cleavage of the endoplasmic chaperone binding immunoglobulin protein (BiP) by its A-subunit. This cleavage leads to an unfolded protein response, resulting in apoptosis of the host cell. The B-subunit forms a ring-like homopentameric structure which is responsible for the binding to the receptor *N*-glycolylneuraminic acid (Neu5Gc) and other *O*-glycans.

Although the mode of cytotoxicity of AB_5 toxins have been studied extensively, some mechanisms remain unsolved. The scope of this thesis was to analyze further the mode of action of AB_5 toxins and the gene regulation of *stx* and *subAB*. Both publications included in this thesis combine the characterization of the cytotoxic activity of AB_5 toxins, the regulation of their genes, their subunits, and the combination of subunits of Stx and SubAB.

In the first publication the regulation of gene expression of AB_5 toxins was investigated in more detail. In this study, the gene expression of *subAB*$_1$ was analyzed with a luciferase reporter gene assay and by quantitative real-time polymerase chain reaction. To unravel the regulatory mechanisms, both the laboratory *E. coli* strain DH5α and the STEC O113:H21 strain TS18/08 were used. Expression of *subAB*$_1$ and promoter activity was studied using standard cultivation methods. Moreover, this work shed light on the impact of the global regulatory proteins host factor of bacteriophage Qβ (Hfq) and histone-like nucleoid structuring protein (H-NS) on *subAB*$_1$ gene expression. Therefore, isogenic deletion mutants of *hfq* and *hns* gene were generated in the respective strains. Afterwards, plasmid-based complementation was conducted to verify that the observed effects were due to the deletion. Analysis of *subAB*$_1$ promoter activity revealed impact of both Hfq and H-NS during different growth phases in both strains. In addition, the influence of both regulatory proteins on the expression toxin genes in STEC strain TS18/08 was investigated. This study did not only focus on the expression of *stx*$_{2a}$

and *subAB1*, but also the gene expression of the gene of the cytolethal distending toxin V (*cdtV*) was analyzed. Interestingly, all three toxin genes studied were upregulated in the deletion mutants of Δ*hfq* and Δ*hns*. Those results demonstrate the impact of global regulatory proteins on AB_5 toxin gene expression and show that all three toxin genes investigated are integrated into the same regulatory network.

In the second publication, the mode of action of AB_5 toxins on the example of Stx2a was analyzed in more detail. The paradigm of AB_5 toxin was known as the receptor binding B-subunit which mediates uptake of the enzymatic A-subunit and the subsequent cytotoxic activity. Previous studies have questioned this paradigm by showing cytotoxic effects of the SubA-subunit in absence of its corresponding B-subunit. This work analyzed whether this cytotoxic effect of the A-subunit is not only true for SubAB, but also for Stx. Thus, seperate recombinant expression of StxA2a subunits and subsequent His tag-based purification was performed. Both StxA2a-His and StxB2a-His were analyzed on cytotoxicity separately or in combination with the other subunit. Strikingly, cytotoxic effects of the StxA2a-His was observed in the absence of its corresponding B-subunit cell-type independently on HeLa, Vero B4, and HCT-116 cells. Studies on the B-subunit revealed no cytotoxicity on all cell lines. Additionally, combinations of different A- and B-subunits of Stx2a and SubAB1 proteins were analyzed. The hybrid combination showed that the cytotoxic effect of StxA2a-His on HeLa and HCT-116 cells could be reduced in the presence of the SubB1-His. Contrary, the cytotoxic effects of SubA1-His were unaltered in combination with StxB2a-His. Those results give the assumption that the Stx2aA-subunit binds to a target cell receptor blocked by SubB1-His. Additional experiments on the binding capacity of the Stx2a-subunits to Gb_3 revealed that while StxB2a-His was able to bind to the receptor, no binding of the recombinant A-subunit was observed. The results indicate a cytotoxic effect of StxA2a on different cell types in absence of its corresponding B-subunit, which is designated as “single-A” effect in this work. The role of this effect in STEC pathogenicity, the uptake mechanism and subsequent transport inside the host cells of StxA-subunit need to be further analyzed in the future.

Zusammenfassung

Durch enterohämorrhagische *Escherichia coli* (EHEC) verursachten Lebensmittel-assoziierte Krankheiten stellen weltweit ein ernstes Problem dar. Dabei wird die Pathogenität der EHEC vor allem durch die Fähigkeit der Produktion von Virulenzfaktoren, wie z.B. Toxinen, definiert. Eines dieser Toxine ist das sogenannte Shiga Toxin (Stx), weshalb die EHEC zur Gruppe der Shiga Toxin-produzierenden *E. coli* (STEC) zugeordnet sind.

Stx gehören zur Familie der AB_5 Toxine und bestehen aus zwei Untereinheiten. Davon hemmt die StxA-Untereinheit die Proteinbiosynthese durch die Depurinierung der 28S rRNA der eukaryotischen Ribosomen, indem sie eine *N*-Glycosidase Aktivität aufweist und anschließend zur Apoptose der Zielzelle führt. Die zweite Untereinheit ist die homopentamere B-Untereinheit, welche an den Glykolipid-Rezeptor Globotriaosylceramid Gb_3 auf der Membran der Zielzelle. In den letzten Jahren wurde in STEC neben dem Stx das Subtilase Zytotoxin (SubAB) beschrieben. Auch SubAB gehört zu der Familie der AB_5 Toxine, wobei die A-Untereinheit die zytotoxische Aktivität durch die Spaltung des endoplasmatischen Chaperons Immunoglobulin-Bindeprotein (BiP) aufweist. Diese Spaltung führt zur *unfolded protein response* (dt. ungefaltete Protein-Antwort) und infolgedessen zum Zelltod. Die B-Untereinheit besteht aus fünf identischen Molekülen, welche ringartig angeordnet sind, und bindet an den Rezeptor *N*-glykolyneuraminsäure (Neu5Gc) und andere *O*-Glykane.

Obwohl die Mechanismen der Zytotoxizität der AB_5 Toxine bereits untersucht wurden, bleiben einige Mechanismen ungeklärt. Dabei stellt das Ziel dieser Dissertation die Charakterisierung der zytotoxischen Aktivität und Regulation der Genexpression von *stx* und *subAB* dar. Beide Publikationen im Rahmen dieser Dissertation kombinieren dabei die Charakterisierung der Zytotoxizität dieser AB_5 Toxine, der Regulation ihrer Gene, ihrer Untereinheiten und der Kombination der Untereinheiten von SubAB und Stx.

In der ersten Publikation wurde die Fragestellung der Regulation der Genexpression von AB_5 Toxinen untersucht. Die Genexpression des $subAB_1$ Gens wurde in dieser Studie mit Hilfe der Methoden des Luciferase-Reportergenassays und quantitativer Echtzeit-Polymerase-kettenreaktion (*quantitative real time polymerase chain reaction*) analysiert. Um die Fragestellung der regulatorischen Mechanismen zu untersuchen, wurden sowohl der Laborstamm *E. coli* DH5α als auch der STEC O113:H21 Stamm TS18/08 verwendet. Die Expression und Promoteraktivität des $subAB_1$ wurden unter Standard-Kulturbedingungen gemessen. Des Weiteren wurden vor allem der Einfluss der globalen Regulatorproteinen *host factor of bacteriophage* Qβ (Hfq) und des Histone-ähnlichen Nukleoid bindenden Proteins (H-NS) auf die $subAB_1$ Genexpression untersucht. Dafür wurden isogene Deletionsmutanten der Gene *hfq* und *hns* in den beiden genannten Stämmen erstellt. Um zu beweisen, dass die

gemessenen Effekte auf diesen Deletionen basieren, wurde anschließend eine Plasmid-basierte Komplementation durchgeführt. Die Analyse der Promoteraktivität zeigte, dass beide Regulatorproteine Hfq und H-NS Einfluss auf diese während unterschiedlichen Wachstumsphasen in beiden untersuchten Stämmen haben. Zusätzlich wurde der Einfluss der beiden Regulatorproteine auf die Genexpression der Toxingene im STEC TS18/08 untersucht. Dabei wurden in dieser Arbeit nicht nur die Gene *stx*$_{2a}$, *subAB*$_{1}$ untersucht, sondern auch das Gen des Cytolethalen Distending Toxins V (*cdtV*) betrachtet. Interessanterweise wurden alle drei untersuchten Gene in den Deletionsmutanten Δ*hfq* und Δ*hns* hochreguliert. Die Ergebnisse dieser Studie zeigen den Einfluss von globalen Regulatorproteinen auf die Genexpression von AB_5 Toxinen und weisen auf eine Regulation der untersuchten Gene in einem gemeinsamen Netzwerk hin.

In der zweiten Publikation wurde das Wirkprinzip der AB_5 Toxine am Beispiel von Stx2a näher untersucht. Das bisher geltende Paradigma der AB_5 Toxine umfasst den Wirkmechanismus der Rezeptorbindenden B-Untereinheit, welche die Aufnahme der enzymatischen A-Untereinheit und die damit verbundene Zytotoxizität vermittelt. Dieses Paradigma wurde erstmals durch vorangegangene Studien in Frage gestellt, welche die zytotoxische Aktivität der SubA-Untereinheit in Abwesenheit ihrer zugehörigen B-Untereinheit aufgezeigt hatten. In dieser Arbeit wurde geprüft, ob diese zytotoxische Aktivität der A-Untereinheit nicht nur für SubAB, sondern auch für Stx gilt. Daher wurden die Stx-Untereinheiten rekombinant exprimiert und anschließend separate His-Tag basierte Reinigungen durchgeführt. Sowohl StxA2a-His als auch StxB2a-His wurden auf ihre Zytotoxizität einzeln oder in Kombination mit der jeweils anderen Untereinheit analysiert. Auffallend war dabei die Zelltyp-unabhängige zytotoxische Aktivität der StxA2a-His Untereinheit in Abwesenheit der B-Untereinheit auf HeLa, Vero B4 und HCT-116 Zellen. Versuche mit StxB2a-His resultierten in keinerlei Zytotoxizität auf allen Zelllinien. Zusätzlich wurde die hybride Kombination aus verschiedenen Untereinheiten von SubAB1 und Stx2a untersucht. Dabei wurde gezeigt, dass die durch StxA2a-His ausgelösten Effekte auf HeLa und HCT-116 Zellen durch SubB1-His reduziert wurden. Im Gegensatz dazu blieb die durch SubA1-His induzierte Zytotoxizität bei Kombination mit StxB2a-His unverändert. Diese Versuche lassen auf eine StxA2a-His Zielstruktur auf der Zelloberfläche schließen, welche durch SubB1-His blockiert wird. Zusätzliche Versuche zur Bindungskapazität der Stx2a-Untereinheiten an Gb_3 zeigten, dass obwohl eine Bindung von StxB2a-His zum Rezeptor nachgewiesen wurden, keine Bindung der rekombinanten A-Untereinheit an diesen festgestellt werden konnte. Die Ergebnisse dieser Studie weisen auf einen zytotoxischen Effekt der StxA2a-Untereinheit in Abwesenheit ihrer B-Untereinheit auf, welcher hier als „Single-A“ Effekt bezeichnet wird. Zukünftig soll die Rolle dieses Effektes auf die Pathogenität der STEC, der Aufnahmemechanismus und der nachfolgende Transport der StxA-Untereinheit analysiert werden.

List of publications

Parts of the work of this thesis were presented at conferences or published in peer-reviewed journals. A summary of those is given below in which the first author or the presenting person is underlined.

Published articles

Heinisch L, Zoric K, Krause M, and Schmidt H. 2019. Transcription of the subtilase cytotoxin gene *subAB*$_1$ in Shiga toxin-producing *Escherichia coli* is dependent on *hfq* and *hns.* Applied and Environmental Microbiol. 85:20 e01281-19*;* DOI: 10.1128/AEM.01281-19

Schwidder M, Heinisch L, and Schmidt H. 2019. Genetics, toxicity, and distribution of enterohemorrhagic *Escherichia coli* hemolysin. Toxins (Basel) 11:502.

Heinisch L, Krause M, Roth A, Barth H, and Schmidt H. 2021. Cytotoxic effects of recombinant StxA2-His in the absence of its corresponding B-subunit. Toxins 13:307; DOI: 10.3390/toxins13050307

Poster presentations at conferences

Heinisch L, Krause M, and Schmidt H. 2018. Regulation of subtilase cytotoxin expression by the global regulators Hfq and H-NS in *Escherichia coli*. FoodMicro, 26th international ICFMH Conference, Berlin, Germany.

Oral presentations at conferences

Heinisch L, Krause M, and Schmidt H. 2019. Regulation of virulence gene expression by the global regulators Hfq and H-NS in *Escherichia coli*. Young Scientists Conference "Food Biotechnology" (DECHEMA Summer School 2019), Hohenheim, Germany.

Heinisch L, Krause M, and Schmidt H. 2019. Regulation des Subtilase Zytotoxins durch die globalen Regulatorproteine Hfq und H-NS. Fachsymposium Lebensmittelmikrobiologie (DGHM), Kiel, Germany.

Heinisch L, Krause M, and Schmidt H. 2020. Effect of global regulators on pathogenicity of locus of enterocyte effacement negative Shiga toxin-producing *E. coli*. 6th Joint Conference of DGHM & VAAM 2020, Leipzig, Germany.

Krause M, Heinisch L, Schmidt H. 2021. Purification and cytotoxic activity of Stx2a subunits. Annual Conference of VAAM 2021. Online Seminar.

Information on own contribution to publications

Related to the scope of this thesis two peer-reviewed publications were prepared, in which several co-authors were involved. **Herbert Schmidt** applied for the funding of the DFG-project Schm1360/11-01. He was significantly involved in the conception of the manuscripts, the planning of the experiments as described in chapter 2 and 3 and assisted in writing and correction of the manuscripts. **Maike Krause** was involved in the conception of the experiments described in chapter 2 and assisted in writing and correction of the manuscripts. Her contribution to the manuscript in chapter 3 are described below.

Publication 1 (chapter 2)

Laura Heinisch. I was involved in the conception of the experiments described in this publication. I conducted all experiments described besides the construction of the luciferase reporter gene plasmid pKMD3. In detail, I generated isogenic deletion mutants of *E. coli* DH5α and STEC strain TS18/08, constructed the complementation plasmids, and performed luciferase reporter gene experiments. Subsequently, I performed RNA isolation and quantitative real-time PCR experiments. Statistical analysis of data was performed by me. I wrote and edited the manuscript.

Katharina Zoric constructed the luciferase reporter gene plasmid pKMD3.

Publication 2 (chapter 3)

Maike Krause and **Laura Heinisch** contributed equally to this work.

Laura Heinisch. I was involved in the conceptualization of the work and experiments. In detail, I was involved in purification of the Stx2a-subunits. Additionally, I performed cell culture experiments using Vero B4, HeLa, and HCT-116 cells including cytotoxicity assays, microscopic experiments, and statistical analysis. Subsequently, I have conducted the experiments on hybrid toxins of Stx2a and SubAB1. I wrote and edited the manuscript.

Maike Krause was involved in conceptualization of the work and experiments. She was involved in the establishment of the purification strategy of separate recombinant Stx2a-subunits. She performed purification and biochemical characterization of Stx2a-subunits including size exclusion chromatography, mass spectrometry, and circular dichroism spectrometry. Additionally, she performed the Gb_3-based ELISA and was involved in analysis of mass spectrometry data. She wrote and edited the manuscript.

Astrid Roth was involved in the establishment of the purification strategy of Stx2a-subunits. She conducted preliminary cytotoxic experiments of StxA2a-His on HeLa cells.

Holger Barth was involved conceptualization of the manuscript and the funding DFG project Ba2087/6-1. Moreover, he was involved in writing and editing of the manuscript.

_____ _____

Place, Date Signature Supervisor

Chapter 1 – Introduction

Escherichia coli (*E. coli*) are commensal bacteria found in the gastrointestinal tract of human and animals but can be present in the environment as well. Due to their manifold characteristics and their high adaptability *E. coli* strains are present widely in the environment and are used as laboratory model organisms. Due to the acquisition of virulence factors, *E. coli* strains are defined as pathogens can be a major concern to human health (1). The diseases caused by pathogenic *E. coli* are mainly diarrhea or extraintestinal diseases, which are either transmitted through contaminated food or water, or direct contact to infected animals or persons (1). Pathogenic *E. coli* are divided into six pathotypes that can cause human disease. They are differentiated based on their ability to produce toxins and to adhere or to invade to epithelial cells. Those pathotypes include enteroaggregative *E. coli* (EAEC), enteropathogenic *E. coli* (EPEC), enterotoxigenic *E. coli* (ETEC), enteroinvasive *E. coli* (EIEC), diffusely adherent *E. coli* (DAEC), and enterohemorrhagic *E. coli* (EHEC) (1). The latter are defined as a subgroup of Shiga toxin-producing (STEC), which are the focus of this thesis.

1. Shiga toxin-producing *Escherichia coli* (STEC)

Having a long history of research, the difference between apathogenic and pathogenic bacteria has been studied in detail and virulence factors that contribute to the pathogenicity have been designated. The group of Shiga toxin-producing *Escherichia coli* (STEC) is classified by the production of one or more Shiga toxin genes (1). The main reservoir of STEC are ruminants, especially cattle (2, 3). But many other ruminants such as bovines, sheep, goats, alpacas, elks, yaks, and various deer have been described as reservoir for STEC (reviewed in (4)). It is noticeable that STEC do not cause any disease in animals leading to asymptomatic cases. Although being asymptomatic in animals carrying STEC can be shed to the environment (5, 6). After shedding, cross-contamination of humans can occur, and due to this, the transmission of STEC is obscure.

After shedding to the environment, STEC bacteria can enter the food chain and cause diseases. Foodborne diseases such as diarrhea, hemorrhagic colitis, and the hemolytic uremic syndrome (HUS) are caused by EHEC, a subgroup of STEC (7, 8). Those extraintestinal diseases can range from mild courses to dead induced by HUS. The triad of HUS is characterized by microangiopathic hemolytic anemia, thrombocytopenia, and renal failure (7). The development of HUS is highly increased in young children being the leading cause of acute renal failure in children in developed countries (8). Moreover, the production of Stxs is related to the development of renal and neurological diseases causing central nervous system abnormalities (9, 10). Transmission of EHEC can easily occur due to its small infection dose of 1 to 100 cells (11). EHEC can be transmitted via food sources such as raw meat, raw

cheese, meat, or plant products (reviewed in (12, 13)). Infection can occur via direct contact with animals or infected people as well (4, 14).

The most prominent serotype associated with the development of human diseases is O157:H7, but other EHEC O-serotypes such as O26, O103, O111, and O145 have been commonly described (15). The first two EHEC-outbreaks were reported in 1982 in the United States, with STEC isolates showing the production of Stx (16). Since then, STEC-associated outbreaks have increased over the years leading to an estimation by the World Health Organization of about 1 million illnesses and 100 deaths associated with EHEC in 2010 (17). Each infection case associated with EHEC-derived enteritis is designated as a notifiable disease in Germany, with about 1.300 cases reported in 2020 (18).

2. Virulence factors of STEC

Virulence factors of bacteria are essential factors in their pathogenesis, most of which are encoded on mobile genetic elements such as prophages, plasmids, transposons, or pathogenicity islands (PAI) (19–21). To adapt to the niches which are not the normal habitat of *E. coli* such as the small intestine, pathogenic bacteria possess different adherence factors.

2.1 Adherence/ colonization factors

Bacterial attachment to intestinal epithelial cells is one crucial step in STEC infection (22). To colonize and adhere to different habitats, pathogenic *E. coli* produce morphological structures. This step is mainly initiated by adhesins. The family of adhesins compromises fimbriae, also designated as pili, and fibrillae of outer membrane proteins. Of those, pili are virulence factors important for colonization of the host. Moreover, pili convey to biofilm formation, recognition of host receptors or inter-bacterial aggregation (22). Studies have linked the initial attachment to the presence of fimbrial adhesins, the hemorrhagic coli pili (type IV pilus), the *E. coli* common pilus or flagella (23–25). One of the most commonly produced adhesin is intimin, encoded by the gene *eae*, an outer membrane protein that mediates tight binding to the host cell. Subsequently, intimin binds to the translocated intimin receptor (Tir) which is a virulence factor encoded on and secreted by type III secretion system (T3SS) (26). This T3SS acts as a syringe and injects the effector molecules into eukaryotic cells (27). Those effector molecules can interact with the cytoskeleton of the host cell. As a result, after initial attachment, so-called attaching and effacing lesions are formed (28). Beneath adherent bacteria pedestal-like structures rich in cytoskeletal are formed on the host cell, and effacement of absorptive microvilli occur (29). The factors of the T3SS and several effector proteins are located on the pathogenicity island locus of enterocyte effacement (LEE) (30). The LEE is commonly found in STEC and referred to one of the main pathogenicity factors (30, 31). Although, the LEE is associated as an important virulence factor of EHEC, research in the last decade has indicated

that LEE-negative strains can be associated with human disease. Several studies have indicated the abundance of LEE-negative STEC. For example, an increasing number of human patient isolates of STEC in Switzerland from 2010 to 2014, did not carry the LEE genes (32). Moreover, the German outbreak in 2011 originating from an *E. coli* O104:H4 strain which caused over 3.000 cases and 50 deaths (33) highlights the importance of LEE-negative strains in human disease. LEE-negative STEC strains have been isolated from different sources such as stool samples, animals, food, the environment, and their virulence factors have been extensively studied in the last years (reviewed by (34)).

2.2 Toxins

Besides adherence factors, the major virulence factors of EHEC are toxins. Two different kinds of toxins can be produced by bacteria: lipopolysaccharides (endotoxins) or protein toxins (exotoxins). The lipid A of lipopolysaccharides functions as an endotoxin, which is released after disruption of the cell. Exotoxins are produced inside the cell and subsequently secreted and released to the target. Given that secreted exotoxins can act at distance from the infectious site (35, 36), bacterial protein toxins play a key role in the outcome of diseases. They have a great diversity in functionality and structure. Bacterial protein toxins can bind to host cell surface receptors and trigger intracellular signaling or induce pore-formation, leading to disruption of the host cell bilayer. Furthermore, some protein toxins consist of an A-subunit, which exhibits the enzymatic activity, and a B-subunit that mediates receptor binding. Alternatively, bacterial protein toxins can be delivered inside the host cells by injection with a needle, such as the toxins of the T3SS (reviewed in (37)).

Another important virulence factor of EHEC is the enterohemolysin or EHEC-hemolysin (38). Many research studies have indicated the importance of enterohemolysin for bacterial virulence (reviewed in (39)). The gene of enterohemolysin *ehxA,* also termed EHEC *hly-A*, to EHEC *hlyD* is encoded on the large virulence plasmid pO157 (38). The combination of four genes was later termed EHEC *hly*-operon. The product of this operon, the enterohemolysin, is a pore-forming cytotoxin and belongs to the family-of-repeats in toxins (RTX) (40). This classification is due to the repeats of nonapeptides which are glycine-rich. The toxin is present in many pathogenic *E. coli* strains and has even been reported as a marker for EHEC strains (39). This heat-labile enterohemolysin causes lysis of various eukaryotic cell lines. Hence, free enterohemolysin can induce cell lysis by pore formation on the host cell (39, 41). Besides the free form, enterohemolysin can be present in outer membrane vesicles (OMVs) causing intracellular damage and apoptosis (42).

A further toxin encoded in the STEC chromosome is the cytolethal distending toxin (Cdt). The Cdt mediates its cytotoxic effect by breaking double DNA strands in eukaryotic host cells (43).

The three genes *cdtA*, *cdtB*, and *cdtC* are encoded on one operon, and their transcription products have been shown to be cytotoxic to various cell lines *in vitro*. Five variants of Cdt are found in pathogenic *E. coli*, of which the gene for Cdt-V (*cdtV*) is known to be the most prominent gene variant in STEC (44). Moreover, *cdtV* has been proposed to increase STEC pathogenicity (45). Thus, Friedrich et al. (43). have shown in the subtyping of various *E. coli* O157:H7 strains that the prevalence of *cdtV* was around 5% in the analyzed genomes. The three subunits of CdtA, CdtB and CdtC assemble in an AB_2 formation (46). Consequently, it belongs to the family of AB toxins, characterized by a catalytic A-subunit and a receptor-binding B-subunit (47). In AB toxins, the B-subunit can be present as a single moiety or oligomerized. These A- and B-subunits consist of two independent polypeptide chains. The enzymatic A-subunit enters the cell due to translocation by the B-subunit inside the target cells. Inside the cell the A-subunit functions as an effector and catalyzes reactions such as adenosine diphosphate (ADP)-ribosylation of host proteins (reviewed in (47, 48)).

AB toxins represent a versatile group of toxins which are produced by many bacterial pathogens and plant species (48). Besides the above-described toxins, the group of AB_5 toxins is essential for this work. AB_5 toxins can be produced by several pathogens including *Vibrio cholera*, *Shigella dysenteriae* and pathogenic *E. coli* strains (49).

2.2.1 AB_5 toxins

AB_5 toxins consist of a catalytic A-subunit which exhibits the enzymatic activity but are characterized by the B-subunit of that has a pentameric structure and mediates glycan receptor binding to the host cell. After binding, the holotoxin is taken up and retrogradely transported to its target inside the cell. On its target structure, the A-subunit exhibits an enzymatic activity (49). Besides the cholera toxin of *Vibrio cholerae*, the heat-labile enterotoxins, the Stx, and the SubAB of *Escherichia coli* belong to the family of AB_5 toxins (50).

2.2.1.1 Shiga toxin

The most crucial AB_5 toxin produced by *Shigella dysenteriae* type 1 and STEC is Stx. Stx was first described by Kiyoshi Shiga in 1897 (51) and has been intensively investigated since then. The Stx of *E. coli* was initially identified by its cytopathic effects on Vero cells and was originally named verotoxin (52). Subsequently, its similarity to the *S. dysenteriae* type 1 toxin was analyzed giving it the name of Shiga-like toxin (16). Due to molecular analysis, the identity to the *S. dysenteriae* Stx has been designated to Stx1 of *E. coli* as they share the B-subunit and differ only in one amino acid in the A-subunit (53, 54). Stx2 shows less identity of around 56% to the previous types and is immunological different to Stx1 (55, 56). The two genetic variants of stx_1 and stx_2 have been reported in *E. coli* (54). Both *E. coli* Stx types comprise of many subtypes and variants, which can correlate with epidemiological significance. The subtypes

Stx1a to Stx1d and Stx2a to Stx2g may show great differences in biologic activity (57). Currently, up to 107 variants of Stx have been described in *E. coli* (57) which differ in one or more amino acids (58). While some STEC strains express only one subtype, others have been described to express a combination of variants of both types (58). However, Stx2a has been mostly associated with the development of HUS (58).

Belonging to the family of AB_5 toxins, Stx consists of an A-subunit and five identical B-subunits having a molecular size of 32 kDa and 7.7 kDa per monomer, respectively (59). The latter mediates the receptor binding to the glycolipid globotriaosylceramide Gb_3, also designated as CD77 (60–62). This receptor is found on many human cell types including the renal epithelium and endothelium, microvascular cells of the intestine, as well as smooth muscle cells of the digestive tract. Moreover, the presence of Gb_3 has been described on endothelial cells, neurons of the central nervous system, and on lung cells (reviewed in (63)).

After binding to Gb_3, the homopentameric B-subunit mediates the uptake of the A-subunit inside the host cell (64). After the retrograde transport, the A-subunit executes its enzymatic activity by altering ribosomal activity. The StxA-subunit belongs to the family of ribosome-inactivating proteins (60). In detail, it exhibits a *N*-glycosidase activity on the adenine 4324 of 28S ribosome RNA (rRNA) of the 60S ribosomal unit leading to inhibition of protein synthesis followed by cell apoptosis (48, 65). The polypeptide chain of StxA-subunit consists of two domains A1 (27.5 kDa) and A2 (4.5 kDa), which are connected by a disulfide bond. This bond forms a protein loop in which the A-subunit is cleaved by the host enzyme furin by recognizing the consensus motif (Arg-XX-Arg) (66). Although cleavage, the two domains are still connected by the disulfide bond which is subsequently reduced inside the endoplasmic reticulum (ER). Afterwards, the A1 domain is released inside the cytosol exhibiting the enzymatic activity on its target (67).

The *stx*$_1$ and *stx*$_2$ genes are usually located in the genome of lambdoid prophages (31). Those Stx-phages can vary in size and genetic composition, which compromises highly mobile genetic elements (68). On the phages, *stx* operons are located upstream of the lysis cassette and downstream of the anti-terminator gene Q that enables regulation of late phage genes (69). Due to this genetic position, Stx is released during phage-induced host cell lysis (70). Because bacteria can possess multiple Stx variants, they are able to carry more than one Stx-phage which increases the occurrence of recombination between the phage elements (68).

While STEC can express one or more *stx* gene, studies on epidemiological data have implicated that the occurrence of *stx*$_{2a}$ is most linked to the development of HUS (71). A recent *in vivo* study by Hauser et. al (72) has indicated that the expression levels of Stx2a lead to

increased virulence. Moreover, increased Stx2a levels in stool samples increased lethality in mice.

2.2.1.2 Subtilase cytotoxin

Besides carrying the *stx* genes, LEE-negative STEC strains can encode for the subtilase cytotoxin (SubAB). SubAB was first identified in an HUS outbreak strain in 1999 in Australia by Paton et al. (73). This *E. coli* O113:H21 strain 98NK2 carried a mega plasmid pO113 encoding the first-described SubAB gene variant (*subAB*$_{1}$). Besides this plasmid-encoded gene, three different chromosomal variants (*subAB*$_{2\text{-}1}$ to *subAB*$_{2\text{-}3}$) have been described up to date (74, 75), but more variants have been suggested (75). Genes for the subunits *subA* and *subB* are encoded on the same operon and have a size of 1047 bp and 426 bp, respectively (74).

SubAB shows the typical AB_5 toxin structure, whereas the enzymatic SubA-subunit has its cytotoxic activity in cleaving the endoplasmic chaperone binding immunoprotein (BiP) or 78-kDa glucose-regulated protein (GRP78). The serine-like protease introduces a single-site cleavage, which leads to the inactivation of BiP/ GRP78 (76), then to an unfolded protein response followed by apoptosis of the cell (77). The homopentameric B-subunit binds to the receptor of *N*- and *O*-glycans but most prominently to the sialic acid *N*-glycolyneuraminic acid (Neu5Gc) on the host cell surface (78, 79). Subsequently to binding, the B-subunit mediates the transport of the holotoxin inside of the cell, which is in a clathrin-dependent way (77). Interestingly, the glycan side-chain Neu5Gc cannot be produced by human cells themselves, but has to be integrated into the glycan matrix of human cells on the cell surface by dietary uptake of red meat or dairy products (80). Besides Neu5Gc other target structures for SubB such as *N*- and *O*-glycans have been suggested in the recent years (79).

In studies performed in mice, SubAB has been shown to induce symptoms characteristic for the development of Stx-associated HUS. This included the development of thrombosis, microvascular damage, and necrosis in organs such as the kidney, liver, and brain (81). Moreover, cytotoxicity assays using recombinant SubAB have indicated even higher activity on Vero cells compared to Stx (82). Furthermore, Tozzoli et al. (83) revealed the presence of *subAB* in *stx*-negative *E. coli* strains isolated from childhood diarrhea. This study proved that SubAB production can be present even in the absence of Stx, highlighting the importance of this AB_5 toxin and its role in STEC pathogenicity.

3. Regulation of virulence genes

The virulence genes in STEC bacteria can be regulated by the impact of environmental factors such as temperature, salt, acidity, and quorum sensing (84–87). Shiga toxin genes (*stx*) are encoded on lambdoid prophages between the lysis enzymes and the anti-terminator Q and

are regulated by genes involved in the bacteriophage life cycle (88). Thus, *stx* genes can be co-transcribed with the late phage genes. Due to this connection, *stx* genes can be regulated by SOS response, when prophages are induced.

The bacterial SOS response can be triggered by compounds such as hydrogen peroxide or antibiotics and consequently, promote the expression of *stx* genes (89). Antibiotics like mitomycin C cause prophage induction through activation of the bacterial SOS response. Thus, studies have demonstrated the induction of bacteriophages followed by increased Stx production through different antibiotics (90, 91). During infection STEC encounter host cells such as neutrophils that produce nitric oxide and hydrogen peroxide (89). Both compounds are known to induce SOS response and DNA damage in bacterial cells. Moreover, a study by Łos et al. (92) has demonstrated bacteriophage induction after hydrogen peroxide treatment. Not only environmental factors can regulate *stx* gene regulation, but it was shown that global regulatory proteins are integrated in the regulatory pathway of *stx* gene expression.

3.1 Global regulator host factor of bacteriophage Qβ

The global regulator host factor of bacteriophage Qβ (Hfq) is known to inhibit stx_{2a} gene regulation. It has been described that the deletion of the *hfq* gene in EHEC leads to an increase in stx_{2a} expression (93). Besides regulating the expression of *stx* genes, Hfq is involved in regulating other virulence factors such as the factors of LEE (94).

The protein Hfq has a hexameric ring structure and a size of 12 kDa (95, 96). Being a pleiotropic posttranscriptional regulator, Hfq belongs to the family of Sm and Sm-like proteins (97). Hfq itself can bind to RNA. For example it interferes with small non-coding RNAs (sRNAs), and is involved in processing them, indicating its function as an RNA chaperone (98). Its functionality is as a global regulator resides in initiating translation repression via Hfq-dependent sRNAs or introduction of decay by binding on *trans*-encoded mRNAs (99). Thus, Hfq or the RNAs processed by it have impact in many cellular processes such as metabolism (100), oxidative stress response (97), acid stress response(101, 102), or quorum sensing (87). In those processes, Hfq or the sRNAs regulated by it act mainly as repressors of the gene regulation. Hfq and Hfq-dependent RNAs can regulate genes involved in motility (103) and virulence of STEC bacteria (104, 105). Moreover, adaptation to stresses plays an important role in pathogenicity of STEC behavior and consequently, by regulating factors of response to that (106) Hfq is implicated in pathogenicity of bacteria (107, 108). In a study by Kendall et al. (93) the stx_{2a} expression was increased in a Δ*hfq* deletion mutant indicating an inhibitory effect of Hfq on virulence factors.

As described above, the global regulator Hfq is involved in various cellular processes. In Figure 1 the processes which are regulated by Hfq are schematically depicted.

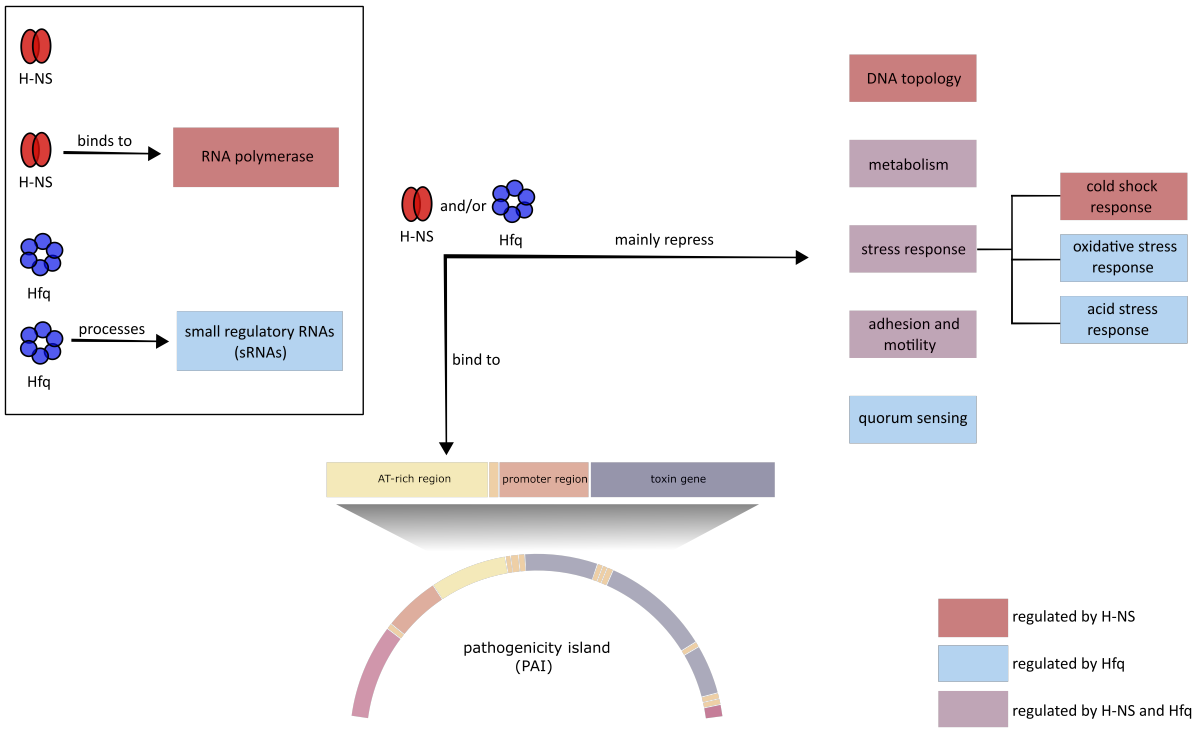

Figure 1 Schematic representation of impact of global regulators H-NS and Hfq in pathogenic *E. coli.* Processes regulated by H-NS itself or due to the binding of H-NS to the RNA polymerase are displayed in red. Bacterial processes which are regulated by Hfq and its subsidiaries sRNAs are shown in blue. Processes which are regulated by both H-NS and Hfq are displayed in violet.

All processes regulated by Hfq are shown in blue, the bacterial mechanisms regulated by H-NS are shown in red. In those, Hfq can either directly have regulatory effects or is integrated in the regulation pathway due to its related sRNAs. Besides the global regulator Hfq, another pleiotropic regulator has been associated with the regulation of virulence genes in pathogenic bacteria: the histone-like nucleoid structuring protein (H-NS). Processes regulated by H-NS are depicted in Figure 1 in red and will be discussed in detail in the following chapter.

3.2 Global regulator histone-like nucleoid structuring protein

The protein H-NS is one of the most abundant proteins inside the cell and has a mass of 15.5 kDa (96, 109). Belonging to the group of DNA-binding proteins (110), H-NS can interfere directly with RNA polymerase (111) or with the DNA (112, 113). By binding to the DNA, the topology is altered and hence, transcription and gene expression is changed (113, 114). H-NS is involved in the regulation of many cellular processes being a transcriptional repressor (115–117). Preferably, H-NS binds to adenine and thymine rich (AT-rich) regions, indicating its role in the regulation of foreign acquired DNA (112). It has been shown that DNA acquired by phages or gene transfer is high in AT-content. As a result, H-NS can be a regulator of virulence genes in *E. coli*.

Just as the Hfq protein, H-NS is implicated in regulating horizontal and lateral acquired DNA which is AT-rich (118–120). It has been shown that up to one third of the genes present on the pathogenicity island of pO157 are silenced by H-NS, which were amongst others the Stx genes *stx*$_1$ and *stx*$_2$ (121). Moreover, several loci of the LEE in EHEC are regulated by H-NS as well (86). Regulation by those virulence factors occurs mainly as repression (115, 117), this was analyzed by several studies that have indicated upregulation of virulence factors in deletion mutants of *hns*. The upregulation of the enterohemolysin in an EHEC deletion mutant of *hns* was shown (122, 123). Both virulence factors Hfq and H-NS have impact in many cellular processes as well as in the regulation of virulence factors. A summary of the implications of both regulators is schematically displayed in Figure 1, in which the bacterial mechanisms regulated by H-NS are shown in red. H-NS can bind the DNA and alter its topology or interacts with the RNA polymerase and thus, be implicated in many cellular processes. Both (shown in Figure 1 in violet) regulate the expression of genes responsible for stress response, adhesion and motility, and metabolic processes. Additionally, H-NS and Hfq can bind to xenogenic acquired DNA present on pathogenicity islands and have impact in the regulation of virulence genes in STEC bacteria.

4. *Escherichia coli* O113:H21 strain TS18/08

For the work presented in chapter 2 of this thesis *E. coli* O113:H21 strain TS18/08 was used because it is LEE-negative and encodes for multiple toxin genes. The strain *E. coli* O113:H21 was originally isolated from minced meat in 2008 by Slanec et al. (124). Besides the most prominent O-serotype strains, the importance of LEE-negative strains has been noted in the recent years. In the performed screening study, *E. coli* TS18/08 was found to harbor genes for Stx2a, SubAB, enterohemolysin, and CdtV.

The finding that *E. coli* strain TS18/08 encodes for multiple toxins leads to the question of how those factors act together. This issue was first addressed in a study by Hauser et al. (125) in which the expression rates of the three genes stx_{2a}, $subAB_1$, and *cdt-V* were analyzed. Using quantitative real time polymerase chain reaction (PCR) experiments it was shown that all three genes were transcribed within different time points during standard cultivation conditions. Moreover, transcription levels of the three toxins did vary between each other (125). This study gives the first hint on the relation of expression different toxins produced during standard cultivation of STEC strains.

5. Aims of the study

The current study addresses two main open questions regarding the knowledge on AB_5 toxins. This thesis was integrated in a project funded by the German Research Foundation (DFG) with the corresponding grant number SCHM-1360/11-1.

First, the characterization of the regulation of the SubAB1 gene expression was addressed. Although many studies have been performed to investigate the enzymatic activity of the SubAB, the regulation pathway in which this cytotoxin is integrated remained unclear. In this study, the impact of global regulatory proteins such as Hfq and H-NS on gene regulation of *subAB$_1$* was investigated. To identify the regulation of the *subAB$_1$* gene, luciferase reporter gene assay and quantitative real-time PCR experiments were conducted. The gene expression of *subAB$_1$* was studied in laboratory strain *E. coli* DH5α and the STEC strain O113:H21 TS18/08, which combines the expression of *stx$_{2a}$*, *subAB$_1$*, and *cdtV*. Thus, isogenic deletion mutants of *hfq* and *hns* gene in STEC TS18/08 and *E. coli* DH5α were generated. Cultivation experiments using standard conditions were performed, and promoter activity was evaluated. Subsequently, quantitative real-time PCR was used to analyze the gene expression of *stx$_{2a}$*, *subAB$_1$*, and *cdtV* in the influence of deletion of *hfq* and *hns*. To verify that the determined effects were caused by the deletions, complementation of respective genes was performed and compared in all experiments. Results of this study are shown in chapter 2.

Secondly, the functionality of AB_5 toxins was characterized in this thesis. As the cytotoxic activity of those has been studied intensively in the past years, the question of whether the enzyme needs both subunits to exhibit cytotoxic activity was further addressed in this thesis. In the second study, the cytotoxic activity of AB_5 toxins was investigated using Stx2a as a model toxin. For this reason, a purification strategy for the separate expression and purification of recombinant Stx2a-subunits was established. Biochemical characteristics of the purified StxA2a-His and StxB2a-His were verified using size exclusion chromatography, mass spectrometry, and circular dichroism spectrometry. The results of this study are shown in chapter 3, in which Maike Krause and myself contributed equally to the work. The focus of this thesis is the analysis of cytotoxic activity of the A-subunit. After purification, recombinant StxA2a-His and StxB2a-His were analysed on cytotoxic activity either separately or in a molar combination of 1:5 on HeLa, Vero B4, and HCT-116 cells. For all cell lines, StxA2a-His showed cytotoxic effects in absence of its B-subunit. Cytotoxicity assays using crystal violet staining and subsequent spectrophotometric analysis were performed comparing cell viabilities with or without treatment. Additionally, microscopic analysis of all cell types investigated was performed to observe visual cytotoxic effect of the respective subunits. Moreover, it was investigated whether subunits of Stx2a and SubAB1 can exhibit cytotoxic activity in

combination. These experiments were conducted again in crystal violet staining cytotoxicity assays. Further details and results of this work will be presented in chapter 3.

Chapter 2

Transcription of the subtilase cytotoxin gene *subAB*$_1$ in Shiga toxin-producing *Escherichia coli* is dependent on *hfq* and *hns*

Laura Heinisch[a], Katharina Zoric[a], Maike Krause[a], and Herbert Schmidt[a]

[a]Institute of Food Science and Biotechnology, Department of Food Microbiology and Hygiene, University of Hohenheim, Stuttgart, Germany

Published in Applied and Environmental Microbiology Volume 85 Issue 20 e01281-19
DOI: 10.1128/AEM.01281-19

Belonging to this article is additional supplementary data which can be found at https://doi.org/10.1128/AEM.01281-19.

AMERICAN SOCIETY FOR MICROBIOLOGY | Applied and Environmental Microbiology®

GENETICS AND MOLECULAR BIOLOGY

Transcription of the Subtilase Cytotoxin Gene *subAB*$_1$ in Shiga Toxin-Producing *Escherichia coli* Is Dependent on *hfq* and *hns*

Laura Heinisch,[a] Katharina Zoric,[a] Maike Krause,[a] Herbert Schmidt[a]

[a]Institute of Food Science and Biotechnology, Department of Food Microbiology and Hygiene, University of Hohenheim, Stuttgart, Germany

ABSTRACT Certain foodborne Shiga toxin-producing *Escherichia coli* (STEC) strains carry genes encoding the subtilase cytotoxin (SubAB). Although the mode of action of SubAB is under intensive investigation, information about the regulation of *subAB* gene expression is currently not available. In this study, we investigated the regulation of the chromosomal *subAB*$_1$ gene in laboratory *E. coli* strain DH5α and STEC O113:H21 strain TS18/08 using a luciferase reporter gene assay. Special emphasis was given to the role of the global regulatory protein genes *hfq* and *hns* in *subAB*$_1$ promoter activity. Subsequently, quantitative real-time PCR was performed to analyze the expression of Shiga toxin 2a (Stx2a), SubAB1, and cytolethal distending toxin V (Cdt-V) genes in STEC strain TS18/08 and its isogenic *hfq* and *hns* deletion mutants. The deletion of *hfq* led to a significant increase of up to 2-fold in *subAB*$_1$ expression, especially in the late growth phase, in both strains. However, deletion of *hns* showed different effects on the promoter activity during the early and late exponential growth phases in both strains. Furthermore, upregulation of *stx*$_{2a}$ and *cdt-V* was demonstrated in *hfq* and *hns* deletion mutants in TS18/08. These data showed that the expression of *subAB*$_1$, *stx*$_{2a}$, and *cdt-V* is integrated in the regulatory network of global regulators Hfq and H-NS in *Escherichia coli*.

IMPORTANCE Shiga toxin-producing *Escherichia coli* (STEC) strains are responsible for outbreaks of foodborne diseases, such as hemorrhagic colitis and the hemolytic uremic syndrome. The pathogenicity of those strains can be attributed to, among other factors, the production of toxins. Recently, the subtilase cytotoxin was detected in locus of enterocyte effacement (LEE)-negative STEC, and it was confirmed that it contributes to the cytotoxicity of those STEC strains. Although the mode of action of SubAB1 is under intensive investigation, the regulation of gene expression is currently not known. The global regulatory proteins H-NS and Hfq have impact on many cellular processes and have been described to regulate virulence factors as well. Here, we investigate the role of *hns* and *hfq* in expression of *subAB*$_1$ as well as *stx*$_{2a}$ and *cdt-V* in an *E. coli* laboratory strain as well as in wild-type STEC strain TS18/08.

KEYWORDS STEC, Shiga toxin-producing *Escherichia coli*, gene expression, global regulator, *hfq*, *hns*, subtilase cytotoxin

Shiga toxin-producing *Escherichia coli* (STEC) strains are a major cause of serious foodborne diseases, leading to diarrhea, hemorrhagic colitis, and the hemolytic uremic syndrome (HUS) (1, 2). The main virulence factors described so far are the production of Shiga toxins (Stx) (3) and the components of the locus of enterocyte effacement (LEE) (4). Although the LEE is widely distributed in STEC, many LEE-negative STEC strains have been isolated and characterized (5, 6). Characterization of those strains led to identification of other putative virulence factors, such as the subtilase cytotoxin (SubAB). So far, SubAB was found to be produced only by LEE-negative STEC strains and was first identified in *E. coli* O113:H21 strain 98NK2, involved in an HUS outbreak (7). SubAB belongs to the family of AB$_5$ toxins and consists of a

Citation Heinisch L, Zoric K, Krause M, Schmidt H. 2019. Transcription of the subtilase cytotoxin gene *subAB*$_1$ in Shiga toxin-producing *Escherichia coli* is dependent on *hfq* and *hns*. Appl Environ Microbiol 85:e01281-19. https://doi.org/10.1128/AEM.01281-19.

Editor Maia Kivisaar, University of Tartu

Address correspondence to Herbert Schmidt, herbert.schmidt@uni-hohenheim.de.

Received 6 June 2019
Accepted 30 July 2019
Accepted manuscript posted online 2 August 2019
Published 1 October 2019

catalytic A subunit and a homopentameric B subunit, the latter mediating binding to the terminal sialic acids of glycoproteins of the host cell (8). The catalytic activity of SubA is the cleavage of the endoplasmic chaperone BiP/GRP78, leading to an unfolded protein response and apoptosis (9, 10).

Recent studies demonstrated the contribution of SubAB to STEC cytotoxicity (11, 12). Until now, three genetic *subAB* variants have been described in STEC strains. Whereas $subAB_1$ is located on the virulence plasmid pO113, the variants $subAB_{2\text{-}1}$, $subAB_{2\text{-}2}$, and $subAB_{2\text{-}3}$ are located on the chromosome (13, 14). The regulatory pathways leading to increased expression of *subAB* are currently not known.

Global regulatory proteins regulate many cellular processes in bacteria. The host factor of bacteriophage Qβ (Hfq) is an RNA chaperone and interacts with mRNA and small regulatory RNAs in *E. coli* (15). Hfq itself or the RNAs that are processed by Hfq are implicated in regulation of metabolism, quorum sensing, and regulation of adhesion and motility (16, 17). Moreover, Hfq regulates many stress responses, such as response to acids or oxidative stress (18, 19). In addition to Hfq, the histone nucleoid structuring protein H-NS is a pleiotropic regulator. It regulates transcription by binding directly to DNA or to the RNA polymerase (20). H-NS is known to alter DNA topology (20) and to regulate many processes during the bacterial life cycle. It regulates metabolic processes and is integrated in the regulatory pathway of genes involved in motility (21). Moreover, H-NS plays a role in stress response, such as cold shock response (22). Regulation of cellular processes by Hfq and H-NS have been studied extensively in recent years. Both Hfq and H-NS are integrated in the regulation of virulence factors of pathogenic bacteria as well. Kendall et al. identified the role of Hfq in regulation of virulence in enterohemorrhagic *E. coli* (EHEC) O157:H7. In this study, it was shown that deletion of the *hfq* gene led to an increase of stx_{2AB} expression (23). The nucleoid binding protein H-NS silences foreign DNA with high percentages of adenosine and thymine (A/T) content (24) and is therefore integrated in regulation of virulence genes. H-NS was also identified to regulate genes of the LEE. H-NS also regulates expression of genes of the hemolysin in EHEC (25).

First insights in gene expression of $subAB_1$ were given by Hauser et al. (12). In STEC strain TS18/08, isolated from minced meat, the expression of $subAB_1$ was analyzed using quantitative real-time PCR (qRT-PCR). It was shown that the expression of $subAB_1$ was highest in the exponential growth phase under standard batch culture conditions (12).

The aim of this study was to investigate whether $subAB_1$ expression is under the control of Hfq and H-NS. Therefore, deletion of *hfq* and *hns* genes was performed, and the expression of $subAB_1$ was measured with a luciferase reporter gene assay in laboratory *E. coli* strain DH5α and the foodborne STEC strain TS18/08 (26). *E. coli* TS18/08 produces three toxins: the subtilase cytotoxin SubAB1, Shiga toxin 2a (Stx2a), and the cytolethal distending toxin V (Cdt-V) (11). Therefore, we were interested in whether the expression of the corresponding toxin genes is dependent on the global regulators Hfq and H-NS. Quantitative real-time PCR was applied to study *in vitro* transcription of those toxin genes in *E. coli* TS18/08.

RESULTS

Transcription of cloned *hfq* or *hns* genes present on complementation plasmids. Prior to the use of plasmids pLH01 and pLH02 for complementation studies, expression of cloned *hfq* and *hns* genes on these plasmids was investigated. Therefore, deletion mutants DH5α Δ*hfq*/pHL01 and DH5α Δ*hns*/pHL02 were grown under standard batch conditions and total RNA was isolated. Transcription analyses of *hfq* and *hns* were conducted as described previously. PCR analysis with *hfq*- and *hns*-specific primers and subsequent agarose gel electrophoresis of the resulting cDNA demonstrated PCR products with the molecular size of *hfq* (309 bp) and *hns* (414 bp). Laboratory strain *E. coli* DH5α (positive control), as well as its *E. coli* DH5α Δ*hfq* and DH5α Δ*hns* (negative controls) isogenic deletion mutants, were also applied in the procedure. cDNAs of the *hfq* gene and *hns* gene were not amplified in either control, as representatively shown

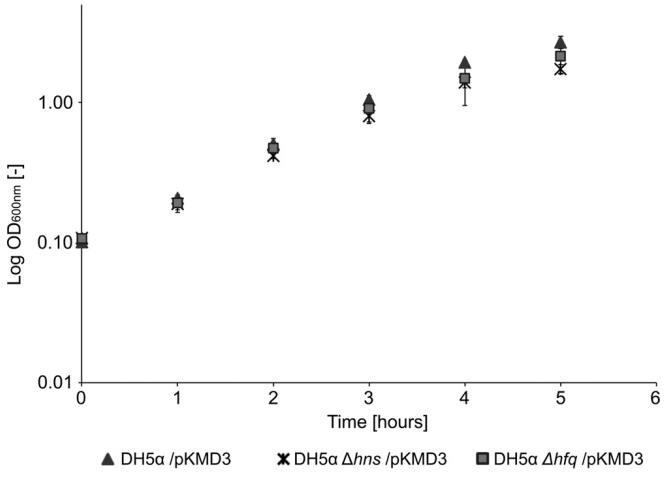

FIG 1 Growth curves of *E. coli* DH5α wild-type and mutant strains. Cultivation was conducted for 5 h in LB at 37°C with aeration. The OD_{600} was determined over a period of 5 h for *E. coli* DH5α/pKMD3, DH5α Δ*hns*/pKMD3, and DH5α Δ*hfq*/pKMD3 strains. Data represent mean values and standard deviations from three biological replicates.

for the *E. coli* DH5α Δ*hfq* strain (see Fig. S1 in the supplemental material). For both the wild-type strain and the *E. coli* DH5α Δ*hfq*/pLH01 and DH5α Δ*hns*/pLH02 complemented strains, bands with an expected size of around 300 bp and 414 bp, respectively, were visible on the agarose gels.

Reverse transcriptase negative controls show that no cross-contamination with DNA occurred during the experimental procedure. This indicated that the plasmids pLH01 and pLH02 expressed the genes of interest and can be used for complementation of deletion mutants.

Deletion of *hfq* and *hns* leads to slower growth in STEC TS18/08. In order to investigate the effects of *hfq* and *hns* on *subAB* gene expression, growth curves of *E. coli* DH5α (Fig. 1) and STEC strain *E. coli* TS18/08 (Fig. 2), as well as of their respective *hfq* and *hns* mutants, were initially compared. It could be shown that deletion of either *hfq* or *hns* led to a minor decrease in growth in DH5α and both mutants, whereas the highest decreases in values of optical density at 600 nm (OD_{600}) were measured as 1.6-fold in the DH5α Δ*hns* strain and 1.8-fold in the DH5α Δ*hfq* strain in the late growth

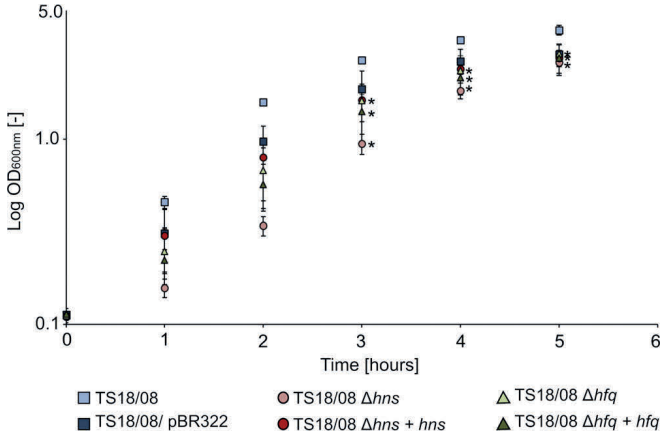

FIG 2 Impact of deletion of genes *hfq* and *hns* on growth of STEC O113:H21 strain TS18/08. Optical density of wild-type strain (TS18/08), TS18/08/pKMD3 + pBR322 (TS18/08/pBR322) empty vector backbone control, TS18/08 Δ*hns*/pKMD3 (TS18/08 Δ*hns*) and TS18/08 Δ*hfq*/pKMD3 (TS18/08 Δ*hfq*) deletion mutants, and TS18/08 Δ*hns*/pKMD3 + pLH02 (TS18/08 Δ*hns* + *hns*) and TS18/08 Δ*hfq*/pKMD3 + pLH01 (TS18/08 Δ*hfq* + *hfq*) complemented strains is shown for measurements over 5 h. Data from three biological replicates are shown; error bars indicate standard deviations from mean values. Asterisks indicate statistical significance ($P < 0.05$) compared to values for TS18/08.

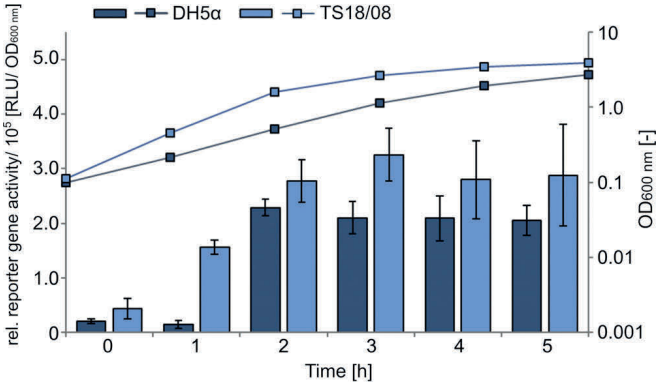

FIG 3 Comparison of *PsubAB*$_1$ promoter activities in DH5α and TS18/08. Relative reporter gene activity (RLU/OD$_{600}$) is shown. Bars represent data for *E. coli* DH5α (dark blue) and an STEC strain (TS18/08, light blue). OD$_{600}$ is shown as squares. Cultivation was conducted for 5 h in LB at 37°C with aeration. Data from three biological replicates are shown; error bars indicate standard deviations from mean values.

phase. This effect was stronger in STEC TS18/08 than in DH5α. The deletion mutants showed significantly lower OD$_{600}$ values over the cultivation period. Whereas deletion of *hns* led to a decrease of up to 4.6-fold in the exponential growth phase, the decline in OD$_{600}$ values was 2.3-fold lower in the TS18/08 Δ*hfq* strain than in the wild type. After 5 h of incubation, decrease rates diminished up to 1.5-fold and 1.3-fold in TS18/08 Δ*hns* and TS18/08 Δ*hfq* strains, respectively. The reduction in OD$_{600}$ values in the TS18/08 Δ*hns* strain could be restored after complementation with the wild-type gene on plasmid pLH02 (Fig. 2). However, reduction in OD$_{600}$ values could not be restored in the TS18/08 Δ*hfq* strain by complementation with plasmid pLH01. Although TS18/08 Δ*hfq* and TS18/08 Δ*hns* deletion mutants grew more slowly than wild-type TS18/08, all strains reached the exponential growth phase in a period of 5 h. Therefore, a growth period spanning 5 h was chosen for further investigations of *PsubAB*$_1$ activity.

***E. coli* DH5α/pKMD3 is suitable for measuring *subAB*$_1$ promoter activity.** Promoter activity of *subAB*$_1$ was measured as described above in *E. coli* DH5α, *E. coli* TS18/08, and their respective Δ*hfq* and Δ*hns* mutants. As shown in Fig. 3, the relative promoter activity of *subAB*$_1$ (*PsubAB*$_1$) of *E. coli* DH5α/pKMD3 significantly increased up to 11-fold compared to the starting value in the exponential growth phase, showing the highest activity of 2.29 $\times$ 10^5 relative light units (RLU)/OD$_{600}$ after 2 h of cultivation. This activity did not increase any further. Similar to the activity measured in *E. coli* DH5α/pKMD3, the *PsubAB*$_1$ activity of TS18/08/pKMD3 increased significantly up to 7-fold compared to the starting value in the exponential growth phase and did not increase further. The highest *PsubAB*$_1$ activity in STEC TS18/08 was detected with 3.3 $\times$ 10^5 RLU/OD$_{600}$ after 3 h of cultivation (Fig. 3). The results of these experiments demonstrated that the luciferase reporter system worked well for measuring *subAB*$_1$ promoter activity.

Hfq represses *PsubAB*$_1$ activity in *E. coli* DH5α and TS18/08 in the late exponential growth phase. In Fig. 4, the effect of the *hfq* deletion in *E. coli* DH5α (Fig. 4A) and *E. coli* TS18/08 (Fig. 4B) on *PsubAB*$_1$ activity is shown. In the *E. coli* DH5α Δ*hfq*/pKMD3 mutant, the relative reporter gene activity was significantly increased up to 1.8-fold compared to that of wild-type DH5α/pKMD3 in the exponential growth phase and reached its highest activity of 4.0 $\times$ 10^5 RLU/OD$_{600}$ after 5 h of growth. Moreover, the observed effects were reduced in the DH5α Δ*hfq*/pKMD3 + pLH01 strain to a level similar to that of the wild type. TS18/08 Δ*hfq*/pKMD3 deletion mutants showed behavior similar to that of the DH5α deletion mutants. The relative reporter gene activity was significantly increased up to 2-fold in the late growth phase, showing its highest activity of 5.6 $\times$ 10^5 RLU/OD$_{600}$ after 4 h of growth. The effects were reduced to the wild-type level after complementation of the TS18/08 Δ*hfq*/pKMD3 strain with pLH01. Moreover, DH5α and TS18/08 did not show great differences in *PsubAB*$_1$ activity

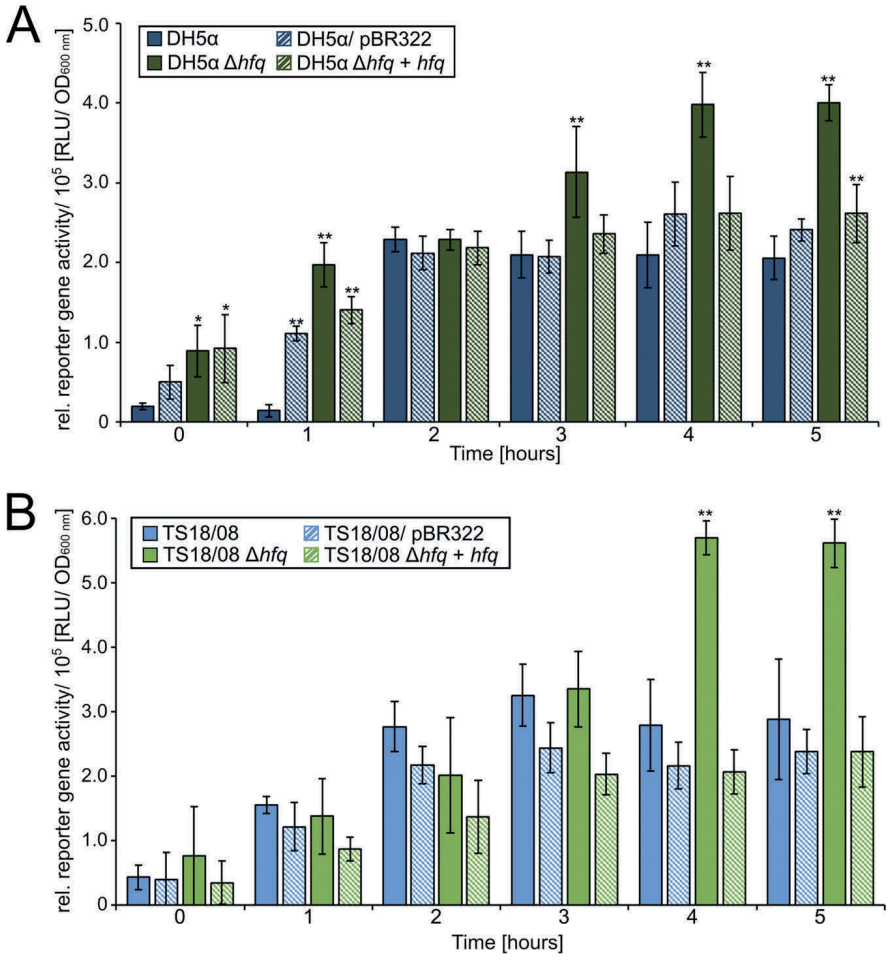

FIG 4 Impact of Hfq on *PsubAB*$_1$ activity in *E. coli* DH5α (A) and STEC *E. coli* TS18/08 (B). Relative reporter gene activity (RLU/OD$_{600}$) is shown. Bars represent data from the wild-type strain (DH5α/pKMD3 [A] or TS18/08/pKMD3 [B], solid blue) and an empty vector control (DH5α/pKMD3 + pBR322 [A] or TS18/08/pKMD3 + pBR322 [B], dashed blue). Additionally, data from *E. coli* DH5α Δ*hfq*/pKMD3 (DH5α Δ*hfq*) (A) and *E. coli* TS18/08 Δ*hfq*/pKMD3 (TS18/08 Δ*hfq*) (B) (solid green) deletion mutants and DH5α Δ*hfq*/pKMD3 + pLH01 (DH5α Δ*hfq* + *hfq*) (A) and TS18/08 Δ*hfq*/pKMD3 + pLH01 (TS18/08 Δ*hfq* + *hfq*) (B) (dashed green) complemented strains are depicted. Data are presented for measurements over 5 h of cultivation in LB at 37°C with aeration. Data from three biological replicates are shown; error bars indicate standard deviations from mean values. Statistical significance compared to the wild-type strain is indicated (*, $P < 0.05$; **, $P < 0.01$).

in either complemented strains or empty vector controls (pBR322-harboring strains). This result indicated the pBR322 backbone had no effect on the *PsubAB*$_1$ promoter activity.

The deletion of *hfq* led to a significant increase of *PsubAB*$_1$ activity in the late growth phase for both *E. coli* DH5α and STEC TS18/08. Moreover, observed effects were restored to the wild-type level if complementation was performed. These results indicate that Hfq represses *subAB*$_1$ promoter activity under wild-type conditions.

***PsubAB*$_1$ activity is dependent on H-NS in *E. coli* strains.** The impact of deletion of the *hns* gene on *PsubAB*$_1$ activity is depicted in Fig. 5. Relative reporter gene activity was significantly increased to a value of 1.9×10^5 RLU/OD$_{600}$ in the DH5α Δ*hns*/pKMD3 laboratory strain compared to that of the control DH5α/pKMD3 after 1 h of cultivation. After 2-, 3-, and 4-h time points, the *PsubAB*$_1$ activity of the DH5α Δ*hns*/pKMD3 strain was similar to that of the corresponding wild type. However, in the late exponential growth phase, the activity decreased up to a significant reduction of 1.5-fold relative reporter gene activity compared to that of the control. Nevertheless, the effects detected in the deletion mutant were restored in the complemented strain to levels comparable to that of *E. coli* DH5α.

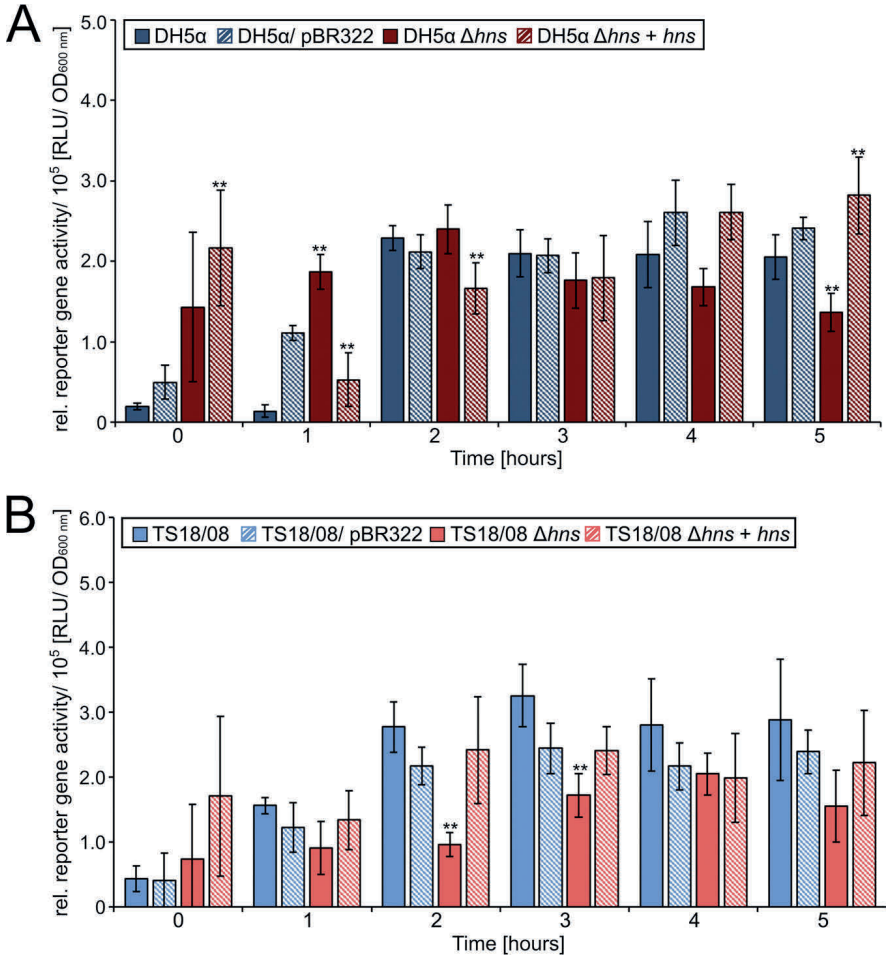

FIG 5 Impact of H-NS on *PsubAB*$_1$ activity in *E. coli* DH5α (A) and STEC TS18/08 (B). Relative (rel.) reporter gene activity (RLU/OD$_{600}$) is shown. Bars represent data from the wild-type strain (DH5α/pKMD3 [A] or TS18/08/pKMD3 [B], blue) and an empty vector control (DH5α/pKMD3 + pBR322 [A] or TS18/08/pKMD3 + pBR322 [B], dashed blue). Additionally, data from *E. coli* DH5α Δ*hns*/pKMD3 (DH5α Δ*hns*) (A) and *E. coli* TS18/08 Δ*hns*/pKMD3 (TS18/08 Δ*hns*) (B) (solid red) deletion mutants and DH5α Δ*hns*/pKMD3 + pLH01 (DH5α Δ*hns* + *hns*) (A) and TS18/08 Δ*hns*/pKMD3 + pLH01 (TS18/08 Δ*hns* + *hns*) (B) (dashed red) complemented strains are depicted. Data are presented for measurements over 5 h of cultivation in LB at 37°C with aeration. Data from three biological replicates are shown; error bars indicate standard deviations from mean values. Statistical significance compared to the wild-type strain is indicated (**, $P < 0.01$).

The increase of *PsubAB*$_1$ activity after 1 h of cultivation in the *hns* deletion mutant was not detected in STEC strain TS18/08, but, comparable to the case in *E. coli* DH5α, the deletion of *hns* led to a decrease of *PsubAB*$_1$ activity. In the TS18/08 Δ*hns*/pKMD3 strain, the decrease in relative reporter gene activity was measured during the whole period of cultivation, reaching a decrease of up to 2.9-fold compared to that of the wild-type strain. As described above for DH5α, the plasmid-based complementation led to a reduction of those effects.

These results suggested an impact of the global regulator H-NS on *PsubAB*$_1$ activity. Repression of *subAB*$_1$ by H-NS in early growth phase and activation in the exponential growth phase were measured for *E. coli* DH5α. In STEC strain TS18/08, only activation of the *subAB*$_1$ promoter activity was detected.

The global regulators Hfq and H-NS control expression of *subAB*$_1$, *stx*$_{2a}$, and *cdt-V*. Since TS18/08 was previously shown to express the three toxin genes *subAB*$_1$, *stx*$_{2a}$, and *cdt-V*, transcription analysis of wild-type and mutant strains was carried out by qRT-PCR. The gene expression of the three toxins was analyzed and normalized to expression of the reference gene *rrsB* (ΔC_T value, where C_T is threshold cycle). Tran-

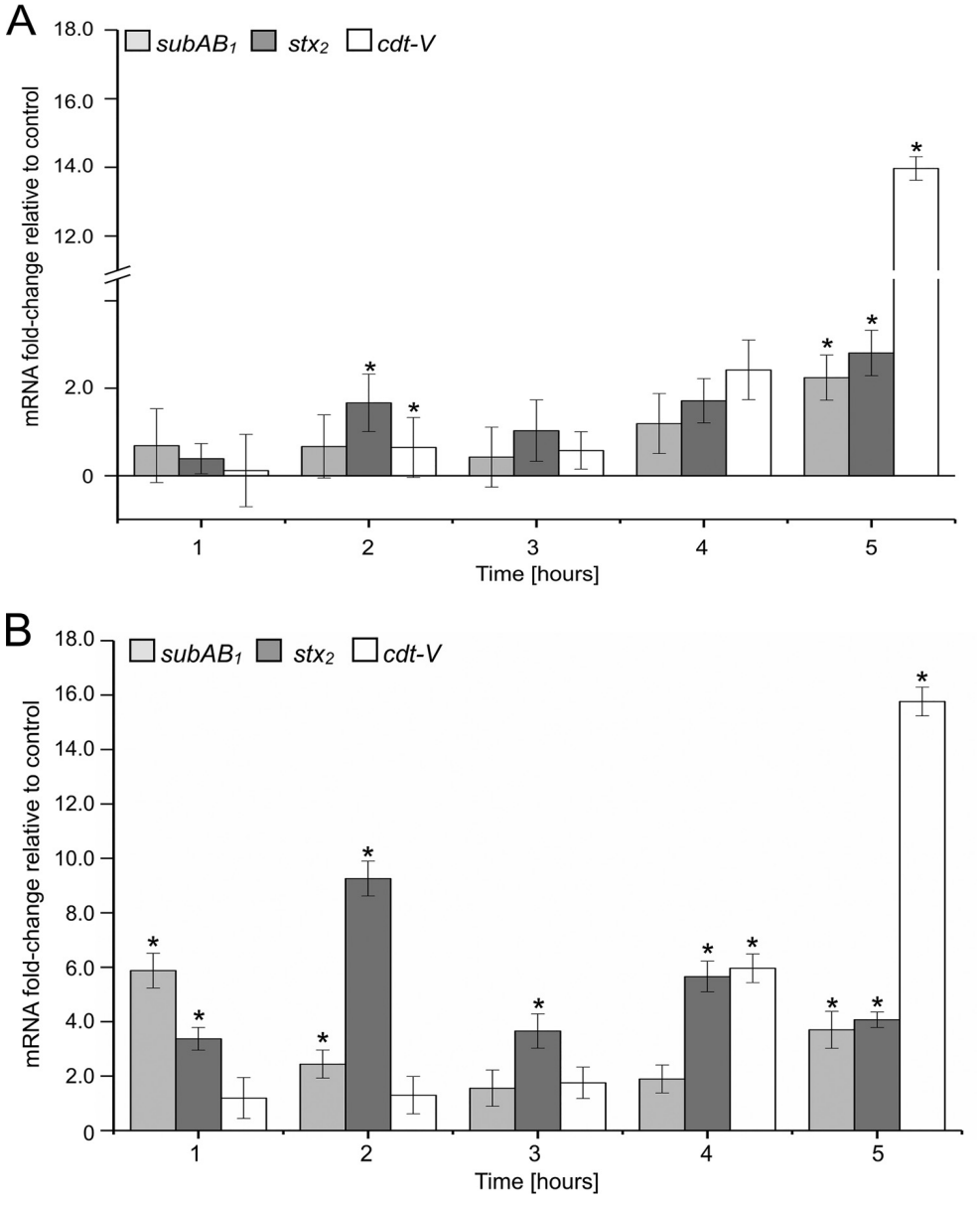

FIG 6 Expression of $subAB_1$, stx_2, and *cdt-V* in *E. coli* TS18/08 Δ*hfq* (A) and TS18/08 Δ*hns* (B) strains. Transcription is shown as fold change relative to the level of the control (*E. coli* TS18/08). Gene expression was measured under standard batch conditions (LB medium, 37°C, with aeration) using quantitative real-time PCR. Quantification was conducted using *rrsB* as a reference gene. Error bars indicate standard deviations from the mean values. Data from three biological replicates are shown. Asterisks indicate significance in fold change compared to the level for the control ($P < 0.05$).

scription of all investigated strains was normalized to transcription of TS18/08 ($\Delta\Delta C_T$ value) at each time point separately. The effect of the deletion of the *hfq* gene (Fig. 6A) and the *hns* gene (Fig. 6B) in *E. coli* TS18/08 is shown as fold change of mRNA levels in Fig. 6. The expression of $subAB_1$ was increased significantly up to 2-fold in the *E. coli* TS18/08 Δ*hfq* strain in the late exponential growth phase. The transcription of stx_{2a} in this strain showed a similar pattern, whereas a 2.8-fold increase was measured after 5 h of cultivation compared to the level for TS18/08. The highest upregulation was detected for *cdt-V* expression. Similar to that of the other toxins, the 14-fold upregulation was measured in the late growth phase.

Upregulation of the expression of all three toxins was also found in the *E. coli* TS18/08 Δ*hns* strain. $subAB_1$ transcription increased up to 6-fold after 1 h of cultivation and up to 3-fold in the late growth phase at 5 h of cultivation. The expression of *cdt-V*

increased up to 16-fold in the late growth phase and therefore was comparable to the one obtained in the *E. coli* TS18/08 Δ*hfq* strain. The expression of stx_{2a} increased over the whole bacterial life cycle in the *E. coli* TS18/08 Δ*hns* strain and was 10-fold upregulated after 2 h of cultivation.

The results obtained by qRT-PCR showed that both Hfq and H-NS have an impact on the expression of the toxins produced by STEC TS18/08. The strongest effects were detected in the late growth phase. In comparisons of the expression of the three toxins, the highest increase was detected in the *E. coli* TS18/08 Δ*hns* for stx_{2a} transcription. Therefore, the results of these experiments let us conclude that Hfq and H-NS had a strong impact on toxin gene transcription in STEC TS18/08.

DISCUSSION

Regulation of transcription of virulence factors is of major importance for pathogens, since maximum transcription of such factors at the site of infection may be advantageous for the colonization and infection process. In recent years, STEC strains have been analyzed frequently for the presence and absence of genes encoding virulence factors, such as Shiga toxins, type III effectors, adhesins, and EHEC-hemolysin, or for the qualitative description of their expression (14, 27–30). In some cases, data on the regulation of virulence factors have been published. For example, Shiga toxin expression is included in the phage induction cycle and is *recA* dependent (31). Moreover, the complex regulation of the LEE operon is well elucidated, and there is some knowledge on regulation of EHEC-hemolysin.

During recent years, STEC strains that carry genes encoding a subtilase cytotoxin have been described increasingly, and it was demonstrated that this toxin contributes to virulence of STEC (11). In a recent study, we could show that the subtilase is expressed during the bacterial growth cycle in batch culture, but the dependence of regulators is currently not known (12). Therefore, we were interested in getting deeper insight into the transcription regulation of $subAB_1$.

In this study, we investigated the effects of *hfq* and *hns* deletions in laboratory strain *E. coli* DH5α and wild-type STEC O113:H21 strain TS18/08. Both strains showed their highest promoter activity in the exponential growth phase. Hauser et al. (12) have demonstrated that transcription of $subAB_1$ was highest after 3 h of cultivation under standard batch conditions, showing a 7-fold increase in transcription compared to the initial value. This is similar to the results obtained in our study. Interestingly, the promoter activity varied only slightly between the two tested strains.

Moreover, we could show that Hfq acts as a repressor of $subAB_1$ promoter activity in the late growth phase. This finding was strain independent. Hfq is a pleiotropic regulator and has an impact on the expression of many virulence genes (23, 32–35). In former studies, the regulation of toxin gene expression by Hfq was shown. Kendall et al. studied EHEC O157:H7 strain 86-24 and its mutant with a *hfq* deletion and its respective Shiga toxin expression. They could show that transcription of stx_{2AB} was increased in this deletion mutant (23). This result could be reproduced in our study with the *E. coli* TS18/08 Δ*hfq* strain. In addition, upregulation of *cdt-V* was detected in the same mutant strain, assuming that Hfq is integrated in the regulation of different toxins. Both SubAB and Shiga toxin belong to the family of AB_5 toxins (36, 37), whereas the Cdt-V toxin is an AB_2 toxin consisting of three subunits (Cdt-A, Cdt-B, and Cdt-C) (38). The regulation by Hfq seems not to be dependent on the type of toxin.

Hfq can directly interact with DNA and regulate transcription, but most processes described indicate regulation by Hfq-dependent small regulatory RNAs (sRNAs) (25, 34, 39). In recent studies, the prevalence of sRNAs in gene regulation were shown (40). Oogai et al. have shown that the regulation of expression of Cdt-V is dependent on sRNAs in *Aggregatibacter actinomycetemcomitans* (41). We suggest that this is the same regulatory pathway in STEC strain TS18/08. Regulation of toxins could be integrated in networks regulated by sRNAs due to the fast response to environmental changes. This cascade is controlled by the RNA chaperone Hfq.

Regulation of toxin gene expression was reported not only for sRNAs and Hfq but

TABLE 1 Strains and plasmids used in this study

Strain or plasmid	Relevant geno- and phenotype[a]	Reference or source
E. coli		
DH5α	*tonA lacZ*ΔM15 *endA1 recA1 thi-1 supE44 phoA gyrA96 hsdR17* Δ(*lacZYA-argF*)*U169 relA1*	Invitrogen
DH5α Δ*hns*	*tonA lacZ*ΔM15 *endA1 recA1 thi-1 supE44 phoA gyrA96 hsdR17* Δ(*lacZYA-argF*)*U169 relA1* Δ*hns*	This study
DH5α Δ*hfq*	*tonA lacZ*ΔM15 *endA1 recA1 thi-1 supE44 phoA gyrA96 hsdR17* Δ(*lacZYA-argF*)*U169 relA1* Δ*hfq*	This study
HB101	F^- *mcrB mrr hsdS20*(r_B^- m_B^-) *recA13 leuB6 ara-14 proA2 lacY1 galK2 xyl-5 mtl-1 rpsL20* (Sm^r) *supE44* λ^-	52
TS18/08	O113:H21, *cdt-V*$^+$ $subAB_1^+$ stx_2^+	26
TS18/08 Δ*hns*	O113:H21, *cdt-V*$^+$ $subAB_1^+$ stx_2^+ Δ*hns*	This study
TS18/08 Δ*hfq*	O113:H21, *cdt-V*$^+$ $subAB_1^+$ stx_2^+ Δ*hfq*	This study
Plasmids		
pKD46	Contains genes of red recombinase system under control of *araB* promoter, Amp^r	46
pKD4	Template plasmid for kanamycin resistance cassette, Amp^r, Kan^r	46
pCP20	Contains genes for FLP recombinase, Amp^r	46
pKMD3	Luciferase reporter gene plasmid containing the $subAB_1$ promoter region	This study
pBR322	Cloning vector, pMB1 origin of replication, Amp^r, Tet^r	53
p3121	Luciferase reporter gene (*luc*) template vector, Amp^r, Kan^r	54
pWSK29	Cloning vector (low copy number), Amp^r	55
pLH01	Complementation plasmid, pBR322 backbone, with *hfq* gene under control of its own promoter, Tet^r	This study
pLH02	Complementation plasmid, pBR322 backbone, with *hns* gene under control of its own promoter, Tet^r	This study

[a]Amp^r, ampicillin resistance gene; Kan^r, kanamycin resistance gene; Tet^r, tetracycline resistance gene.

also for H-NS. Wan et al. revealed, by RNA sequencing, the repressing role of H-NS on expression of the hemolysin and Shiga toxin in EHEC (42). In our study, we showed by quantitative real-time PCR that H-NS repressed the expression of not only stx_{2a} but also *cdt-V* and $subAB_1$. Upregulation of $subAB_1$ expression in the TS18/08 Δ*hns* strain was detected in the early and late growth phases. For the *E. coli* DH5α Δ*hns* strain, upregulation could be confirmed only in the early growth phase. Moreover, we measured a decreased promoter activity in the latter strain in the late growth phase. This result might be due to the different methods applied, and factors such as RNA decay could influence the results. Another possibility is that the toxin genes studied are not regulated directly by H-NS but are integrated in the regulatory pathway of H-NS. Wan et al. identified, by RNA sequencing, up to 983 genes which are regulated by H-NS in EHEC (42). H-NS is an important factor in xenogeneic gene silencing. Genes involved in response to environmental stimuli, such as the acidic environment, temperature, pH value, or host signal peptides, could have a direct impact on promoter activity and posttranscriptional processes. Moreover, H-NS interacts directly with other nucleoid binding proteins, such as the DNA binding protein StpA (24). Those proteins regulate gene expression if H-NS is not present (43, 44). Moreover, it has been shown that StpA in combination with Hfq could reduce effects of an *hns* deletion mutant. Thus, it was shown that phenotypic characteristics of a Δ*hns* mutant were counteracted by *hfq* on a multicopy plasmid (45). This counteraction by Hfq and StpA might be the reason why different results were acquired for $subAB_1$ expression in the TS18/08 Δ*hns* strain in this study by comparing the luciferase reporter gene assay and qRT-PCR.

Given the fact that both global regulators showed influence on gene expression of three important STEC toxins, the role of these proteins in virulence and pathogenicity of STEC should be further investigated.

Conclusion. In this study, we demonstrated that expression of $subAB_1$, stx_{2a}, and *cdt-V* is dependent on functional global regulatory proteins Hfq and H-NS in both *E. coli* DH5α and STEC strain TS18/08. The presented data reveal that the expression of the virulence factors is integrated in the circuit of global regulatory proteins. Further studies will be necessary to elucidate the complex regulatory network.

MATERIALS AND METHODS

Bacterial strains and plasmids. Bacterial strains and plasmids used in this study are shown in Table 1. Strains were routinely grown in Luria-Bertani (LB) broth consisting of 1.0% (wt/vol) tryptone, 0.5% (wt/vol) yeast extract, and 1.0% (wt/vol) sodium chloride, adjusted to pH 7.0. For solid media, 1.5% (wt/vol) agar-agar was added. If necessary, ampicillin, kanamycin, and tetracycline were added to the

medium in final concentrations of 100 μg/ml, 50 μg/ml, and 10 μg/ml, respectively. Overnight cultures were prepared by incubating two colonies in 10 ml LB medium in 100-ml Erlenmeyer flasks at 37°C on a rotary shaker at 180 rpm.

Plasmids were prepared using a QIAprep spin miniprep kit (Qiagen, Germany) by following the manufacturer's recommendations (QIAprep miniprep handbook from July 2006; Qiagen). Genomic DNA for cloning procedures was isolated using a DNeasy Blood and Tissue kit (Qiagen) according to the procedure described in the DNeasy Blood and Tissue handbook (July 2006). Concentration and purity of nucleic acids were determined using a NanoDrop 2000 spectrophotometer (ThermoScientific, USA) and by agarose gel electrophoresis.

Construction of deletion mutants. Deletion of genes was conducted as described by Datsenko and Wanner (46), with minor modifications. Briefly, the genes of interest were exchanged with a kanamycin resistance cassette by homologous recombination. Primers were designed with Serial Cloner, version 2.6.1 (SerialBasics; Franck Perez, Paris, France). Whole-genome sequences of *E. coli* DH5α (NCBI accession number NZ_JRYM01000001), *E. coli* K-12 MG1655 (GenBank accession number NC_000913.3), and *E. coli* TS18/08 (NCBI accession number ASM199093v1) were used to design primers targeting *hfq* and *hns*, including their surrounding regions. Moreover, the genomic backgrounds of *hfq* and *hns* were compared in both strains by DNA sequencing. Thus, surrounding regions, meaning 86-bp upstream and 76-bp downstream sequences for the gene *hfq* and 144-bp upstream and 300-bp downstream sequences for the gene *hns*, were amplified using the primers stated in Table 1. Substitution of the kanamycin cassette was carried out using the helper plasmid pKD46, encoding the recombinase genes γ, β, and *exo*. Using a second helper plasmid, pCP20, which encodes FLP recombinase, the resistance cassettes were excised. Transformation of plasmids and linear fragments was performed as described below. Primers used for mutagenesis are shown in Table 2. Deletion mutants were verified by PCR with subsequent agarose gel electrophoresis and DNA sequencing. The *E. coli* DH5α Δ*hns*, *E. coli* DH5α Δ*hfq*, *E. coli* TS18/08 Δ*hns*, and *E. coli* TS18/08 Δ*hfq* deletion mutants were analyzed for a presumable 2nd copy of these genes by PCR using primers hfq_for, hfq_rev, hns_for, and hns_rev (Table 2).

Electroporation. Transformation of PCR products and plasmids was conducted by electroporation (GenePulser Xcell electroporation system; Bio-Rad, USA), and competent cells were prepared as described previously (47). To each cell aliquot, 300 ng of PCR products or 30 ng of plasmid DNA was added. Transformation was performed in electroporation cuvettes (2 mm; Bio-Rad) at 25 μF, 200 Ω, 2.5 kV, and 5 $\pm$ 0.2 ms. Residual steps were carried out as described previously (47).

Construction of reporter gene plasmid pKMD3. The luciferase reporter gene plasmid pKMD3 was constructed using the isothermal Gibson Assembly (NEB, USA) strategy. Therefore, a 405-bp region upstream of $subAB_1$, including the putative $subAB_1$ promoter region, was cloned from *E. coli* O113:H21 strain TS18/08. The plasmid map is shown in Fig. 7. The vector backbone consisted of plasmid pWSK29, which was linearized by restriction with PvuII and subsequent purification by agarose gel extraction using a QIAeX II gel extraction kit (Qiagen, Germany) according to the manufacturer's instructions (QIAeX II handbook, March 2015; Qiagen). The luciferase gene (*luc*) insert (1,653 bp) was amplified using plasmid p3121 as the target using primers luc-gibson_for and luc-gibson_rev (Table 2). The promoter region of the $subAB_1$ gene was amplified with primers subAB-gibson_for and subAB-gibson_rev (Table 2) using genomic DNA of *E. coli* TS18/08. The isothermal assembly was performed at 60°C for 50 min with an insert-to-vector ratio of 2:1. The assembly mixture was directly transformed by electroporation in competent *E. coli* DH5α cells as described previously. Cloning of the reporter gene plasmid was verified by PCR and DNA sequencing.

Luciferase assay. Analysis of subtilase cytotoxin promoter activity ($PsubAB_1$) was conducted using a luciferase reporter system (Promega, Madison, WI) by following the recommendations of the manufacturer (luciferase assay system, technical bulletin from 2015; Promega Corporation). Strains harboring the reporter gene plasmid pKMD3 (Table 1) were grown in LB medium at 37°C, 180 rpm, for 16 h. Twenty-four milliliters of LB medium in a 100-ml Erlenmeyer flask was inoculated with an overnight culture to an initial OD_{600} of 0.1 (unless stated otherwise) and further incubated at 37°C, 180 rpm, for 5 h. During cultivation, hourly sample taking and measurement of the OD_{600} was conducted in duplicates for each culture. In addition, samples were collected to measure luciferase activity. Thus, 400-μl samples were taken in duplicates for each strain and centrifuged at 6,000 $\times$ *g*, 4°C, for 5 min. Supernatants were discarded and pellets were resuspended in 90 μl of 1$\times$ cell culture lysis reagent (CCLR; Promega, USA) containing 10 mg/ml bovine serum albumin (albumin fraction V; Carl Roth, Germany). Subsequent adding of 90 μl 1$\times$ CCLR containing 10 mg/ml lysozyme (Sigma-Aldrich, Germany) was performed, and samples were frozen immediately at −70°C. Thawing of samples was conducted by incubation at 23°C with 300 rpm for 20 min in a heating block.

Measurement of luciferase activity was performed as described here and prepared in duplicates for each sample. Fifty-microliter aliquots of thawed samples were transferred to a white microtiter plate (LUMITRAC 600; Greiner). As a substrate, 50 μl of luciferase assay reagent (Promega) was added to samples, and luminescence was measured immediately at 562 nm using a microplate reader (Infinite M200; Tecan). To compare the results during cultivation, relative reporter gene activity was defined as the ratio of relative light units (RLU) to the respective OD_{600}. All experiments were performed three times, each on a different day.

Cloning of vectors for complementation experiments. For complementation experiments, plasmids were constructed containing *hfq* and *hns*, including their putative promoter regions, as shown in Fig. 8. The medium-copy-number plasmid pBR322 (Table 1) was chosen as a cloning vector due to its compatibility with the luciferase reporter gene plasmid pKMD3. The plasmid was double digested with restriction enzymes PvuI (NEB, USA) and AseI (NEB, USA). The reaction was carried out using 1 μg of DNA

TABLE 2 Oligonucleotide primers used in this study

Primer and/or category	Use	Nucleotide sequence[a] (5′ to 3′)	Source
Hfq_for	Detection of *hfq* gene	ATGGCTAAGGGGCAATCTTTACAAG	This study
Hfq_rev	Detection of *hfq* gene	TTATTCGGTTCTTCGCTGTCCTG	This study
Hns_for	Detection of *hns* gene	TTATTGCTTGATCAGGAAATCGTCG	This study
Hns_rev	Detection of *hns* gene	ATGAGCGAAGCACTTAAAATTCTG	This study
Mutagenesis			
Del_hfq_for	Deletion of *hfq* gene, creation of resistance cassette	AATGTGTACAATTGAGACGTATCGTGCGCATTTTTTCAGAATCGCGATTGTGTAGGCTGGAGC	This study
Del_hfq_rev	Deletion of *hfq* gene, creation of resistance cassette	AGCGTATAACCCTCTAAATAGATCAGCGGGGAACGCAGGATCCATGGTCCATATGAATATCCTCC	This study
Hfq + 186up_for	Verification of deletion of *hfq*	CCTGGCTGCGTGGTTGGGAAG	This study
Hfq-176down_rev	Verification of deletion of *hfq*	ACCAGAGATTCAAACTCCTGGAGGTC	This study
Del-hns_for	Deletion of *hns* gene, creation of resistance cassette	ACATCCGTATCGGTGTTACCACGAAACGGCGTTGAGCAATCGCGATTGTGTAGGCTGGAGC	This study
Del-hns_rev	Deletion of *hns* gene, creation of resistance cassette	ATAGGGAATTCTCGTAAACACAACTAATACAGAAGACTGAAAGGCATGGTCCATATGAATATCCTCC	This study
Hns + 244up_for	Verification of deletion of *hns*	TAGGTTACATGCAGGCCTTCGTTG	This study
Hns-705down_rev	Verification of deletion of *hns*	ACAGTGCGCATGCCGCGTTCC	This study
Construction of complementation plasmids			
Hfq + 86up_AseI_for	Complementation studies	GGGGGGGGGGattaatAATGTGTACAATTGAGACGTATCGTGCGCAATTTTTTCAGAATC	This study
Hfq-76down_PvuI_rev	Complementation studies	GGGGGcgatcgAGCGTATAACCCTCTAAATAGATCAGCGGGGAACGCAGGATC	This study
Hns + 144up_AseI_for	Complementation studies	CCCCCCaattaatACATCCGTATCGGTGTTATCCACGAAACGGCGTTGAGCAATC	This study
Hns-300down_PvuI_rev	Complementation studies	CCCCCCcgatcgATAGGGAATTCTCGTAAACACAACTAATACAGAAGACTGAAAGG	This study
Construction of luciferase reporter gene plasmid pKMD3			
subAB-gibson_for	Cloning of $subAB_1$ promoter region for pKMD3	TTCGCTATTACGCCAGCTGAACGGTATCGATCCG	This study
subAB-gibson_rev	Cloning of $subAB_1$ promoter region for pKMD3	GTCTTCCATAAGCTCCTCCAGTTAGTAC	This study
luc-gibson_for	Cloning of *luc* for pKMD3	AGGAGCTTATGGAAGACGCCAAAAAC	This study
luc-gibson_rev	Cloning of *luc* for pKMD3	CCGATTCATTAATGCAGTCACAATTTGGACTTTCCG	This study
Gibson-1_for	Verification of pKMD3	ACACCCGCCGCGCTTAATGC	This study
Seq 2-gibson_rev	Verification of pKMD3	GATACCGCTCGCCGCAGCCG	This study
Seq 3-gibson_for	Verification of pKMD3	GGTTGTGGATCTGGATGCCG	This study
Seq 4-gibson_rev	Verification of pKMD3	AGGGCGTATCTCTTCATAGC	This study

[a]Underlined bases depict homologous regions in mutagenesis, and underlined lowercase letters depict restriction sites for cloning strategy.

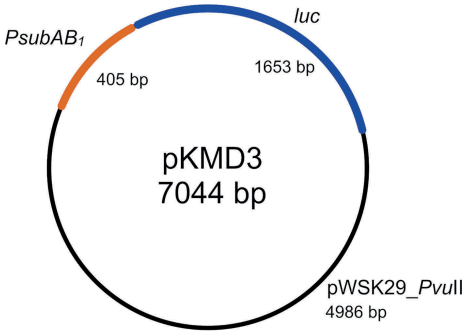

FIG 7 Plasmid map of the luciferase reporter gene plasmid pKMD3. The putative promoter region of *subAB*$_1$ (405 bp; *PsubAB*$_1$) was cloned upstream of the luciferase reporter gene *luc* (1,652 bp) in the pWSK29 backbone restricted with PvuII (pWSK29_PvuII).

template, 10 U of each enzyme, and NEB buffer 3.1. Restriction was performed at 37°C for 60 min. Inserts of the sequences were cloned, 86-bp upstream and 76-bp downstream sequences for the gene *hfq* and 144-bp upstream and 300-bp downstream sequences for the gene *hns*, and were amplified using primers with restriction sites at their 3′ ends as shown in Table 2. Amplification was conducted using genomic DNA of *E. coli* strain DH5α (DNeasy Blood and Tissue kit; Qiagen, Germany) as the template. Oligonucleotides (Eurofins MWG Operon, Germany) were designed using Serial Cloner, version 2.6.1 (SerialBasics; Franck Perez, Paris, France). Purification of linearized vector DNA was conducted by excising the respective band on an agarose gel (1%, wt/vol) and subsequently isolated using a Wizard SV gel and PCR clean-up system (Promega, USA). The amplified inserts were digested with PvuI and AseI as stated above and purified using a PCR purification kit (Qiagen, Germany) by following the manufacturer's recommendations (QIAquick spin handbook, April 2015; Qiagen). Ligation of vector and the respective insert was performed with T4 DNA ligase (ThermoFisher Scientific) at 22°C for 1 h using a vector-to-insert ratio of 1:5. After ligation, the resulting plasmids pLH01 and pLH02 were transformed in competent *E. coli* DH5α cells as described previously, and transformants were selected on agar plates containing tetracycline (10 μg/ml). Recombinant plasmids were then verified by DNA sequencing using the respective primers listed in Table 2 and finally transformed in reporter strains and deletion mutants using electroporation as described previously.

Analysis of gene transcription on complementation plasmids. The expression of the cloned genes on the recombinant plasmids used for complementation was verified by transcription analysis as described earlier (48). Briefly, RNA was isolated using the RNeasy minikit (Qiagen, Germany). Strains harboring complementation plasmids were grown in LB medium at 37°C with agitation to an OD_{600} of 1.0. Five hundred microliters of the culture was added to 1 ml of RNAprotect bacterial reagent (Qiagen, Germany). Isolation of RNA was conducted by following the manufacturer's recommendation, and DNA

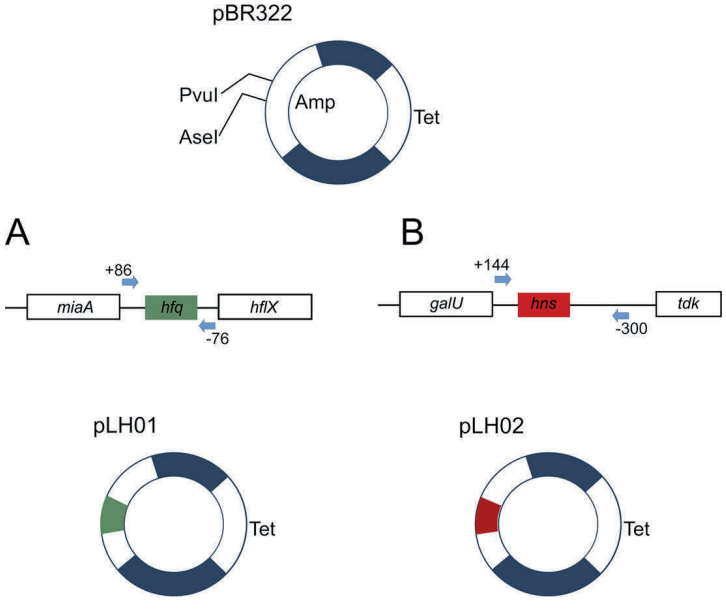

FIG 8 Cloning strategy of complementation vectors pLH01 (A) and pLH02 (B). Positions of *hns* and *hfq* genes refer to the genome sequence of *E. coli* DH5α (NCBI accession number NZ_JRYM01000001).

TABLE 3 Oligonucleotide primers used for transcription analysis by qRT-PCR

Primer	Nucleotide sequence (5′ to 3′ direction)	PCR product size and conditions	Reference
rrsB-for	GCATAACGTCGCAAGACCAAA	91 bp; 95°C, 10 s; 60.0°C, 30 s; 72°C, 10 s	51
rrsB-rev	GCCGTTACCCCACCTACTAGCT		
RTsubAB-2-for	GCAGGTATTATGGGATGTCT	177 bp; 95°C, 15 s; 60.3°C, 20 s; 72°C, 10 s	12
RTsubABrev	GCAGGCACTTATGGAGGAG		
Upper-stx2	TCATATCTGGCGTTAATGGAGTTC	99 bp; 95°C, 10 s; 52.4°C, 30 s; 72°C, 10 s	51
Lower-stx2	GCGTAAGGCTTCTGCTGTG		
RTCDTA-for	CCGATGGTAACACGCAATG	184 bp; 95°C, 10 s; 53.0°C, 30 s; 72°C, 10 s	12
RTCDTA-rev	GCCTTAATGGTTCGCTTATGG		

was digested using a DNA-free kit (Thermo Fisher Scientific, USA) according to the manual (user guide, October 2012; Life Technologies Corporation). RNA concentration and purity were determined spectrophotometrically using a NanoDrop 2000 device (Thermo Scientific, USA), followed by visual inspection on denaturing agarose gel electrophoresis (data not shown). Transcription to cDNA was performed using 1 μg RNA, a SuperScript II reverse transcriptase kit (Bio-Rad, USA), and primer for detection of the *hfq* (hfq_for and hfq_rev) or *hns* (hns_for and hns_rev) gene (Table 2) by following the manufacturer's recommendations (manual of SuperScript II from 2010; Life Technologies Corporation). As a control, cDNA synthesis was performed using random primers as given in the SuperScript II reverse transcriptase kit (random hexamer oligonucleotides). For each approach, the reverse transcriptase negative control was applied to avoid false-positive results due to residual DNA present in samples. Synthesized cDNA was analyzed by PCR using primers specific for genes *hfq* and *hns* as stated above. Subsequently, amplification was investigated by agarose gel electrophoresis. Expression control was performed in three biological replicates independently, each on different days.

RNA isolation. Erlenmeyer flasks containing 24 ml LB medium were inoculated with overnight culture to an OD_{600} of 0.1. *E. coli* TS18/08 was cultivated at 37°C, 180 rpm, for 5 h, and samples were taken hourly for RNA isolation. Therefore, 1.0×10^9 cells were transferred to a 2-fold volume of RNAprotect bacterial reagent (Qiagen, Germany). The suspensions were mixed immediately for 5 s, followed by an incubation at room temperature for 5 min. Centrifugation was then performed at room temperature at 5,000 $\times$ *g* for 10 min, and the supernatants were discarded. Pellets were stored at −70°C until further processing. RNA isolation was performed as described in the manual of the RNAprotect bacterial reagent (Qiagen, Germany) and RNeasy minikit (Qiagen, Germany) by following the protocol for enzymatic lysis and proteinase K digestion (protocol 4) and subsequent purification of total RNA (protocol 7). RNA purity and concentration were determined using a spectrophotometer (NanoDrop 2000; Thermo Scientific, USA), and integrity of RNA was examined using formaldehyde-based denaturing agarose gel electrophoresis.

Transcription analysis. Prior to cDNA synthesis, residual DNA was degraded in the samples using a DNA-free kit (ThermoScientific, USA) by following the recommendations stated in the manual (user guide, October 2012; Life Technologies Corporation). Reverse transcription was performed using an iScript cDNA synthesis kit (Bio-Rad, USA) with the following procedure: 500 ng of the RNA samples was used for reverse transcription and incubated according to the protocol stated by the manufacturer (manual from 2000; Bio-Rad Laboratories). For each sample, a reverse transcription-negative approach was conducted as a control to detect residual DNA. Synthesized cDNA was used for quantitative real-time PCR in a CFX96 system (Bio-Rad, USA) by following the experimental procedure described previously (12). Therefore, 10 μl of SsoAdvanced universal SYBR green supermix (Bio-Rad, USA), 2.8 ng of cDNA, 0.75 μl of each primer (10 pmol/μl), and nuclease-free water to the end volume of 20 μl were used for each qRT-PCR approach. Primers and respective PCR conditions are shown in Table 3. Analysis was performed in duplicates and with three biological replicates. Analysis of data was performed using the $2^{-\Delta\Delta CT}$ method described by Pfaffl et al. (49, 50). Thus, expression data for genes $subAB_1$, stx_2, and *cdt-V* were normalized to expression of reference gene *rrsB* (16S rRNA gene) (ΔC_T). Subsequently, ΔC_T values were normalized to the values of *E. coli* TS18/08 ($\Delta\Delta C_T$). The data were analyzed for each point of time independently. For all targets, standard curves of recombinant plasmids were used to identify target efficiency as described previously (12, 51). No-template controls and reverse transcription-negative controls were applied in each approach and showed C_T values after 35 to 40 cycles of PCR (data not shown). Each sample was analyzed in at least two technical replicates, and experiments were conducted in three independent experiments on different days (biological replicates).

Statistical analysis. Means from biological replicates were used for statistical analysis. Data were analyzed on normal distribution using the Grubb's test. If data sets of two different time points measured were compared for one strain, paired Student's *t* test was used, and if data were not normally distributed, Mann-Whitney test was applied. Data sets of different strains at identical time points measured were analyzed by application of analysis of variance (ANOVA). The variance homogeneity was identified by residual plots (Q-Q-plots). If requirements were given, one-way ANOVA was performed using a *post hoc* Tukey test ($\alpha = 0.05$). If requirements were not met, data were analyzed using Welch's ANOVA and *post hoc* Games-Howell test. Statistical analysis was performed using the software SPSS Statistics 25 (IBM, USA), and statistical significance was given if the *P* value was $<\alpha$.

SUPPLEMENTAL MATERIAL

Supplemental material for this article may be found at https://doi.org/10.1128/AEM.01281-19.

SUPPLEMENTAL FILE 1, PDF file, 0.1 MB.

ACKNOWLEDGMENTS

We thank Lydia Pertschy and Markus Kranz (University of Hohenheim, Stuttgart) for skillful technical assistance. We gratefully thank Hans-Peter Piepho (University of Hohenheim, Stuttgart) for his advice on the statistical analysis of the data.

This work was funded by the German Research Foundation (DFG) grant number SCHM-1360/11-1.

We have no conflicts of interest to declare.

REFERENCES

1. Karch H, Tarr PI, Bielaszewska M. 2005. Enterohaemorrhagic *Escherichia coli* in human medicine. Int J Med Microbiol 295:405–418. https://doi.org/10.1016/j.ijmm.2005.06.009.
2. Nataro JP, Kaper JB. 1998. Diarrheagenic *Escherichia coli*. Clin Microbiol Rev 11:142–201. https://doi.org/10.1128/CMR.11.1.142.
3. O'Brien AD, Newland JW, Miller S, Holmes RK, Smith HW, Formal SB. 1983. Shiga-like toxin-converting phages from *Escherichia coli* strains that cause hemorrhagic colitis or infantile diarrhea. Science 226:694–696. https://doi.org/10.1126/science.6387911.
4. McDaniel TK, Jarvis KG, Donnenberg MS, Kaper JB. 1995. A genetic locus of enterocyte effacement conserved among diverse enterobacterial pathogens. Proc Natl Acad Sci U S A 92:1664–1668. https://doi.org/10.1073/pnas.92.5.1664.
5. Galli L, Miliwebsky E, Irino K, Leotta G, Rivas M. 2010. Virulence profile comparison between LEE-negative Shiga toxin-producing *Escherichia coli* (STEC) strains isolated from cattle and humans. Vet Microbiol 143:307–313. https://doi.org/10.1016/j.vetmic.2009.11.028.
6. Chui L, Li V, Fach P, Delannoy S, Malejczyk K, Patterson-Fortin L, Poon A, King R, Simmonds K, Scott AN, Lee MC. 2015. Molecular profiling of *Escherichia coli* O157:H7 and non-O157 strains isolated from humans and cattle in Alberta, Canada. J Clin Microbiol 53:986–990. https://doi.org/10.1128/JCM.03321-14.
7. Paton AW, Woodrow MC, Doyle RM, Lanser JA, Paton JC. 1999. Molecular characterization of a Shiga toxigenic *Escherichia coli* O113:H21 strain lacking *eae* responsible for a cluster of cases of hemolytic-uremic syndrome. J Clin Microbiol 37:3357–3361.
8. Yahiro K, Satoh M, Morinaga N, Tsutsuki H, Ogura K, Nagasawa S, Nomura F, Moss J, Noda M. 2011. Identification of subtilase cytotoxin (SubAB) receptors whose signaling, in association with SubAB-induced BiP cleavage, is responsible for apoptosis in HeLa cells. Infect Immun 79:617–627. https://doi.org/10.1128/IAI.01020-10.
9. Paton AW, Beddoe T, Thorpe CM, Whisstock JC, Wilce MCJ, Rossjohn J, Talbot UM, Paton JC. 2006. AB_5 subtilase cytotoxin inactivates the endoplasmic reticulum chaperone BiP. Nature 443:548–552. https://doi.org/10.1038/nature05124.
10. Le Nours J, Paton AW, Byres E, Troy S, Herdman BP, Johnson MD, Paton JC, Rossjohn J, Beddoe T. 2013. Structural basis of subtilase cytotoxin SubAB assembly. J Biol Chem 288:27505–27516. https://doi.org/10.1074/jbc.M113.462622.
11. Funk J, Biber N, Schneider M, Hauser E, Enzenmüller S, Förtsch C, Barth H, Schmidt H. 2015. Cytotoxic and apoptotic effects of recombinant subtilase cytotoxin variants of Shiga toxin-producing *Escherichia coli*. Infect Immun 83:2338–2349. https://doi.org/10.1128/IAI.00231-15.
12. Hauser E, Bruederle M, Reich C, Bruckbauer A, Funk J, Schmidt H. 2016. Subtilase contributes to the cytotoxicity of a Shiga toxin-producing *Escherichia coli* strain encoding three different toxins. Int J Food Microbiol 217:156–161. https://doi.org/10.1016/j.ijfoodmicro.2015.10.023.
13. Funk J, Stoeber H, Hauser E, Schmidt H. 2013. Molecular analysis of subtilase cytotoxin genes of food-borne Shiga toxin-producing *Escherichia coli* reveals a new allelic *subAB* variant. BMC Microbiol 13:230. https://doi.org/10.1186/1471-2180-13-230.
14. Fierz L, Cernela N, Hauser E, Nüesch-Inderbinen M, Stephan R. 2017. Characteristics of Shiga toxin-producing *Escherichia coli* strains isolated during 2010–2014 from human infections in Switzerland. Front Microbiol 8:1471. https://doi.org/10.3389/fmicb.2017.01471.
15. Moll I, Leitsch D, Steinhauser T, Bläsi U. 2003. RNA chaperone activity of the Sm-like Hfq protein. EMBO Rep 4:284–289. https://doi.org/10.1038/sj.embor.embor772.
16. De Lay N, Schu DJ, Gottesman S. 2013. Bacterial small RNA-based negative regulation: Hfq and its accomplices. J Biol Chem 288:7996–8003. https://doi.org/10.1074/jbc.R112.441386.
17. Meng X, Meng X, Zhu C, Wang H, Wang J, Nie J, Hardwidge PR, Zhu G. 2013. The RNA chaperone Hfq regulates expression of fimbrial-related genes and virulence of *Salmonella enterica* serovar Enteritidis. FEMS Microbiol Lett 346:90–96. https://doi.org/10.1111/1574-6968.12206.
18. Zhang A, Altuvia S, Tiwari A, Argaman L, Hengge-Aronis R, Storz G. 1998. The OxyS regulatory RNA represses *rpoS* translation and binds the Hfq (HF-I) protein. EMBO J 17:6061–6068. https://doi.org/10.1093/emboj/17.20.6061.
19. Zhang A, Wassarman KM, Ortega J, Steven AC, Storz G. 2002. The Sm-like Hfq protein increases OxyS RNA interaction with target mRNAs. Mol Cell 9:11–22. https://doi.org/10.1016/S1097-2765(01)00437-3.
20. Tupper AE, Owen-Hughes TA, Ussery DW, Santos DS, Ferguson DJ, Sidebotham JM, Hinton JC, Higgins CF. 1994. The chromatin-associated protein H-NS alters DNA topology in vitro. EMBO J 13:258–268. https://doi.org/10.1002/j.1460-2075.1994.tb06256.x.
21. Bertin P, Terao E, Lee EH, Lejeune P, Colson C, Danchin A, Collatz E. 1994. The H-NS protein is involved in the biogenesis of flagella in *Escherichia coli*. J Bacteriol 176:5537–5540. https://doi.org/10.1128/jb.176.17.5537-5540.1994.
22. Atlung T, Ingmer H. 1997. H-NS: a modulator of environmentally regulated gene expression. Mol Microbiol 24:7–17. https://doi.org/10.1046/j.1365-2958.1997.3151679.x.
23. Kendall MM, Gruber CC, Rasko DA, Hughes DT, Sperandio V. 2011. Hfq virulence regulation in enterohemorrhagic *Escherichia coli* O157:H7 strain 86-24. J Bacteriol 193:6843–6851. https://doi.org/10.1128/JB.06141-11.
24. Srinivasan R, Scolari VF, Lagomarsino MC, Seshasayee A. 2015. The genome-scale interplay amongst xenogene silencing, stress response and chromosome architecture in *Escherichia coli*. Nucleic Acids Res 43:295–308. https://doi.org/10.1093/nar/gku1229.
25. Li H, Granat A, Stewart V, Gillespie JR. 2008. RpoS, H-NS, and DsrA influence EHEC hemolysin operon (*ehxCABD*) transcription in *Escherichia coli* O157:H7 strain EDL933. FEMS Microbiol Lett 285:257–262. https://doi.org/10.1111/j.1574-6968.2008.01240.x.
26. Slanec T, Fruth A, Creuzburg K, Schmidt H. 2009. Molecular analysis of virulence profiles and Shiga toxin genes in food-borne Shiga toxin-producing *Escherichia coli*. Appl Environ Microbiol 75:6187–6197. https://doi.org/10.1128/AEM.00874-09.
27. Krause M, Barth H, Schmidt H. 2018. Toxins of locus of enterocyte effacement-negative Shiga toxin-producing *Escherichia coli*. Toxins (Basel) 10:241–219. https://doi.org/10.3390/toxins10060241.
28. Akiyama Y, Futai H, Saito E, Ogita K, Sakae H, Fukunaga M, Tsuji H, Chikahira M, Iguchi A. 2017. Shiga toxin subtypes and virulence genes in *Escherichia coli* isolated from cattle. Jpn J Infect Dis 70:181–185. https://doi.org/10.7883/yoken.JJID.2016.100.
29. Baranzoni GM, Fratamico PM, Gangiredla J, Patel I, Bagi LK, Delannoy S, Fach P, Boccia F, Anastasio A, Pepe T. 2016. Characterization of Shiga

toxin subtypes and virulence genes in porcine Shiga toxin-producing *Escherichia coli*. Front Microbiol 7:574. https://doi.org/10.3389/fmicb.2016.00574.
30. Alonso MZ, Krüger A, Sanz ME, Padola NL, Lucchesi P. 2016. Serotypes, virulence profiles and *stx* subtypes of Shigatoxigenic *Escherichia coli* isolated from chicken derived products. Rev Argent Microbiol 48:325–328. https://doi.org/10.1016/j.ram.2016.04.009.
31. Ichimura K, Shimizu T, Matsumoto A, Hirai S, Yokoyama E, Takeuchi H, Yahiro K, Noda M. 2017. Nitric oxide-enhanced Shiga toxin production was regulated by Fur and RecA in enterohemorrhagic *Escherichia coli* O157. Microbiologyopen 6:e00461-17. https://doi.org/10.1002/mbo3.461.
32. Hansen AM, Kaper JB. 2009. Hfq affects the expression of the LEE pathogenicity island in enterohaemorrhagic *Escherichia coli*. Mol Microbiol 73:446–465. https://doi.org/10.1111/j.1365-2958.2009.06781.x.
33. Kulesus RR, Diaz-Perez K, Slechta ES, Eto DS, Mulvey MA. 2008. Impact of the RNA chaperone Hfq on the fitness and virulence potential of uropathogenic *Escherichia coli*. Infect Immun 76:3019–3026. https://doi.org/10.1128/IAI.00022-08.
34. Khandige S, Kronborg T, Uhlin BE, Møller-Jensen J. 2015. sRNA-mediated regulation of P-fimbriae phase variation in uropathogenic *Escherichia coli*. PLoS Pathog 11:e1005109-23. https://doi.org/10.1371/journal.ppat.1005109.
35. Bojer MS, Jakobsen H, Struve C, Krogfelt KA, Løbner-Olesen A. 2012. Lack of the RNA chaperone Hfq attenuates pathogenicity of several *Escherichia coli* pathotypes towards *Caenorhabditis elegans*. Microbes Infect 14:1034–1039. https://doi.org/10.1016/j.micinf.2012.06.002.
36. Paton AW, Srimanote P, Talbot UM, Wang H, Paton JC. 2004. A new family of potent AB_5 cytotoxins produced by Shiga toxigenic *Escherichia coli*. J Exp Med 200:35–46. https://doi.org/10.1084/jem.20040392.
37. Fraser ME, Chernaia MM, Kozlov YV, James M. 1994. Crystal structure of the holotoxin from *Shigella dysenteriae* at 2.5 A resolution. Nat Struct Biol 1:59–64. https://doi.org/10.1038/nsb0194-59.
38. Cortes-Bratti X, Frisan T, Thelestam M. 2001. The cytolethal distending toxins induce DNA damage and cell cycle arrest. Toxicon 39:1729–1736. https://doi.org/10.1016/S0041-0101(01)00159-3.
39. Papenfort K, Vogel J. 2014. Small RNA functions in carbon metabolism and virulence of enteric pathogens. Front Cell Infect Microbiol 4:91. https://doi.org/10.3389/fcimb.2014.00091.
40. Gottesman S. 2005. Micros for microbes: non-coding regulatory RNAs in bacteria. Trends Genet 21:399–404. https://doi.org/10.1016/j.tig.2005.05.008.
41. Oogai Y, Gotoh Y, Ogura Y, Kawada-Matsuo M, Hayashi T, Komatsuzawa H. 2018. Small RNA repertoires and their intraspecies variation in *Aggregatibacter actinomycetemcomitans*. DNA Res 25:207–215. https://doi.org/10.1093/dnares/dsx050.
42. Wan B, Zhang Q, Tao J, Zhou A, Yao YF, Ni J. 2016. Global transcriptional regulation by H-NS and its biological influence on the virulence of enterohemorrhagic *Escherichia coli*. Gene 588:115–123. https://doi.org/10.1016/j.gene.2016.05.007.
43. Srinivasan R, Chandraprakash D, Krishnamurthi R, Singh P, Scolari VF, Krishna S, Seshasayee A. 2013. Genomic analysis reveals epistatic silencing of "expensive" genes in *Escherichia coli* K-12. Mol Biosyst 9:2021–2033. https://doi.org/10.1039/c3mb70035f.
44. Prieto A, Urcola I, Blanco J, Dahbi G, Muniesa M, Quiros P, Falgenhauer L, Chakraborty T, Huttener M, Juarez A. 2016. Tracking bacterial virulence: global modulators as indicators. Sci Rep 6:25973. https://doi.org/10.1038/srep25973.
45. Shi X, Bennett GN. 1994. Plasmids bearing *hfq* and the *hns*-like gene *stpA* complement *hns* mutants in modulating arginine decarboxylase gene expression in *Escherichia coli*. J Bacteriol 176:6769–6775. https://doi.org/10.1128/jb.176.21.6769-6775.1994.
46. Datsenko KA, Wanner BL. 2000. One-step inactivation of chromosomal genes in *Escherichia coli* K-12 using PCR products. Proc Natl Acad Sci U S A 97:6640–6645. https://doi.org/10.1073/pnas.120163297.
47. Saile N, Voigt A, Kessler S, Stressler T, Klumpp J, Fischer L, Schmidt H. 2016. *Escherichia coli* O157:H7 strain EDL933 harbors multiple functional prophage-associated genes necessary for the utilization of 5-N-acetyl-9-O-acetyl neuraminic acid as a growth substrate. Appl Environ Microbiol 82:5940–5950. https://doi.org/10.1128/AEM.01671-16.
48. Bondì R, Chiani P, Michelacci V, Minelli F, Caprioli A, Morabito S. 2017. The gene *tia*, harbored by the subtilase-encoding pathogenicity island, is involved in the ability of locus of enterocyte effacement-negative Shiga toxin-producing *Escherichia coli* strains to invade monolayers of epithelial cells. Infect Immun 85:e00613-17. https://doi.org/10.1128/IAI.00613-17.
49. Pfaffl MW. 2004. Real-time RT-PCR: Neue Ansätze zur exakten mRNA Quantifizierung. BIOspektrum 10:92–95.
50. Fleige S, Walf V, Huch S, Prgomet C, Sehm J, Pfaffl MW. 2006. Comparison of relative mRNA quantification models and the impact of RNA integrity in quantitative real-time. Biotechnol Lett 28:1601–1613. https://doi.org/10.1007/s10529-006-9127-2.
51. Slanec T, Schmidt H. 2011. Specific expression of adherence-related genes in *Escherichia coli* O157:H7 strain EDL933 after heat treatment in ground beef. J Food Prot 74:1434–1440. https://doi.org/10.4315/0362-028X.JFP-11-018.
52. Boyer HW, Roulland-Dussoix D. 1969. A complementation analysis of the restriction and modification of DNA in *Escherichia coli*. J Mol Biol 41:459–472. https://doi.org/10.1016/0022-2836(69)90288-5.
53. Bolivar F, Rodriguez RL, Greene PJ, Betlach MC, Heyneker HL, Boyer HW, Crosa JH, Falkow S. 1977. Construction and characterization of new cloning vehicles II. A multipurpose cloning system. Gene 2:95–113. https://doi.org/10.1016/0378-1119(77)90000-2.
54. Gerlach RG, Hölzer SU, Jäckel D, Hensel M. 2007. Rapid engineering of bacterial reporter gene fusions by using red recombination. Appl Environ Microbiol 73:4234–4242. https://doi.org/10.1128/AEM.00509-07.
55. Wang RF, Kushner SR. 1991. Construction of versatile low-copy-number vectors for cloning, sequencing and gene expression in *Escherichia coli*. Gene 100:195–199. https://doi.org/10.1016/0378-1119(91)90366-J.

Chapter 3

Cytotoxic effects of recombinant StxA2-His in the absence of its corresponding B-subunit

Laura Heinisch[a*], Maike Krause[a*], Astrid Roth[a], Holger Barth[b], and Herbert Schmidt[a]

[a]Institute of Food Science and Biotechnology, Department of Food Microbiology and Hygiene, University of Hohenheim, Stuttgart, Germany

[b]Institute of Pharmacology and Toxicology, University of Ulm Medical Center, Ulm, Germany

[*]Laura Heinisch and Maike Krause contributed equally to this work

Published in Toxins Volume 13 of 2021, Article 307

DOI: 10.3390/toxins13050307

The supplemental material of this article can be found at https://www.mdpi.com/2072-6651/13/5/307.

toxins

MDPI

Article

Cytotoxic Effects of Recombinant StxA2-His in the Absence of Its Corresponding B-Subunit

Laura Heinisch [1,†], Maike Krause [1,†], Astrid Roth [1], Holger Barth [2] and Herbert Schmidt [1,*]

[1] Department of Food Microbiology and Hygiene, Institute of Food Science and Biotechnology, Garbenstraße 28, University of Hohenheim, 70599 Stuttgart, Germany; laura.heinisch@uni-hohenheim.de (L.H.); maike.krause@uni-hohenheim.de (M.K.); astrid.roth.94@web.de (A.R.)

[2] Institute of Pharmacology and Toxicology, University of Ulm Medical Center, Albert-Einstein-Allee 11, 89081 Ulm, Germany; holger.barth@uni-ulm.de

* Correspondence: herbert.schmidt@uni-hohenheim.de; Tel.: +49-711-459-22305

† Laura Heinisch and Maike Krause contributed equally to this work.

Abstract: AB_5 protein toxins are produced by certain bacterial pathogens and are composed of an enzymatically active A-subunit and a B-subunit pentamer, the latter being responsible for cell receptor recognition, cellular uptake, and transport of the A-subunit into the cytosol of eukaryotic target cells. Two members of the AB_5 toxin family were described in Shiga toxin-producing *Escherichia coli* (STEC), namely Shiga toxin (Stx) and subtilase cytotoxin (SubAB). The functional paradigm of AB toxins includes the B-subunit being mandatory for the uptake of the toxin into its target cells. Recent studies have shown that this paradigm cannot be maintained for SubAB, since SubA alone was demonstrated to intoxicate human epithelial cells in vitro. In the current study, we raised the hypothesis that this may also be true for the A-subunit of the most clinically relevant Stx-variant, Stx2a. After separate expression and purification, the recombinant Stx2a subunits StxA2a-His and StxB2a-His were applied either alone or in combination in a 1:5 molar ratio to Vero B4, HeLa, and HCT-116 cells. For all cell lines, a cytotoxic effect of StxA2a-His alone was detected. Competition experiments with Stx and SubAB subunits in combination revealed that the intoxication of StxA2a-His was reduced by addition of SubB1-His. This study showed that the enzymatic subunit StxA2a alone was active on different cells and might therefore play a yet unknown role in STEC disease development.

Keywords: Shiga toxin; Stx2a; subtilase cytotoxin; SubAB; enzyme subunit; cytotoxicity; protein purification strategies; GB_3 ELISA; Vero B4; HeLa; HCT-116

Key Contribution: We implemented recombinant protein expression and purification protocols for the A- and B-subunits of the AB_5 toxin Shiga toxin 2a (Stx2a) and showed, for the first time, that the A-subunit of Stx2a alone can exhibit a cytotoxic effect on different eukaryotic cell cultures independently of its B-subunit.

Citation: Heinisch, L.; Krause, M.; Roth, A.; Barth, H.; Schmidt, H. Cytotoxic Effects of Recombinant StxA2-His in the Absence of Its Corresponding B-Subunit. *Toxins* **2021**, *13*, 307. https://doi.org/10.3390/toxins13050307

Received: 12 March 2021
Accepted: 23 April 2021
Published: 26 April 2021

1. Introduction

Particular Shiga toxin (Stx)-producing *Escherichia coli* (STEC) strains produce, in addition to Stx, another AB_5 toxin, the subtilase cytotoxin (SubAB) [1,2]. AB_5 toxins consist of a catalytic A-subunit and five receptor-binding B-subunits, which form a homopentamer [2]. The production of one or more Stx variants is a major pathogenicity factor of enterohemorrhagic *E. coli* (EHEC). EHEC comprise a STEC subgroup being able to cause gastrointestinal diseases and extraintestinal sequelae such as the life-threatening hemolytic-uremic syndrome (HUS) [3].

Stx belongs to the family of ribosome-inactivating proteins (RIPs) (reviewed in [4]). The A-subunit StxA causes an irreversible removal of an adenine residue from the 28S rRNA in eukaryotic cells [5]. Due to this rRNA *N*-glycosidase activity, protein synthesis is

inhibited and apoptosis of the affected cell is initiated [6]. The 32 kD A-subunit is a single polypeptide chain that consists of the two domains A1 and A2, which are inter-connected by a disulfide bond. The 27.5 kD A1-domain exhibits the catalytic activity, whereas the 4.5 kD A2-domain consists of an α-helix, which connects the A-subunit to the B-subunit [1]. The StxB-subunit has a molecular weight of 7.7 kD per monomer [1] and binds mainly to the glycosphingolipid receptor globotriaosylceramide (Gb_3 or CD77) on the host cell surfaces [4,7,8]. Following receptor recognition, Stx is taken up by endocytosis and transported retrogradely to the Golgi apparatus and subsequently to the endoplasmic reticulum (ER). After processing in the endoplasmic reticulum, the StxA1-domain is translocated into the cytosol to reach the ribosomes (reviewed in [9]).

Stx comprise a family of structurally related toxins, including the two major groups Stx1 and Stx2, each of which is represented by multiple genetic variants. All known Stx variants are encoded in a single operon consisting of *stxA* and *stxB* genes, which are located in lambdoid prophages in the STEC genome [9,10]. Among these, Stx2a is most frequently associated with the development of HUS [11].

The similarly structured subtilase cytotoxin (SubAB) was originally identified in the *E. coli* O113:H21 strain 98NK2, which was isolated from a patient suffering from HUS [12]. The catalytic SubA-subunit is a serine protease which cleaves specifically the ER chaperone BiP/GRP78 [13]. This cleavage leads to an unfolded protein response and eventually apoptosis of target cells [14]. The SubB-subunits bind to the receptor *N*-glycolylneuraminic acid (Neu5Gc) [15], but recent studies indicated other *N*- and *O*-glycans as further target structures for SubB [16]. The SubA-subunit has a molecular weight of approximately 33 kD, whereas SubB has a molecular weight of approximately 14 kD per monomer [17]. Four different genetic variants have been identified for SubAB to date [12,18,19], but more variant genes have been suggested in recent years [20].

Studies on bacterial AB_5 toxins have demonstrated that the preassembly of the A- and B-subunits to toxin complexes is not essential for cytotoxicity and that the A-subunit alone can exhibit cytotoxic effects [17,21,22]. Funk et al. [22] previously demonstrated such a cytotoxic effect for SubA in Vero B4 cells. Moreover, Pellino et al. [21] have shown that the A and B_5 preassembly of AB_5 toxins, by the example of Stx2a, is not required for the in vivo toxicity in mice.

Genes for both, *stx* and *subAB*, can be present in the chromosomes of particular foodborne STEC strains. One of these is *E. coli* O113:H21 strain TS18/08, which was isolated in a previous study [23]. It harbors the stx_{2a} genes as well as the plasmid-located $subAB_1$ genes [23]. Quantitative real-time PCR (qRT-PCR) experiments showed that both genes were transcribed similarly during laboratory cultivation of this strain, having their transcription optimum after three hours of cultivation [24]. Furthermore, additional qRT-PCR data indicated the role of the global regulators Hfq and H-NS in the regulation of both stx_{2a} and $subAB_1$ [25].

Bowman et al. [26] demonstrated that hybrid formation of the A-subunit of cholera toxin and the B-subunit of *E. coli* heat-labile toxin is possible. Hybrid toxin formation might have implications for co-infections with different AB_5 toxin producing strains or infection with strains expressing different AB_5 toxins in parallel.

In the current study, we hypothesize that the A-subunit of Stx2a alone can intoxicate eukaryotic cells without the corresponding B-subunit. Therefore, separate purification protocols for recombinantly expressed StxA2a-His and StxB2a-His subunits were developed, since common purification strategies mainly focus on the purification of the holotoxin or the separated B-subunit [27–30]. After identification of the purified subunits by mass spectrometry, the secondary structure and oligomerization of the separate subunits were analyzed using circular dichroism (CD) spectroscopy and size exclusion chromatography, respectively. Separately purified subunits were analyzed alone or in combination in cytotoxicity assays with Vero B4, HeLa, and HCT-116 cells.

Since *subAB* genes have frequently been found in *stx*-positive, *eae*-negative STEC strains, an interaction of both AB_5 toxin subunits is hypothesized. Therefore, we inves-

tigated whether SubA/StxB or SubB/StxA hybrid toxins may be formed. Consequently, recombinants of Stx2a and SubAB1 subunits were used to identify their collaborative cytotoxic potential in cell culture assays. This study aims to give further insight to the cytotoxic activity of Stx2a, unbiased from the paradigm of B-subunit receptor-mediated uptake of the AB_5 toxin.

2. Results

2.1. Purification of Stx2a-His Subunits

The genes $stxA_{2a}$ and $stxB_{2a}$ were cloned separately in expression vector pET22b(+) as described in the Materials and Methods section. After confirmation of the correct sequence of the recombinant plasmids by Sanger sequencing, expression tests in *E. coli* BL21 (DE3), C41 (DE3), and C43 (DE3) in ZYM-5052, 2YT, and LB broth were performed using different temperatures and incubation times (data not shown). For StxA2a-His, the expression in *E. coli* C43 and auto-induction medium at 37 °C initial growth and 20 °C incubation overnight resulted in the highest protein levels in the soluble fraction of the bacterial cell. After cell lysis, StxA2a-His could be purified using a HisTrap™ column followed by a gel filtration step as described below.

In contrast, StxB2a-His revealed the highest amount of protein in the culture supernatant when expressed with *E. coli* C41 cultivated in LB broth at initially 37 °C, and 20 °C overnight. After concentration of the culture supernatant, the B-subunit was captured on a HisTrap™ column in the first step and after elution further purified on a Superdex® 75 pg column. A schematic procedure of the expression and purification of the subunits is given in Figure 1A,B.

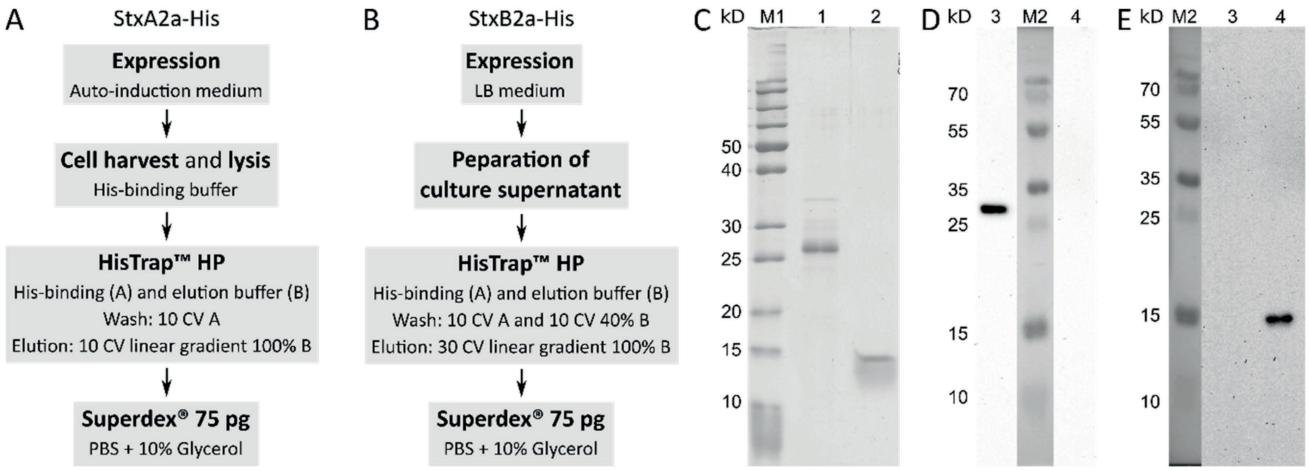

Figure 1. The purification procedures for Stx2a A- and B-subunits are schematically given in (**A**) (StxA2a-His) and (**B**) (StxB2a-His). Gradient elutions are given in column volume (CV). If not otherwise stated, isocratic elutions were applied. Both purifications lead to preparations which show single protein bands in SDS-PAGE, as representatively shown in (**C**). (**C**) PageRuler™ Unstained Protein Ladder (M1; Thermo Fisher Scientific™), 1 µg of StxA2a-His (lane 1), and 1 µg StxB2a-His (lane 2) were applied to 12.5% (*v*/*v*) SDS-PAGE run under reducing conductions. Western blots, given in (**D**,**E**), detected with subunit-specific peptide antibodies Anti-StxA2 and Anti-StxB2, resulted in one band for each purification corresponding to the results of the SDS-PAGE. A total of 500 ng of StxA2a-His (lane 3) and StxB2a-His (lane 4) were subjected to western blot analyses. PageRuler™ Plus Prestained Protein Ladder was used as marker (M2; Thermo Fisher Scientific™).

Representative pools of the protein purification products were applied to a 12.5% (*v*/*v*) SDS-PAGE and are shown in Figure 1C. StxB2a-His preparation was homogenous. StxA2a-His showed some impurities between 30 and 35 kD, which could be identified as *E. coli* proteins. For StxA2a-His and StxB2a-His, one dominant band is visible at approximately 25 kD and close to 15 kD, respectively. The theoretic size of StxA2a-His is 36.8 kD and that of monomeric StxB2a-His is 10.9 kD.

To ensure the purification of the right proteins, preparations of both subunits were submitted to in-gel trypsin digestion (see below). Tryptic peptides were analyzed by Nano-LC-ESI-MS/MS. The obtained spectra of peptides were compared to the protein sequence data base from Uniprot (https://www.Uniprot.org accessed on 1 September 2019) of *E. coli* K12, which was extended by adding Stx2a reference sequences for the A- and B-subunit (StxA2a: NC_002695.1 and StxB2a: NC_002695.1). Both subunits were clearly identified in their respective samples with a total sequence coverage of 63.1% for StxA2a-His and 86.5% for StxB2a-His, respectively. The sequence coverage of both subunits with identified tryptic peptides is depicted in Figure S1. As described above, the StxA2a-His preparation ran at a rather small size of 25 kD compared to expected 36.8 kD on the SDS-PAGE. Although this behavior was unexpected, peptides of all domains of the A-subunit were detected in comparable amounts by mass spectrometry analysis. These findings proved that the subunits were completely expressed and purified, and no degradation of the protein was responsible for the smaller size observed on SDS-PAGE. The observed size of StxB2a-His in the SDS-PAGE is consistent with the literature [28].

2.2. Biochemical Characterization of Stx2a Subunits

The folding of the purified proteins was assessed by their secondary structure composition. To determine these, samples of the separated Stx2a subunits were evaluated by CD spectroscopy in the far-UV range. Spectra between 260 and 195 nm were recorded and are shown in Figure 2A with the black and grey curves representing StxA2a-His and StxB2a-His, respectively. Based on the crystal structure of Stx2a, the A-subunit should consist of mainly α-helices and have only a minor amount of β-sheets [1]. This is well represented in the far-UV spectrum (see Figure 2A, black curve) with minima at 208 and 220 nm, which are typical for α-helical proteins. The B-subunit of Stx2a, in contrast, contains a large amount of β-sheets. This was also reflected in the CD spectrum (see Figure 2A, grey curve). Here, a minimum at approximately 222 nm and a maximum at 190 nm were expected, due to the rise of the curve towards smaller wavelengths. The quite broad minimum of the StxB2a-His curve also indicates that some part consists of α-helices. Both subunits denatured irreversibly between 50 and 60 °C when heated to 95 °C in temperature transition experiments, obtained by measuring the changes in the CD signal at 218 nm for StxA2a-His and StxB2a-His, respectively (see Figure S3).

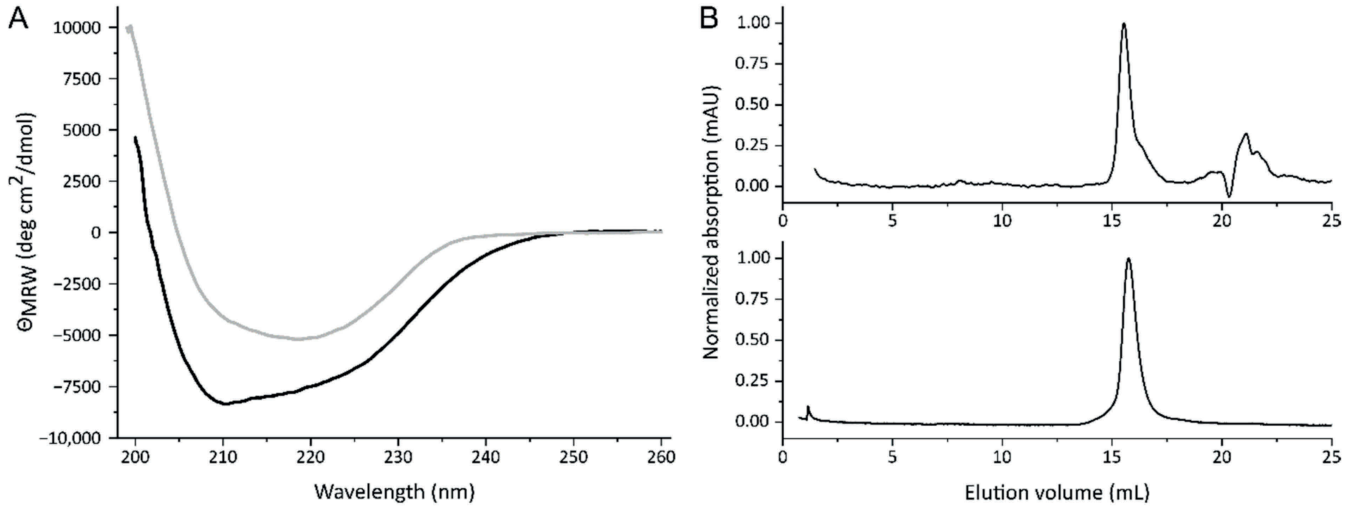

Figure 2. Far-UV spectra (**A**) of StxA2a-His (black curve) and StxB2a-His (grey curve) and size exclusion chromatography (**B**) of StxA2a-His (upper panel) and StxB2a-His (lower panel). All CD and SEC measurements were performed in PBS and with 200 µg/mL samples.

Figure 2B shows the typical elution profiles of the separated Stx2a subunits on a Superdex® 200 increase column running in PBS, whereas 100 µL samples of 200 µg/mL

were analyzed. Both subunits eluted as one single peak. Based on the calibration of the column (see Figure S3) 36.3 ± 0.3 kD and 32.5 ± 0.6 kD were calculated for StxA2a-His and StxB2a-His, respectively. Compared to the size indicated by SDS-PAGE (see Figure 1C), StxA2a-His revealed the expected molecular weight in the SEC experiments. In contrast, StxB2a-His revealed a much smaller molecular weight than expected. The theoretic molecular weight of a StxB2a-His pentamer should be approximately 53.6 kD, so StxB2a-His appeared smaller in the SEC analyses. To ensure that the B-subunit had a stable oligomerization, samples of 400 and 600 µg/mL were analyzed in addition. No concentration dependent increase in the molecular weight was detectable, indicating that the oligomerization of the B-subunit was stable.

To ensure that StxB2a-His was functional in the cytotoxicity assays, a modified Gb_3 enzyme-linked immunosorbent assay (ELISA) based on Zumbrun et al. [31] was performed. Figure 3 shows the absorption at 450 nm obtained by evaluating the binding of StxB2a-His, StxA2a-His, and a combination of both subunits in a 1:5 molar ratio to decreasing amounts of Gb_3. This mixture of StxA2a-His and StxB2a-His is designated as StxAB2a-His in the following text. Murine ER chaperone BiP/GRP78 (mBiP) labeled with a His-tag was used as negative control for the detection with anti-His antibody. Less bound StxB2a-His and StxAB2a-His were detected with decreasing amounts of Gb_3. These results are consistent with previously published data [31]. They prove that StxB2a-His alone is basically functional, and that StxA2a-His alone is not able to bind Gb_3.

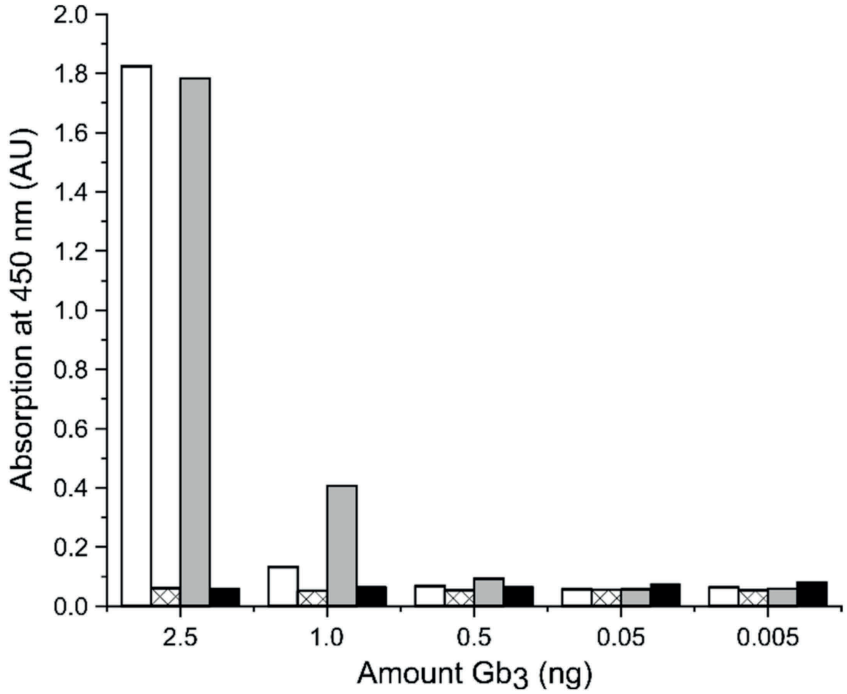

Figure 3. Representative result of the binding of StxB2a-His (white bars), StxA2a-His (crossed bars), and StxAB2a-His (light grey bars) to Gb_3, detected by ELISA. Wells were coated with different amounts of Gb_3. A negative control His-tag labeled mBiP was used (black bars). Binding to Gb_3 was detected at 450 nm through tetramethylbenzidine (TMB) turnover.

2.3. Cytotoxic Effect of StxA2a-His on Different Cell Cultures in the Absence of the B-Subunit

To identify in vitro cytotoxic effects of the recombinant A-subunit of Stx2a, each purified subunit, alone or in combination, was applied to different cell cultures. As a control, Dulbecco's phosphate-buffered saline (DPBS) instead of the toxin solutions was used. After 48 h of intoxication, the amount of attached cells was analyzed by crystal violet staining. Staining intensity was transformed to cell viability using the values of the

DPBS-treated samples as 100% viability. Figure 4 shows the cytotoxic effect of StxA2a-His on HeLa, Vero B4, and HCT-116 cells.

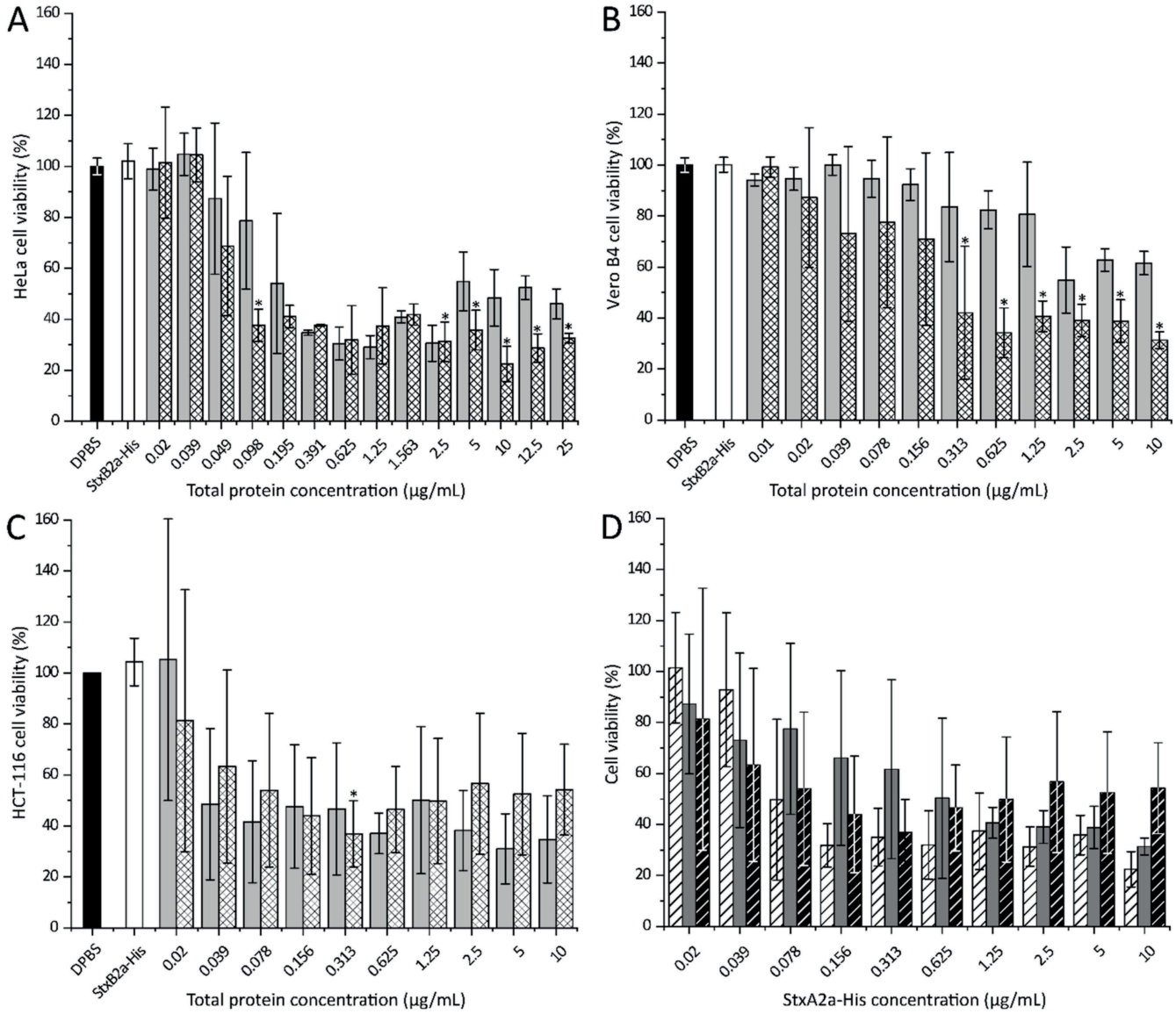

Figure 4. Cytotoxic effects of StxA2a-His on HeLa (**A**), Vero B4 (**B**), and HCT-116 (**C**) cells. Cell viabilities after intoxication with Dulbecco's phosphate-buffered saline (DPBS, control, black bars), StxB2a-His (white bars), StxA2a-His in a molar ratio of 1:5 with StxB2a-His (StxAB2a-His, light grey bars), and StxA2a-His (crossed bars) are shown. Data of at least three biological replicates are depicted. Cell viability is shown in correlation to total protein concentration and values of DPBS, and StxB2a-His are mean values of all dilutions measured. Comparison of cell viability in presence of StxA2a-His between cell cultures is depicted in (**D**), whereas data of HeLa (dashed white bars), Vero B4 (dark grey bars), and HCT-116 cells (dashed black bars) are shown. Data of at least three biological replicates are depicted. Error bars represent standard deviations, asterisks (*) indicate statistical significance of $p < 0.05$ between StxA2a-His and StxAB2a-His at each toxin concentration for panel (**A**) to (**C**).

As depicted in Figure 4A, the cytotoxic effect of StxA2a-His on HeLa cells (crossed bars) was comparable in strength to the effect observed for the combined subunits (StxAB2a-His, light grey bars) at low total protein concentrations. With increasing total protein concentration, the HeLa cell viability decreased to a minimum of 22 ± 6% when 10 µg/mL StxA2a-His was applied. A significant reduction in cell viability was shown when cells were incubated with StxA2a-His in comparison to cells incubated with StxAB2a-His. As control,

StxB2a-His was applied to the cells (white bars), which resulted in no cytotoxic effect after 48 h incubation. Cells treated with 0.02 to 25 µg/mL StxB2a-His showed a comparable amount of attached cells to the control cells (DPBS treated cells, black bars). Independent of the StxB2a-His concentration applied, 100% viable HeLa cells were observed (see Figure S4).

In order to show that the effects of the subunits of Stx2a were not cell-type dependent, the same experiments were performed with Vero B4 and HCT-116 cells (see Figure 4B,C).

A combination of both subunits (StxAB2a-His, light grey bars) showed a cytotoxic effect in a concentration-dependent manner in Vero B4 cells (see Figure 4B). The same effect was observed when StxA2a-His was applied separately (crossed bars), but in this case the cytotoxic effect was more prominent compared to the observations obtained for HeLa cells. At a concentration of 10 µg/mL of StxA2a-His, 31 $\pm$ 3% of viable cells was determined. Significant differences in the cytotoxic effect of StxA2a-His compared to StxAB2a-His were observed at concentrations higher than 0.313 µg/mL. Similarly, the progression of the cytotoxic activity curve on HCT-116 (see Figure 4C) shows effects of StxA2a-His and StxAB2a-His. For this cell line, StxA2a-His showed comparable cytotoxic activity to StxAB2a-His and no statistical significance was given. Comparable to the effects observed on HeLa cells, application of StxB2a-His or DPBS to the cells resulted in no effects on the viability of the Vero B4 and HCT-116 cells.

The significantly higher cytotoxic effects of StxA2a-His in comparison to StxAB2a-His on HeLa and Vero B4 cells, normalized to the total protein concentration, should be interpreted with caution (see Figure 4A,B). Since StxA2a-His and StxB2a-His were combined in a 1:5 molar ratio, the concentration of the A-subunit was smaller than in those samples containing StxA2a-His alone. For example, this resulted in 4.03 µg/mL StxA2a-His in the 10 µg/mL total protein concentration of StxAB2a-His. If the cell viability data was normalized to the StxA2a-His concentration, no significant difference in the progress of cytotoxicity was observed between StxA2a-His and StxAB2a-His for all cell lines (see Figure S5). The cytotoxic effect of StxA2a-His alone or in combination with StxB2a-His (StxAB2a-His) showed similar effects on the cell viability of HeLa and HCT-116 cells. Similar cytotoxic effects were observed at lower StxA2a-His concentrations on Vero B4 cells. Higher cytotoxic effects of StxA2a-His without its B-subunit on Vero B4 cells at values of 1.0 to 10 µg/mL StxA2a-His concentration were shown. Similar StxA2a-His concentrations in the StxAB2a-His holotoxin resulted in an increased viability of Vero B4 cells. This effect was not observed for HeLa or HCT-116 cells (Figure 4). The normalization to StxA2a-His concentration verifies the assumption that similar cytotoxic effects were observed for StxA2a-His in the presence or absence of its B-subunit (see Figure S5).

By comparing the cytotoxic effect of StxA2a-His on different cell cultures, a concentration-dependent decrease in cell viability was observed for all cell lines (see Figure 4D). At concentrations of 630 ng/mL StxA2a-His, all cell lines showed a decreased viability by more than 50%. Whereas HeLa (see Figure 4D, dashed white bars) and Vero B4 (see Figure 4D, dark grey bars) showed the minimum cell viability at 10 µg/mL StxA2a-His, the minimum cell viability for HCT-116 cells (see Figure 4D, dashed black bars) was reached already at a toxin concentration of 310 ng/mL StxA2a-His. No significant difference of the cytotoxic activity of StxA2a-His among the cell lines could be detected, which indicates that the cytotoxic effect of StxA2a-His was not dependent on the cell lines tested in this study.

To visualize possible differences between the cytotoxic effect of StxA2a-His alone or in combination with StxB2a-His, microscopic analysis was conducted. As shown in Figure 5, no difference in the treatment of HeLa cells with DPBS or StxB2a-His was observed. The cells showed a fibroblast-like morphology with elongated shape. This observation reflects the effects from the cytotoxicity assays.

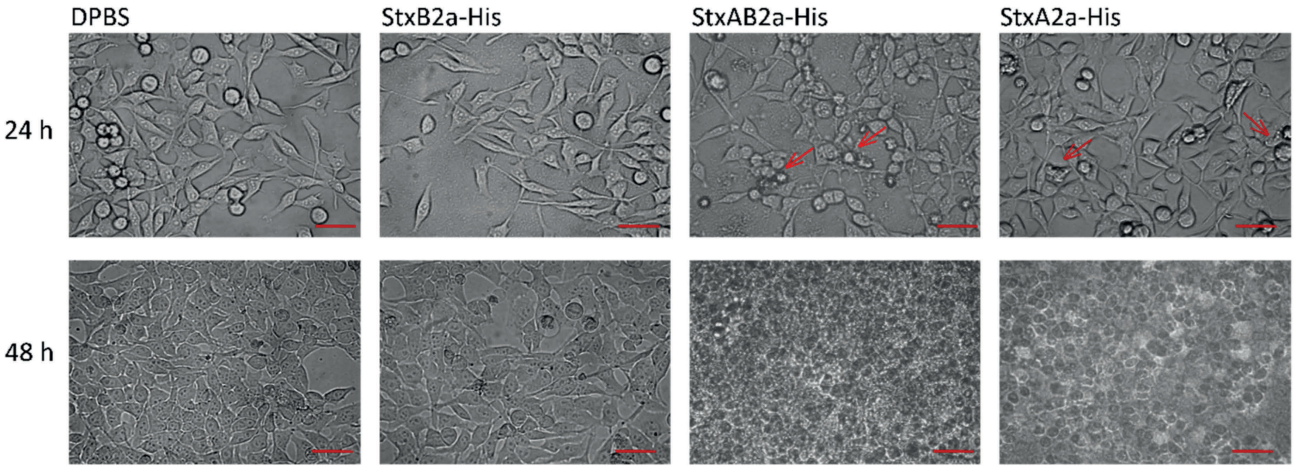

Figure 5. Microscopic analysis of cytotoxic effect of StxA2a-His on HeLa cells. Cells grown in 8-well Nunc permanox chambers and incubated with Dulbecco's phosphate-buffered saline (DPBS, control), StxB2a-His and StxA2a-His in a molar ratio of 1:5 with StxB2a-His (StxAB2a-His), and StxA2a-His are shown after 24 and 48 h incubation at 37 °C, 5.0% CO_2. One data set of three biological replicates is shown representatively. Red arrows indicate changes in cell morphology. Scale bar: 50 µm.

After 24 h, a changed morphology of cells, such as rounding and irregular shapes, was detected in StxA2a-His- and StxAB2a-His-treated cells (see Figure 5, red arrows). Rounding of the cells resulted in detachment, which can be seen in the results of the cytotoxicity assay by the reduced cell viability. After 48 h, complete lysis of cells was observed in the treated samples. Those effects depicted for HeLa cells were representative for all cell cultures (see Figure S6).

These results show that the cytotoxic effect of StxA2a-His in the absence of its B-subunit can be detected in cell morphology and is consistent with the results described for the crystal violet staining assay of the holotoxin of StxA2a-His and StxB2a-His.

2.4. Cytotoxic Effect of StxA2a-His Is Reduced in Presence of SubB1-His

We were further interested in the question of whether hybrid toxins can be formed by the two AB_5 toxins present in STEC. Thus, combinations of StxA2a-His and SubB1-His or SubA1-His and StxB2a-His were investigated for their cytotoxic potential. In Figure 6, the effect of combined Stx2a- and SubAB1-subunits on HeLa (upper panels) and HCT-116 cells (lower panels) is depicted.

The cell viability of HeLa and HCT-116 cells was reduced with increasing StxA2a-His concentration (see Figure 6A,C, white squares) as described above. When samples of StxA2a-His/SubB1-His hybrids were applied to the cells, the cytotoxic effect was significantly reduced compared to the effects measured for StxA2a-His alone. The HeLa cells treated with StxA2a-His/SubB1-His showed only a slight increase in cell viability, showing 122 ± 28% at a total protein concentration of 1 µg/mL. In contrast, intoxication with 1 µg/mL StxA2a-His resulted in 57 ± 2% cell viability (see Figure 6A). The same effect was observed for HCT-116 cells (see Figure 6C). The combination of StxA2a-His with SubB1-His resulted in a reduced cytotoxic effect compared to the cells treated only with StxA2a-His. Incubation with SubA1-His resulted in diminished HeLa cell viability in a concentration-dependent manner. In contrast to the results gained for StxA2a-His in combination with SubB1-His, the addition of StxB2a-His showed no effect on the reduction in the cell viability compared to the treatment with SubA1-His alone (see Figure 6B). In HeLa cells the cytotoxic effect of SubA1-His/StxB2a-His resulted in 36 ± 8% cell viability, whereas SubA1-His alone lead to 32 ± 14% viability at a total protein concentration of 10 µg/mL. No statistically significant difference was given, if SubA1-His was applied separately or in combination with StxB2a-His. The results correlate with the results obtained for HCT-116 cells (see Figure 6D).

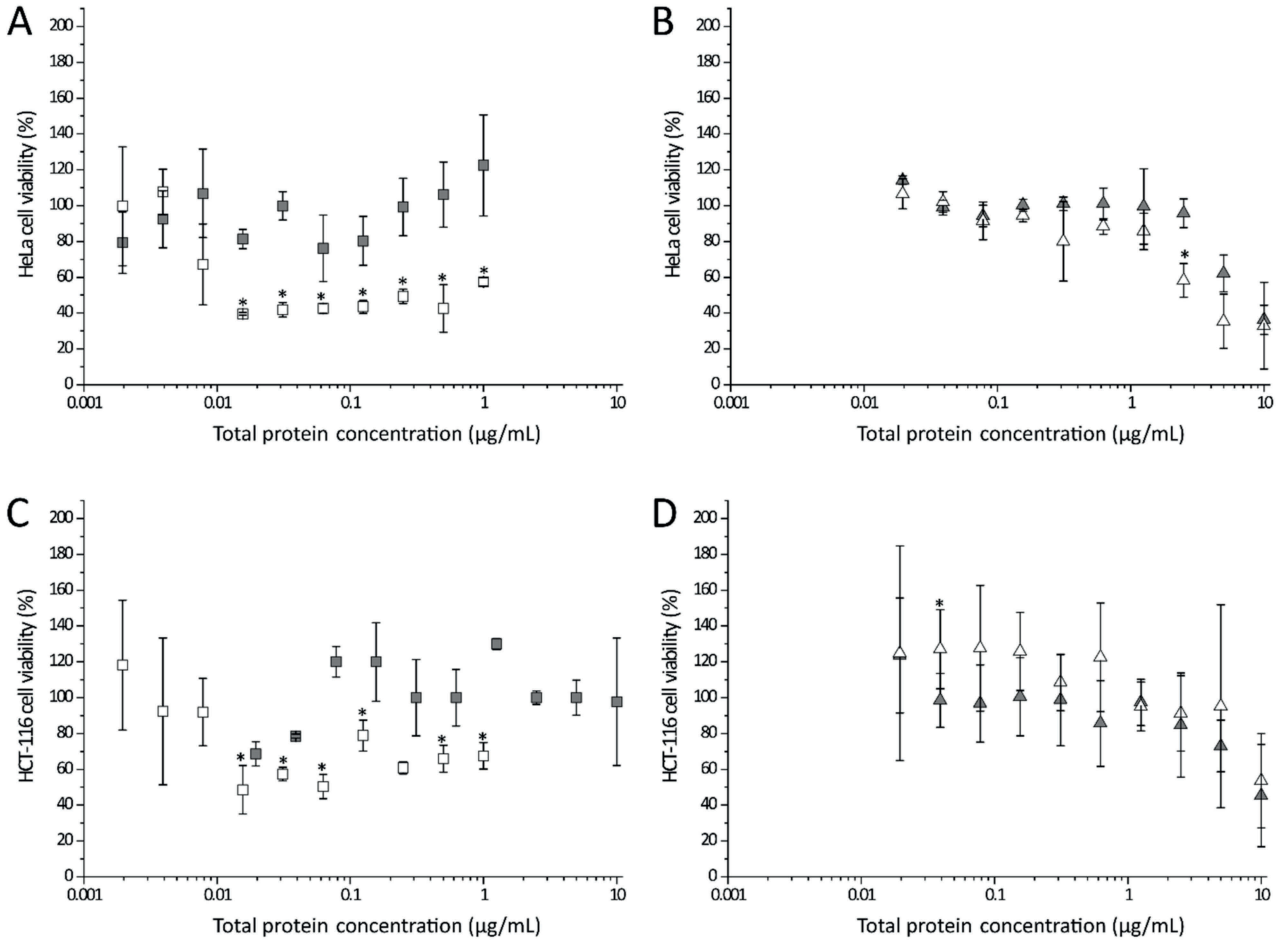

Figure 6. Cytotoxic effect of Stx2a/SubAB1 hybrids on HeLa (upper panels, **A** and **B**) and HCT-116 cells (lower panels, **C** and **D**). Effects of hybrid combination of StxA2a-His and SubB1-His (grey squares, **A** and **C**) or SubA1-His and StxB2a-His (grey triangles, **B** and **D**) in a molar ratio of 1:5 were compared to effects induced by respective A-subunits of Stx2a (white squares) and SubA1 (white triangles). Cells were incubated with StxA2a-His containing samples for 48 h and incubated with SubA1-His containing samples for 72 h. Data of three biological replicates are depicted, error bars show standard deviations, and asterisks (*) indicate statistical significance if $p < 0.05$ between StxA2a-His and StxA2a-His in combination with SubB1-His (panel **A** and **C**) or between SubA1-His and SubA1-His in combination with StxB2a-His (panel **B** and **D**) for each total protein concentration.

3. Discussion

In this study, we present a new His-tag-based purification approach for separately cloned and expressed Stx2a subunits. This approach allows a fast purification and has the advantage that a cross-contamination of the A- with the B-subunit and vice versa is excluded. The purified A-subunit showed one dominant band and the B-subunit revealed a single band in SDS-PAGE analysis after purification with Ni-NTA and gel filtration. Those bands were clearly identified by mass spectrometry analyses as StxA2a-His and StxB2a-His, respectively. Western blots with subunit-specific peptide antibodies proved that the A- and B-subunits were exclusively detectable in its corresponding preparation. No signal for the respective adversatively subunit was detected (see Figure 1D,E). The folding and oligomerization were investigated by CD spectroscopy and SEC. StxA2a-His and StxB2a-His revealed the expected composition in the secondary structure (see Figure 2). Fraser et al. [1] crystalized Stx from *S. dysenteriae* and showed that the A-subunit was mainly composed of α-helices. Based on this study, the B-subunit consists of six β-sheets and one α-helix. In the current study, CD spectra indicating a high number of

α-helices and β-sheets were detected for Stx2a-His and StxB2a-His, respectively, and were comparable to CD spectra published for Stx2a and StxB2a [30,32].

Determination of the molecular weight revealed the expected 36 kD for StxA2a-His (36.3 kD vs. theoretically 36.8 kD). Nevertheless, the observed smaller band in SDS-PAGE for the A-subunit was rather uncommon for Stx2a [33]. To ensure that the full-length of the A-subunit was applied in the following experiments, mass spectrometry was used to identify peptides of the A1- and A2-domain of StxA2a. Tryptic peptides of StxA2a-His of both domains were found in comparable amounts in all analyses performed. Other studies described a band of 25 kD in their Stx preparation as degraded A-subunit [32], which we can exclude for our preparation, based on the mass spectrometry analysis. However, we assumed that the untypical behavior of StxA2a-His in SDS-PAGE might have been due to an altered ratio of SDS-binding levels to the polypeptide chain [34], which was shown to be dependent on the amino acid sequence [35]. Such observations are in general not unknown for other proteins, but are new for the A-subunit of Stx2a [36].

Contrarily to the results of StxA2a-His, the estimated molecular weight for StxB2a-His based on the SEC analysis was rather small (32.6 kD vs. theoretically 53.6 kD). Conrady et al. [30] performed extensive studies on the oligomerization of the B-subunit for Stx1 and Stx2. They showed by analytical ultracentrifugation that the B-subunit existed in a monomer-pentamer equilibrium. Since different analyzed concentrations of StxB2a-His did not show any changes in the molecular weight of the subunit, we concluded that the oligomerization was stable. Already, other B-subunits of AB_5 toxins showed smaller molecular weight, as expected after SEC analysis [17]. This could be due to a more compact folding of the B-subunit. StxB2a-His and StxAB2a-His were able to bind Gb_3, which was shown by a Gb_3 ELISA (see Figure 3), and showed a comparable behavior to that published for other Stx holotoxin preparations [31].

Purified Stx2a-subunits were used for cytotoxicity assays. In those assays, StxA2a-His, separately or in combination with StxB2a-His (StxAB2a-His), showed cytotoxic activity. The cytotoxic activity observed for the StxA2a-subunit was comparable to the cytotoxicity measured when the combined recombinant StxAB2a-holotoxin was applied to HeLa and HCT-116 cells. The overall achieved cytotoxicity for StxA2a-His and StxAB2a-His was rather low compared to values stated in the literature [37,38]. Nevertheless, control experiments with purified Stx2a holotoxin revealed comparable HeLa cell viabilities to the reconstituted StxAB2a-His holotoxin under our experimental settings. When applied to Vero B4 cells, StxA2a-His showed even higher cytotoxic effects in the absence of its B-subunit compared to the reconstituted holotoxin StxAB2a-His. StxB2a-His itself showed no cytotoxic activity at all, and the cell viability of all analyzed cell cultures was comparable to the control samples (see Figure 4). The results in this study demonstrate the effect of StxA2a-His on HeLa, Vero B4, and HCT-116 cells independent of its B-subunit. Interestingly, the cytotoxic activity of StxA2a-His did not vary between the investigated cell lines and, moreover, no difference in cytotoxic activity between StxA2a-His and StxAB2a-His was observed in HeLa and HCT-116 cells. These results were verified by microscopic analysis, whereas morphological changes in the cell structure were observed after 24 h of incubation. Both treatments with StxA2a-His alone or in combination with its B-subunit showed differences in morphology compared to cells incubated with DPBS or StxB2a-His. The morphological changes observed in the cells with StxA2a-His or StxAB2a-His could not be differentiated. Microscopic analysis verified the apoptotic effect of StxA2a-His in HeLa, Vero B4, and HCT-116 cells.

To our knowledge, the cytotoxicity of the StxA2a-subunit independent of its B-subunit is uniquely described. Thus, we recommend designating this effect as the single-A effect. Funk et al. [22] described a similar effect for SubA on HeLa cells, whereas the cytotoxicity of SubA1 was seen at higher concentrations than the combined holotoxin. Comparable to the results seen in our study, the B-subunit of the AB_5 toxin did not exhibit any cytotoxicity if applied separately to HeLa cells [22].

The results described in this study show that the A-subunit of Stx can exhibit cytotoxic activity independent of the B-subunit. This leaves the question of the mechanism of binding, uptake, and cytotoxicity of the A-subunit without the presence of the B-subunit. Studies have indicated the importance of StxA on the endocytosis process. Torgersen et al. [39] showed that endocytosis of Stx in HeLa and Vero cells, amongst others, was triggered by the surface-bound A-subunit in the holotoxin. In contrast, the binding of the B-subunit to the receptor did not induce endocytosis [39]. Besides the impact of the A-subunit in the holotoxin on endocytosis, a recent study suggested that Stx is not released as a holotoxin and AB_5 pre-assembly is formed at the cell surface [21]. Sessler et al. demonstrated that the A-subunit of AB_5 toxins, such as SubA2-2, can be taken up and transported to the endoplasmic reticulum without its B-subunit [40].

Besides the receptor-mediated endocytosis of Stx, several studies demonstrated an alternative method of uptake. It was shown that toxins could be secreted from *E. coli* O157:H7 cells in outer membrane vesicles (OMVs) [41–43]. Moreover, Bielaszewska et al. [44] showed that OMVs are formed and released at the bacterial cell membrane containing multiple virulence factors and uptake at the host cell functions via dynamin-dependent endocytosis. Inside the cell, Stx2a is separated from the OMVs in the early endosomes and is retrogradely transported to the Golgi complex and further to the endoplasmic reticulum [44]. Furthermore, Kim et al. [45] demonstrated that the StxB-subunit can be transported with OMVs in an *E. coli* O157:H7 Δ*stxA* deletion mutant, indicating that even separated subunits can be transported by this pathway. Thus, we suggest that the subunits of Stx2a, and in particular StxA2a, can be transported separately from the other subunit and even probably independent of the classical Gb_3-binding by pathways such as transport via outer membrane vesicles [45].

Experiments using hybrid combinations of recombinant subunits of Stx and SubAB showed that the cytotoxic effect of StxA2a-His on HeLa and HCT-116 cells is reduced in the presence of SubB1-His (see Figure 6). The B-subunit of SubAB is known to bind to the receptor *N*-glycolyneuraminic acid [15], but recent studies have demonstrated binding to all *N*-glycans presented on the cell surface [16]. Thus, we assume that SubB1-His may bind to the glycosylated structures blocking the target structure for StxA2a-His uptake. In contrast, SubA1-His cytotoxicity was not reduced in combination with StxB2a-His. In this study, we could reproduce the cytotoxic effect of SubA1-His described by Funk et al. [22], whereas SubA1-His exhibited a single-A cytotoxic activity on HeLa and HCT-116 cells. This effect was not reduced by the presence of StxB2a-His. It is known that StxB2a binds specifically to the glycosphingolipid globotriaosylceramide (Gb_3) [7]. Thus, if there was a specific target structure for SubA1 on the cell surface, this would not be blocked due the binding of StxB2a-His, assuming that Gb_3 is not the target structure for SubA1-His.

Several studies have indicated the importance of Gb_3 presence on Stx cytotoxicity in the absence of the receptor-mediated B-subunit. The inhibition of the ceramide glucosyltransferase leading to less Gb_3 presented on the surface of HeLa and Vero cells lead to a protection from cytotoxic effects induced by Stx1 [46]. Furthermore, it could be shown that even in cell culture free systems the binding of Stx2a to the receptor Gb_3 is needed for cytotoxicity induction. Johansson et al. [47] showed in extracellular vesicles that the presence of Gb_3 on the recipient cell is important for Stx-induced change in metabolism or protein translation. Uptake of microvesicles containing Stx2a did not induce changes in metabolism when Gb_3 was reduced on the cell surface of HeLa cells [47]. To the contrary, a study of Schüller et al. [48] demonstrated on in vitro organ culture systems that the human intestinal epithelium showed Stx2-induced damage even in the absence of Gb_3 receptors, which indicates an alternative uptake/transport mechanism for Stx2a cytotoxicity. We conclude that the uptake of StxA2a-His is mediated by a target structure presented on the cell surface which is probably not Gb_3, since binding of StxA2a-His in the Gb_3-ELISA was not observed (see Figure 3).

Although we described the cytotoxic activity, the mechanism by which StxA2a-His is taken up and transported inside the cell remains open and will be the subject of further studies.

4. Conclusions

In the present study, we developed purification strategies for both Stx2a subunits as recombinant proteins, based on affinity chromatography. By mass spectrometry, CD spectrometry, and SEC the expected biochemical characteristics of the respective subunits were analyzed. Moreover, purified subunits alone or a combination with a 1:5 molar ratio of both subunits were applied in cytotoxicity assays using HeLa, Vero B4, and HCT-116 cells. StxA2a-His exhibited a cytotoxic effect in the absence of its B-subunit, an effect that we have designated the single-A effect. This effect was independent of the cell lines investigated. Whereas this study is the first to describe a single-A effect of Stx2a, no conclusion according to the uptake mechanism or intracellular processes induced in the cell metabolism can be drawn. Further research is needed to explore the mechanisms of binding, uptake, and intracellular transport to elucidate this single-A mechanism of StxA2a further.

5. Material and Methods

5.1. Cloning and Expression Tests of Recombinant Stx2a Subunits

To clone the *stx2a* subunit genes, genomic DNA (gDNA) of *E. coli* DH5α/933W (see Table 1) was prepared. Thus, a DNeasy Blood and Tissue kit (Qiagen, Hilden, Germany) was used and gDNA was prepared as described in the protocol provided by the manufacturer using 4 mL of an overnight culture of *E. coli* DH5α/933W (DNeasy Blood and Tissue handbook, July 2006; Qiagen, Hilden, Germany). For amplification of *stxA2a* and *stxB2a*, the purified gDNA and primers StxA2a-pET22_for, StxA2a-pET22_rev, StxB2a-pET22_for, and StxB2a-pET22_rev containing restriction sites for *Nde*I and *Xho*I were used (see Table 2).

Plasmids were prepared using a QIAprep spin miniprep kit (Qiagen, Hilden, Germany) by following the manufacturer's recommendations using 2 mL of the respective overnight cultures (QIAprep miniprep handbook from July 2006; Qiagen, Hilden, Germany). Purity and concentration of nucleic acids were determined spectrophotometrically using a NanoDrop 2000 device (Thermo Fisher Scientific, Waltham, MA, USA).

Table 1. Strains and plasmids used in this study.

Strain or Plasmid	Relevant Geno- or Phenotype	Reference
E. coli DH5α	*tonA lacZ*ΔM15 *endA1 recA1 thi-1 supE44 phoA gyrA96 hsdR17* Δ*(lacZYA-argF)U169 relA1*	Invitrogen
E. coli DH5α/933W	DH5α strain carrying the Stx2a-encoding prophage 933W	This study
E. coli BL21 (DE3)	Expression strain, *dcm ompT hsdS*($r_B^- m_B^-$) *gal*	[49]
E. coli C41 (DE3)	Expression strain derived from *E. coli* BL21, T7 promoter driven expression, *lac*I operon	[50]
E. coli C43 (DE3)	Expression strain derived from *E. coli* BL21, T7 promoter driven expression, *lac*I operon	[50]
E. coli C43 (DE3)/pKR09	Expression strain expressing StxA2a-His subunit	This study
E. coli C41 (DE3)/pKR10	Expression strain expressing StxB2a-His subunit	This study
pET22b(+)	Amp^R, 6x His-tag	Novagen Inc.
pKR09	pET22b(+)-*stxA2a*, Amp^R	This study
pKR10	pET22b(+)-*stxB2a*, Amp^R	This study

Table 2. Oligonucleotide primers used in this study.

Primer Designation	Sequence (5′ to 3′)	Source
StxA2a-pET22_for	CGTGCATATGAAGTGTATATTATTTAAATGGGT	This study
StxA2a-pET22_rev	CCCCTCGAGTTTACCCGTTGTATATAA	This study
StxB2a-pET22_for	CGTGCATATGAAGAAGATGTTTATGGCGG	This study
StxB2a-pET22_rev	CCCCTCGAGGTCATTATTAAACTGCAC	This study
pET-22b-seq-for	GGGTTATGCTAGTTATTGC	This study
pET-22b-seq-rev	GCGAAATTAATACGACTCAC	This study

* underlined letters indicate restriction sites.

PCR products of *stxA2a* and *stxB2a* genes and the cloning vector pET22b(+) were digested with *Xho*I (Thermo Fisher Scientific, Waltham, MA, USA) and *Nde*I (Thermo Fisher Scientific, Waltham, MA, USA) in 2× Tango buffer (Thermo Fisher Scientific, Waltham, MA, USA). For the double digest, 1.0 µg of DNA in a total sample volume of 20 µL was incubated at 37 °C for one hour and the restriction enzymes were then inactivated at 80 °C for 20 min. Restricted samples were purified by a QIAquick PCR purification kit following the manufacturer's recommendations (QIAquick spin handbook, April 2015; Qiagen, Hilden, Germany). The *stxA2a* and *stxB2a* PCR products and the vector were ligated using a molar ratio of vector to insert of 1:5, using 10 µg vector, and T4 DNA ligase (Thermo Fisher Scientific, Waltham, MA, USA). The ligation was conducted at 22 °C for one hour. Subsequently, ligation batches were transformed to chemically competent *E. coli* DH5α as described previously [25].

To verify constructed plasmids, they were sequenced by Sanger sequencing using primers pET22-seq-for and pET22-seq-rev (see Table 2) as described earlier [51]. After confirmation of the correct insertion of the *stxA2a* and *stxB2a* genes in the pET22b(+) expression vector, plasmids were transformed to chemically competent *E. coli* C41 (DE3) or competent *E. coli* C43 (DE3) cells, respectively, as described earlier [25]. The expression plasmids for *stxA2a* and *stxB2a* were designated pKR09 and pKR10, respectively. An overview of the cloning procedure is provided in Figure 7.

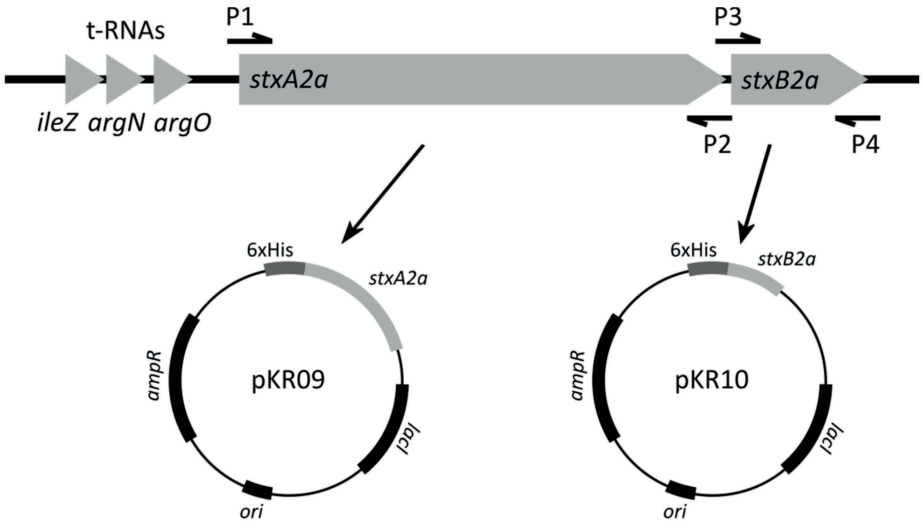

Figure 7. Schematic depiction of the principle of cloning of the stx2a subunits. In the upper part the 933W phage DNA with the binding sites of the primers is shown. P1 refers to the primer StxA2a-pET22_for, P2 to primer StxA2a-pET22_rev, P3 represents primer StxB2a-pET22_for, and P4 primer StxB2a-pET22_rev. A schema of the expression plasmids pKR09 and pKR10 are depicted in the lower row. Besides the position of C-terminal His-Tag (6xHis), the position of the ampicillin resistance gene (ampR) as well as of the lac repressor (lacI) is indicated.

Expression tests for both constructs in *E coli* BL21 (DE3), C41 (DE3), and C43 (DE3) were conducted in LB broth, 2YT broth, and auto-induction medium ZYM-5052 without trace elements as described in [52] (400 mL of ZYM-5052 consisted of 200 mL of two-fold concentrated ZY (2% [w/v] tryptone, 1% [w/v] yeast extract, pH 7.0), 8 mL of 50× M (1.25 mol/L Na_2HPO4, 1.25 mol/L KH_2PO_4, 2.5 mol/L NH_4Cl, 0.25 mol/L Na_2SO_4), 8 mL of 50× 5052 (2.5% [w/v] glycerol, 0.25% [w/v] D-(+)-glucose, 1.0% [w/v] lactose), and 0.8 mL of 1 mol/L $MgSO_4$), respectively. Initial growth temperatures of 37, 25, and 20 °C until induction and 4 h or overnight expression at 25 and 20 °C were applied to increase the subunit expression in the soluble fraction of the bacterial cell pellet or the culture supernatant.

5.2. Recombinant Expression and Purification of Toxin Subunits

The recombinant StxA2a-His subunit was expressed using *E. coli* C43 (DE3)/pKR09 in auto-induction medium ZYM-5052 without trace elements. The expression cultures were supplemented with 150 µg/mL ampicillin and inoculated 1:50 with an LB overnight culture containing 150 µg/mL ampicillin (37 °C, 180 rpm) of the expression strain. After an initial incubation at 37 °C and 180 rpm until an optical density at 600 nm (OD_{600}) of 1.3–1.5, the temperature was decreased to 20 °C and the culture further incubated for 20 h. After expression, the cells were harvested at 5000× g, 4 °C for 15 min and washed with 30 mL phosphate-buffered saline (PBS). Cell lysis was conducted by resuspending the cell pellet in His-binding buffer (50 mmol/L Tris, 300 mmol/L NaCl, pH 8.0) using 5 mL buffer per 1 g cells, the addition of 1 mg/mL lysozyme, and incubation for 1 h on ice. Cell disruption was carried out by ultrasonication using 12 cycles of ultrasonic steps for 10 s each with 20 s cooling on ice in between (Sonifier® SFX150 equipped with a microtip, Branson Ultrasonic Corporation, Danbury, CT, USA). The insoluble fraction was separated by centrifugation 25,000× g, 4 °C for 45 min (Avanti J25 centrifuge, Beckman Coulter, Brea, CA, USA). For the purification of StxA2a-His, the cleared lysate was loaded on a 5 mL HisTrap™ HP column (GE Healthcare, Chicago, IL, USA) equilibrated in His-binding buffer. To remove all unbound components, the column was washed with 6 column volumes (CV) His-binding buffer. Elution was performed with a linear gradient from 0 to 100% of elution buffer (50 mmol/L Tris, 300 mmol/L NaCl, 250 mmol/L imidazole, pH 8.0) over 12 CV. Sodium dodecyl sulphate polyacrylamide gel electrophoresis (SDS-PAGE) as described previously [53] and stained by Quickstain Coomassie® stain solution (SERVA Electrophoresis GmbH, Heidelberg, Germany), as well as western blots, were used to identify StxA2a-His containing fractions. Therefore, SDS-PAGE gels were blotted on a polyvinylidene fluoride (PVDF) immunoblot membrane (Bio-Rad Laboratories Inc., Hercules, CA, USA). Stx2a subunits were detected by synthesized specific primary peptide antibodies Anti-StxA2 and anti-StxB2 (gifted by Alexander Mellmann and Petya Berger, University of Münster, Germany), and a horseradish conjugated secondary antibody (goat anti-rabbit IgG (H+L) secondary antibody, goat/IgG; Thermo Fisher Scientific, Waltham, MA, USA). Detection was performed by chemiluminescence (ECL system) and a BioRad Chemidoc XRS+ device (Bio-Rad Laboratories Inc., Hercules, CA, USA). Positive fractions were subsequently pooled and concentrated using an Amicon Ultra Centrifugal Filter (molecular weight cut off of 3000 Da, Merck Millipore, Germany) following the manufacturer's recommendations. Remaining impurities were removed by a size exclusion chromatography step performed on a Superdex® 75 pg 16/600 (GE Healthcare, Chicago, IL, Chicago, IL, USA) in PBS supplemented with 10% (v/v) glycerol. After sample application the isocratic elution was collected in 2 mL fractions. Again, StxA2a-His-containing fractions were identified with SDS-PAGE followed by western blot and pooled. After concentration and detection of the protein concentration, StxA2a-His was aliquoted in 100 µL portions and stored at −70 °C until further usage.

The recombinant expression of StxB2a-His was conducted with *E. coli* C41 (DE3)/pKR10 in LB broth supplemented with 150 µg/mL ampicillin. A 400 mL expression culture was inoculated with an overnight culture as described above and incubated at 37 °C and

180 rpm. At an OD_{600} of 0.4 the expression was induced by the addition of 250 µmol/L isopropyl β-D-1-thiogalactopyranoside (IPTG) and the temperature subsequently reduced to 20 °C. After 20 h further incubation the cells were harvested as described above and the supernatant used for further processing. The culture supernatant was filtered with a 0.2 µm Nalgene filter (Nalgene, USA) and concentrated to less than 50 mL by cross flow using a Vivaflow200 ultrafiltration module (Sartorius Stedim Lab LTD, Winterbach, Germany). StxB2a-His was purified in a two-column approach consisting of an affinity chromatography and a size-exclusion chromatography step operated on an ÄKTA pure system. First, the concentrated supernatant was loaded on a HisTrap™ HP column. After washing of the column with 6 CV His-binding buffer, impurities were removed by a second wash step of 10 CV with 40% elution buffer. StxB2a-His was eluted with a linear gradient from 40 to 100% elution buffer in 10 CV and 3 mL fractionation. Fractions containing StxB2a-His were identified via SDS-PAGE and western blot as described above and subjected to a Superdex® 75 pg running in PBS supplemented with 10% (*v*/*v*) glycerol as described before. Pure StxB2a-His fractions were pooled, concentrated, and stored in 100 µL aliquots at −70 °C.

Purified Stx subunits were identified after tryptic digestion of protein bands excised from SDS-PAGE using Nano-LC-ESI-MS/MS performed on an Ultimate 3000 RSLCnano system (Dionex, Thermo Fisher Scientific, Waltham, MA, USA) coupled to a Q-Exactive HF-X mass spectrometer (Thermo Fisher Scientific, Waltham, MA, USA) using an EASY-Nano Flex ion source (Thermo Fisher Scientific, Waltham, MA, USA) from the mass spectrometry core facility of the University of Hohenheim.

The SubAB subunits were recombinantly expressed and purified as previously described [17].

5.3. Determination of Protein Concentration

Protein concentrations were determined spectrophotometrically using a NanoDrop® 2000 device (Thermo Fisher Scientific, Waltham, MA, USA). Therefore, absorption was measured at 280 nm and the concentrations were calculated by using the respective theoretical extinction coefficient and molecular mass ascertained by ProtParam (see Table 3). Due to the low extinction coefficient of StxA2a-His, the concentration was determined by a Bradford assay as previously described [54]. The Bio-Rad protein assay dye (Bio-Rad Laboratories Inc., Hercules, CA, USA) was used and a standard curve using bovine serum albumin (BSA, Carl Roth GmbH + Co.KG, Karlsruhe, Germany) was performed. Detection was conducted at 595 nm using a Tecan Infinite M200 device (Tecan, Männedorf, Switzerland).

Table 3. Molecular weight and extinction coefficients of toxin subunits used in this study. Parameters were calculated based on the amino acid sequence with the online tool ProtParam.

Toxin Subunit	Molecular Weight /kDa	Extinction Coefficient /$M^{-1}cm^{-1}$
StxA2a-His	36.8	33,140
StxB2a-His	10.9	13,980
SubA1-His	36.1	41,035
SubB1-His	14.0	26,930

5.4. CD Spectroscopy

Far-UV spectra were measured from 260 to 195 nm at 25 °C with 100 nm/min of continuous scanning, 0.1 nm of data pitch, 4 s of response time, 1 nm of band width, and 10 accumulations at a Jasco J715 CD Spectrometer with a PTC-348 WI Peltier Unit using default settings (Jasco, Pfungstadt, Germany). Raw data was recorded in millidegrees and the signal was converted to the mean residue ellipticity (deg·cm^2/dmol). Prior to the measurements, all samples were dialyzed in standard PBS buffer overnight and the concentration adjusted to 200 µg/mL for each sample. Denaturation curves were recorded at 220 nm for StxA2a-His and 218 nm for StxB2a-His with 1 °C/min of heating rate, 0.1 °C

of data pitch, 1 s of response time, and 1 nm of band width. Denaturation temperatures were estimated with simple logistic fits.

5.5. Size Exclusion Chromatography

For an estimation of the molecular size and oligomerization of the subunits, a Superdex® 200 increase 10/30 GL column (GE Healthcare, Chicago, IL, USA) was calibrated with two sets of calibration proteins, consisting of thyroglobulin, aldolase, ovalbumin, and ribonuclease A and ferritin, conalbumin, carbonic anhydrase, and aprotinin following the manufacture's recommendation (GE Healthcare HMW/LMW calibration kit, GE Healthcare, Chicago, IL, USA). The void volume was detected with Blue dextran. The molecular weight was calculated based on a logarithmic fit by the determination of the K_{av} value. All measurements were performed in PBS and at least thrice of protein samples with 200 µg/mL concentration.

5.6. Gb_3 ELISA

Gb_3 binding was analyzed by a modified ELISA as described by Zumbrun et al. [31]. Briefly, 2HB 96-well plates (Thermo Fisher Scientific, Waltham, MA, USA) were coated with Gb_3 (Matreya LLC, State College, PA, USA) suspended in 96% EtOH p.A. overnight and washed with 100 µL PBST (PBS, 0.05% (*v*/*v*) Tween 20) for 1 h at 4 °C. After blocking with 200 µL PBST + 3% (*w*/*v*) BSA for 2 h at 4 °C and washing twice with 150 µL PBST + 0.2% (*w*/*v*) BSA (PBST/0.2% BSA), 20 ng protein in 100 µL PBST/0.2% BSA was applied to each well and incubated for 1 h at room temperature. For the detection, each well was incubated with 100 µL 6×-His tag monoclonal antibody (His.H8, Thermo Fisher Scientific, Waltham, MA, USA) diluted 1:3000 in PBS after washing the wells thrice with 200 µL PBST/0.2% BSA. After another three times washing with 200 µL PBST/0.2% BSA, goat anti-mouse IgG (H+L) conjugated to horseradish peroxidase (Thermo Fisher Scientific, Waltham, MA, USA) was applied in a 1:2000 dilution in 100 µL PBS as secondary antibody and incubated for 1 h at room temperature. The detection was performed at 450 nm with tetramethylbenzidine (TMB) peroxidase substrate solution (Bio-Rad Laboratories Inc., Hercules, CA, USA) according to the manufacturer's recommendation. The ELISA was performed with StxA2a-His, StxB2a-His, and a 1:5 molar combination of the two subunits (StxAB2a-His). His-tag labeled murine ER-specific chaperone BiP/GRP78 (mBiP) was used as a negative control. The experiment was conducted in three independent biological replicates.

5.7. Cytotoxicity Assays

Cytotoxic activity assays were conducted as described previously [22]. Briefly, human cervix cancer-derived epithelial cell line HeLa cells, human colon carcinoma-derived HCT-116 cells (DMSZ No. ACC581), or Vero B4 cells (DMSZ No. ACC 33) were used. HeLa cells were grown in MEM medium (Gibco®, Thermo Fisher Scientific, Waltham, MA, USA) supplemented with 10% (*v*/*v*) heat-inactivated fetal calf serum (FCS), 1% (*v*/*v*) non-essential amino acid solution (Gibco®, Thermo Fisher Scientific, Waltham, MA, USA), 1% (*v*/*v*) sodium pyruvate (Thermo Fisher Scientific, Waltham, MA, USA), and 2 mmol/L glutamine (Thermo Fisher Scientific, Waltham, MA, USA). HCT-116 cells were grown in DMEM medium containing sodium pyruvate (Gibco®, Thermo Fisher Scientific, Waltham, MA, USA) supplemented with 10% (*v*/*v*) heat-inactivated fetal calf serum (FCS), 1% (*v*/*v*) non-essential amino acid solution (Gibco®, Thermo Fisher Scientific, Waltham, MA, USA), and 2 mmol/L glutamine (Thermo Fisher Scientific, Waltham, MA, USA). Vero B4 cells were cultivated in RPMI 1640 medium (Gibco®, Thermo Fisher Scientific, Waltham, MA, USA) supplemented with 10% (*v*/*v*) heat-inactivated fetal calf serum (FCS). All cultures were passaged by trypsinization and incubated at 37 °C, 5.0% CO_2. Cells were used in passages 5 to 30. For cytotoxicity assays, the cells were seeded in a 96-well chamber at a concentration of 1.0×10^4 cells/well and incubated at 37 °C, 5.0% CO_2 for 24 h. After washing of the cells, subunit solutions were applied in serial dilutions in the respective

medium. For intoxication with Stx2a-subunits, incubation times of 48 and 72 h were used when SubAB1-subunits were applied [22]. Analysis of the assay was performed using crystal violet staining and detection at 570 nm using a Tecan Infinite M200 microtiter plate reader (Tecan, Männedorf, Switzerland). All experiments were conducted in three technical replicates and three independent biological replicates. Cell viability was calculated using the optical density of the control-treated samples, incubated with Dulbecco's phosphate-buffered saline (DPBS), as 100% cell viability.

5.8. Microscopic Analysis

To investigate cytotoxic effects of the Stx2a-subunits on HeLa, Vero B4, and HCT-116 cells, Nunc® permanox 8-well chambers (Thermo Fisher Scientific, Waltham, MA, USA) were used. Cell cultures were grown and passaged as described above. For analysis, 1.0×10^4 cells/well were seeded in the 8-well chamber at a total volume of 400 µL/well. Cells were incubated at 37 °C, 5.0% CO_2 for 24 h. For intoxication, each well was washed with 400 µL DPBS and cell type-dependent fresh medium was added to the cells. Cells were incubated with 0.5 µg/mL total protein concentration and incubated further at 37 °C, 5.0% CO_2. After 24 and 48 h cells were analyzed by microscopy using an inverted microscope Axio Vert.A1 (Zeiss, Oberkochen, Germany) equipped with a color camera (Axiocam 105, Zeiss, Oberkochen, Germany). Pictures were detected using a 40×/1.25 objective (Zeiss, Oberkochen, Germany) and processed by the program ZEN light (Zeiss, Oberkochen, Germany). Experiments were conducted as two technical replicates in at least three biological replicates.

5.9. Statistical Analysis

If not stated differently, all data were analyzed using OriginPro2020 from OriginLab, USA. For statistical analysis of cytotoxic effects, data of cell viability of all biological replicates were used. Initially, data were analyzed on a normal distribution. If the data set was drawn from a normally distributed population, two data sets were compared using the two-tailed Student's *t*-test. Variances of data sets were analyzed with Students *t*-test on variances. Welch's *t*-test was applied to not-normally distributed data sets and if equal variances were not given. Effects compared between all cell cultures were analyzed using one-way analysis of variance (ANOVA) followed by post-hoc Tukey test. Statistical significance was given at values of p smaller than 0.05.

Supplementary Materials: The following are available online at https://www.mdpi.com/article/10.3390/toxins13050307/s1, Figure S1: Sequence coverage of StxA2a-His (A) and StxB2a-His (B) based on the mass spectrometry analysis, Figure S2: Thermal denaturation curves of StxA2a-His (A) and StcB2a-His (B), Figure S3: Logarithmic calibration curve for the Superdex® 200 increase column for the evaluation of the size exclusion experiments, Figure S4: Cytotoxic effect of StxB2a-His on HeLa (A), Vero B4 (B), and HCT-116 (C) cells, Figure S5: Cytotoxic effect of StxA2a-His on HeLa (A), Vero B4 (B), and HCT-116 (C) cells, Figure S6: Microscopic analysis of cytotoxic effect of StxA2a-His on HeLa, Vero B4, and HCT-116 cells.

Author Contributions: Conceptualization, L.H., M.K., H.B. and H.S.; formal analysis, L.H. and M.K.; investigation, L.H., M.K. and A.R.; writing—original draft preparation, L.H. and M.K.; writing—review and editing, L.H., M.K., H.B. and H.S.; visualization, L.H. and M.K.; project administration, M.K. and H.S.; funding acquisition, H.B. and H.S. All authors have read and agreed to the published version of the manuscript.

Funding: This research was funded by the Deutsche Forschungsgemeinschaft, grant numbers Schm 1360/11-01 and Ba2087/6-1.

Institutional Review Board Statement: Not applicable.

Informed Consent Statement: Not applicable.

Data Availability Statement: Data is contained within the article or Supplementary Materials.

Acknowledgments: We thank Annette Bruckbauer, Penelope Sander, and Markus Kranz for excellent technical assistance. We thank Andreas Mellmann and Petya Berger for the generous gift of the StxA2- and StxB2-antibody. Furthermore, we thank Andreas Kuhn for giving access to the CD spectrometer and the Core Facility from the University of Hohenheim for mass spectrometry analysis.

Conflicts of Interest: The authors declare no conflict of interest.

References

1. Fraser, M.E.; Chernaia, M.M.; Kozlov, Y.V.; James, M.N.G. Crystal structure of the holotoxin from *Shigella dysenteriae* at 2.5 A resolution. *Struct. Biol.* **1994**, *1*, 59–64. [CrossRef] [PubMed]
2. Beddoe, T.; Paton, A.W.; Le Nours, J.; Rossjohn, J.; Paton, J.C. Structure, biological functions and applications of the AB_5 toxins. *Trends Biochem. Sci.* **2010**, *35*, 411–418. [CrossRef] [PubMed]
3. Karch, H.; Tarr, P.I.; Bielaszewska, M. Enterohaemorrhagic *Escherichia coli* in human medicine. *Int. J. Med. Microbiol.* **2005**, *295*, 405–418. [CrossRef] [PubMed]
4. Hughes, A.K.; Stricklett, P.K.; Schmid, D.; Kohan, D.E. Cytotoxic effect of Shiga toxin-1 on human glomerular epithelial cells. *Kidney Int.* **2000**, *57*, 2350–2359. [CrossRef]
5. O'Brien, A.D.; LaVeck, G.D.; Thompson, M.R.; Formal, S.B. Production of *Shigella dysenteriae* Type 1-like cytotoxin by *Escherichia coli*. *J. Infect. Dis.* **1982**, *146*, 763–769. [CrossRef]
6. Obrig, T.G.; Moran, T.P.; Brownt, J.E. The mode of action of Shiga toxin on peptide elongation of eukaryotic protein synthesis. *Biochem. J.* **1987**, *244*, 287–294. [CrossRef]
7. Shin, I.S.; Ishii, S.; Shin, J.S.; Sung, K.I.; Park, B.S.; Jang, H.Y.; Kim, B.W. Globotriaosylceramide (Gb3) content in HeLa cells is correlated to Shiga toxin-induced cytotoxicity and Gb3 synthase expression. *BMB Rep.* **2009**, *42*, 310–314. [CrossRef]
8. Shimizu, T.; Sato, T.; Kawakami, S.; Ohta, T.; Noda, M.; Hamabata, T. Receptor affinity, stability and binding mode of Shiga toxins are determinants of toxicity. *Microb. Pathog.* **2007**, *43*, 88–95. [CrossRef]
9. Plunkett, G.; Rose, D.J.; Durfee, T.J.; Blattner, F.R. Sequence of Shiga toxin 2 phage 933 W from *Escherichia coli* O157:H7: Shiga toxin as a phage late-gene product. *J. Bacteriol.* **1999**, *181*, 1767–1778. [CrossRef]
10. Murphy, K.C.; Ritchie, J.M.; Waldor, M.K.; Løbner-Olesen, A.; Marinus, M.G. Dam methyltransferase is required for stable lysogeny of the Shiga toxin (Stx2)-encoding bacteriophage 933W of enterohemorrhagic *Escherichia coli* O157:H7. *J. Bacteriol.* **2008**, *190*, 438–441. [CrossRef]
11. Boerlin, P.; McEwen, S.A.; Boerlin-Petzold, F.; Wilson, J.B.; Johnson, R.P.; Gyles, C.L. Associations between virulence factors of Shiga toxin-producing *Escherichia coli* and disease in humans. *J. Clin. Microbiol.* **1999**, *37*, 497–503. [CrossRef]
12. Paton, A.W.; Srimanote, P.; Talbot, U.M.; Wang, H.; Paton, J.C. A new family of potent AB_5 cytotoxins produced by Shiga toxigenic *Escherichia coli*. *J. Exp. Med.* **2004**, *200*, 35–46. [CrossRef]
13. Paton, A.W.; Beddoe, T.; Thorpe, C.M.; Whisstock, J.C.; Wilce, M.C.J.; Rossjohn, J.; Talbot, U.M.; Paton, J.C. AB_5 subtilase cytotoxin inactivates the endoplasmic reticulum chaperone BiP. *Nature* **2006**, *443*, 548–552. [CrossRef]
14. Chong, D.C.; Paton, J.C.; Thorpe, C.M.; Paton, A.W. Clathrin-dependent trafficking of subtilase cytotoxin, a novel AB_5 toxin that targets the endoplasmic reticulum chaperone BiP. *Cell. Microbiol.* **2008**, *10*, 795–806. [CrossRef]
15. Byres, E.; Paton, A.W.; Paton, J.C.; Löfling, J.C.; Smith, D.F.; Wilce, M.C.J.; Talbot, U.M.; Chong, D.C.; Yu, H.; Huang, S.; et al. Incorporation of a non-human glycan mediates human susceptibility to a bacterial toxin. *Nature* **2008**, *456*, 648–652. [CrossRef]
16. Yamaji, T.; Hanamatsu, H.; Sekizuka, T.; Kuroda, M.; Iwasaki, N.; Ohnishi, M.; Furukawa, J.; Yahiro, K.; Hanada, K. A CRISPR screen using subtilase cytotoxin identifies SLC39A9 as a glycan-regulating factor. *iScience* **2019**, *15*, 407–420. [CrossRef]
17. Krause, M.; Sessler, K.; Kaziales, A.; Grahl, R.; Noettger, S.; Barth, H.; Schmidt, H. Variants of *Escherichia coli* subtilase cytotoxin subunits show differences in complex formation in vitro. *Toxins* **2019**, *11*, 703. [CrossRef]
18. Fierz, L.; Cernela, N.; Hauser, E.; Nüesch-Inderbinen, M.; Stephan, R. Characteristics of Shiga toxin-producing *Escherichia coli* strains isolated during 2010–2014 from human infections in Switzerland. *Front. Microbiol.* **2017**, *8*, 1471. [CrossRef]
19. Funk, J.; Stoeber, H.; Hauser, E.; Schmidt, H. Molecular analysis of subtilase cytotoxin genes of food-borne Shiga toxin-producing *Escherichia coli* reveals a new allelic *subAB* variant. *BMC Microbiol.* **2013**, *13*, 230. [CrossRef]
20. Tasara, T.; Fierz, L.; Klumpp, J.; Schmidt, H.; Stephan, R. Draft genome sequences of five Shiga toxin-producing *Escherichia coli* isolates harboring the new and recently described subtilase cytotoxin allelic variant $subAB_{2-3}$. *Genome Announc.* **2017**, *5*, e01582-16. [CrossRef]
21. Pellino, C.A.; Karve, S.S.; Pradhan, S.; Weiss, A.A. AB_5 preassembly is not required for Shiga toxin activity. *J. Bacteriol.* **2016**, *198*, 1621–1630. [CrossRef]
22. Funk, J.; Biber, N.; Schneider, M.; Hauser, E.; Enzenmüller, S.; Förtsch, C.; Barth, H.; Schmidt, H. Cytotoxic and apoptotic effects of recombinant subtilase cytotoxin variants of Shiga toxin-producing *Escherichia coli*. *Infect. Immun.* **2015**, *83*, 2338–2349. [CrossRef]
23. Slanec, T.; Fruth, A.; Creuzburg, K.; Schmidt, H. Molecular analysis of virulence profiles and Shiga toxin genes in food-borne Shiga toxin-producing *Escherichia coli*. *Appl. Environ. Microbiol.* **2009**, *75*, 6187–6197. [CrossRef] [PubMed]
24. Hauser, E.; Bruederle, M.; Reich, C.; Bruckbauer, A.; Funk, J.; Schmidt, H. Subtilase contributes to the cytotoxicity of a Shiga toxin-producing *Escherichia coli* strain encoding three different toxins. *Int. J. Food Microbiol.* **2016**, *217*, 156–161. [CrossRef]
25. Heinisch, L.; Zoric, K.; Krause, M.; Schmidt, H. Transcription of the subtilase cytotoxin gene $subAB_1$ in Shiga toxin-producing *Escherichia coli* is dependent on *hfq* and *hns*. *Appl. Environ. Microbiol.* **2019**, *85*, e01281-19. [CrossRef]

26. Bowman, C.C.; Clements, J.D. Differential biological and adjuvant activities of cholera toxin and *Escherichia coli* heat-labile enterotoxin hybrids. *Infect. Immun.* **2001**, *69*, 1528–1535. [CrossRef] [PubMed]
27. Smith, M.J.; Carvalho, H.M.; Melton-Celsa, A.R.; O'Brien, A.D. The 13C4 monoclonal antibody that neutralizes Shiga toxin type 1 (Stx1) recognizes three regions on the Stx1 B subunit and prevents Stx1 from binding to its eukaryotic receptor globotriaosylceramide. *Infect. Immun.* **2006**, *74*, 6992–6998. [CrossRef] [PubMed]
28. Smith, M.J.; Melton-Celsa, A.R.; Sinclair, J.F.; Carvalho, H.M.; Robinson, C.M.; O'Brien, A.D. Monoclonal antibody 11E10, which neutralizes Shiga toxin type 2 (Stx2), recognizes three regions on the Stx2 A subunit, blocks the enzymatic action of the toxin in vitro, and alters the overall cellular distribution of the toxin. *Infect. Immun.* **2009**, *77*, 2730–2740. [CrossRef]
29. Brandelli, J.; Griener, T.; Laing, A.; Mulvey, G.; Armstrong, G. The effects of Shiga toxin 1, 2 and their subunits on cytokine and chemokine expression by human macrophage-like THP-1 cells. *Toxins* **2015**, *7*, 4054–4066. [CrossRef]
30. Conrady, D.G.; Flagler, M.J.; Friedmann, D.R.; Vander Wielen, B.D.; Kovall, R.A.; Weiss, A.A.; Herr, A.B. Molecular basis of differential B-pentamer stability of Shiga toxins 1 and 2. *PLoS ONE* **2010**, *5*, e15153. [CrossRef]
31. Zumbrun, S.D.; Hanson, L.; Sinclair, J.F.; Freedy, J.; Melton-Celsa, A.R.; Rodriguez-Canales, J.; Hanson, J.C.; O'Brien, A.D. Human intestinal tissue and cultured colonic cells contain globotriaosylceramide synthase mRNA and the alternate Shiga toxin receptor globotetraosylceramide. *Infect. Immun.* **2010**, *78*, 4488–4499. [CrossRef]
32. Brigotti, M.; Orth-Höller, D.; Carnicelli, D.; Porcellini, E.; Galassi, E.; Tazzari, P.L.; Ricci, F.; Manoli, F.; Manet, I.; Talasz, H.; et al. The structure of the Shiga toxin 2a A-subunit dictates the interactions of the toxin with blood components. *Cell. Microbiol.* **2019**, *21*. [CrossRef]
33. He, X.; Quiñones, B.; McMahon, S.; Mandrell, R.E. A single-step purification and molecular characterization of functional Shiga toxin 2 variants from pathogenic *Escherichia coli*. *Toxins* **2012**, *4*, 487–504. [CrossRef]
34. Rath, A.; Glibowicka, M.; Nadeau, V.G.; Chen, G.; Deber, C.M. Detergent binding explains anomalous SDS-PAGE migration of membrane proteins. *Proc. Natl. Acad. Sci. USA.* **2009**, *106*, 1760–1765. [CrossRef]
35. Ibel, K.; May, R.P.; Kirschner, K.; Szadkowski, H.; Mascher, E.; Lundahl, P. Protein-decorated micelle structure of sodium-dodecylsulfate–protein complexes as determined by neutron scattering. *Eur. J. Biochem.* **1990**, *190*, 311–318. [CrossRef]
36. Melton-Celsa, A.R.; O'Brien, A.D. Shiga toxins of *Shigella dysenteriae* and *Escherichia coli*. In *Bacterial Protein Toxins*; Springer: Berlin/Heidelberg, Germany, 2000; pp. 385–406.
37. Lindgren, S.W.; Samuel, J.E.; Schmitt, C.K.; O'Brien, A.D. The specific activities of Shiga-like toxin type II (SLT-II) and SLT-II-related toxins of enterohemorrhagic *Escherichia coli* differ when measured by Vero cell cytotoxicity but not by mouse lethality. *Infect. Immun.* **1994**, *62*, 623–631. [CrossRef]
38. Tam, P.; Mahfoud, R.; Nutikka, A.; Khine, A.A.; Binnington, B.; Paroutis, P.; Lingwood, C. Differential intracellular transport and binding of verotoxin 1 and verotoxin 2 to globotriaosylceramide-containing lipid assemblies. *J. Cell. Physiol.* **2008**, *216*, 750–763. [CrossRef]
39. Torgersen, M.L.; Lauvrak, S.U.; Sandvig, K. The A-subunit of surface-bound Shiga toxin stimulates clathrin-dependent uptake of the toxin. *FEBS J.* **2005**, *272*, 4103–4113. [CrossRef]
40. Sessler, K.; Papatheodorou, P.; Wondany, F.; Krause, M.; Noettger, S.; Bernhard, D.; Michaelis, J.; Schmidt, H.; Barth, H. The enzyme subunit SubA of Shiga toxin-producing *E. coli* strains demonstrates comparable intracellular transport and cytotoxic activity as the holotoxin SubAB in HeLa and HCT116 cells in vitro. *Arch. Toxicol.* **2021**, *95*. [CrossRef]
41. Kolling, G.L.; Matthews, K.R. Export of virulence genes and Shiga toxin by membrane vesicles of *Escherichia coli* O157:H7. *Appl. Environ. Microbiol.* **1999**, *65*, 1843–1848. [CrossRef]
42. Bauwens, A.; Kunsmann, L.; Marejková, M.; Zhang, W.; Karch, H.; Bielaszewska, M.; Mellmann, A. Intrahost milieu modulates production of outer membrane vesicles, vesicle-associated Shiga toxin 2a and cytotoxicity in *Escherichia coli* O157:H7 and O104:H4. *Environ. Microbiol. Rep.* **2017**, *9*, 626–634. [CrossRef] [PubMed]
43. Yokoyama, K.; Horii, T.; Yamashino, T.; Hashikawa, S.; Barua, S.; Hasegawa, T.; Watanabe, H.; Ohta, M. Production of Shiga toxin by *Escherichia coli* measured with reference to the membrane vesicle-associated toxins. *FEMS Microbiol. Lett.* **2000**, *192*, 139–144. [CrossRef] [PubMed]
44. Bielaszewska, M.; Rüter, C.; Bauwens, A.; Greune, L.; Jarosch, K.-A.; Steil, D.; Zhang, W.; He, X.; Lloubes, R.; Fruth, A.; et al. Host cell interactions of outer membrane vesicle-associated virulence factors of enterohemorrhagic *Escherichia coli* O157: Intracellular delivery, trafficking and mechanisms of cell injury. *PLoS Pathog.* **2017**, *13*, e1006159. [CrossRef] [PubMed]
45. Kim, S.-H.; Lee, S.-R.; Kim, K.-S.; Ko, A.; Kim, E.; Kim, Y.-H.; Chang, K.-T. Shiga toxin A subunit mutant of *Escherichia coli* O157:H7 releases outer membrane vesicles containing the B-pentameric complex. *FEMS Immunol. Med. Microbiol.* **2010**, *58*, 412–420. [CrossRef]
46. Smith, D.C.; Sillence, D.J.; Falguières, T.; Jarvis, R.M.; Johannes, L.; Lord, J.M.; Platt, F.M.; Roberts, L.M. The association of Shiga-like toxin with detergent resistant membranes is modulated by glucosylceramide and is an essential requirement in the endoplasmic reticulum for a cytotoxic effect. *Mol. Biol. Cell* **2006**, *17*, 1375–1387. [CrossRef]
47. Johansson, K.; Willysson, A.; Kristoffersson, A.-C.; Tontanahal, A.; Gillet, D.; Ståhl, A.; Karpman, D. Shiga toxin-bearing microvesicles exert a cytotoxic effect on recipient cells only when the cells express the toxin receptor. *Front. Cell. Infect. Microbiol.* **2020**, *10*, 1–11. [CrossRef]
48. Schüller, S.; Frankel, G.; Phillips, A.D. Interaction of Shiga toxin from *Escherichia coli* with human intestinal epithelial cell lines and explants: Stx2 induces epithelial damage in organ culture. *Cell. Microbiol.* **2004**, *6*, 289–301. [CrossRef]

49. Studier, F.W.; Moffatt, B.A. Use of bacteriophage T7 RNA polymerase to direct selective high-level expression of cloned genes. *J. Mol. Biol.* **1986**, *189*, 113–130. [CrossRef]
50. Miroux, B.; Walker, J.E. Over-production of proteins in *Escherichia coli*: Mutant hosts that allow synthesis of some membrane proteins and globular proteins at high levels. *J. Mol. Biol.* **1996**, *260*, 289–298. [CrossRef]
51. Sanger, F.; Nicklen, S.; Coulson, A.R. DNA sequencing with chain-terminating inhibitors. *Proc. Natl. Acad. Sci. USA* **1977**, *74*, 5463–5467. [CrossRef]
52. Studier, F.W. Protein production by auto-induction in high-density shaking cultures. *Protein Expr. Purif.* **2005**, *41*, 207–234. [CrossRef]
53. Laemmli, U.K. Cleavage of structural proteins during the assembly of the head of bacteriophage T4. *Nature* **1970**, *227*, 680–685. [CrossRef]
54. Bradford, M.M. A rapid and sensitive method for the quantitation of microgram quantities of protein utilizing the principle of protein-dye binding. *Anal. Biochem.* **1976**, *72*, 248–254. [CrossRef]

Chapter 4 - Discussion

This thesis focused on the AB_5 toxin production of STEC. Specifically, the regulation of new AB_5 toxin genes such as *subAB₁* and further, changing the paradigm of functionality of AB_5 toxins by the example of Stx2a were addressed. It was shown that the gene regulation of *subAB₁* is integrated in the regulatory network of Hfq and H-NS and additionally affected by the bacterial life cycle. This result was demonstrated by using luciferase reporter gene assay and quantitative-real time experiments. In both methods, an increase in activity or gene expression was measured in isogenic deletion mutants of *hfq* and *hns*. The highest promoter activity of *PsubAB₁* was measured after three hours of cultivation. Interestingly, the highest activity did not vary between the laboratory strain *E. coli* DH5α or the STEC strain TS18/08 (see chapter 2). This observation is in line with a study of Hauser et al. (125) which found that the gene regulation of *subAB₁* was showing the highest activity after three hours of cultivation. Early studies have indicated the increase in AB_5 toxin production during cultivation on the example of Stx production (126), which was confirmed by a global transcriptome analysis of *E. coli* O157:H7 during exponential and stationary growth phase. The latter showed that *stx* expression was higher in the stationary phase than in the exponential growth phase (127).

In this thesis the luciferase reporter gene assay, the functional connection between the global regulators and the amount of the *subAB₁* gene product could be addressed. Although this connection was proved, there was no information given by this assay on the interaction of Hfq and H-NS and the regulatory region of the gene of *subAB₁*. Important for the analysis of the results of promoter gene assays is the reporter gene unit consisting of the reporter gene and the *subAB₁* promoter. Because of this, the choice of the promoter is crucial for the specificity and reporter gene activity. Up to date, the exact nucleotide sequence of *subAB₁* promoter remains unknown. Therefore, a 405 bp region upstream of the *subAB₁* gene was chosen, which includes the putative promoter region identified in previous studies (82, 125). The *subAB₁* operon is co-transcribed and therefore, the choice of an upstream promoter will resemble the transcription of the whole operon. Paton et al. (82) suggested another putative promoter region upstream of the *subB₁* gene which was not addressed in this study. This promoter is of interest for future studies to investigate the effect of the separate transcription and subsequent production of the separate subunits of SubAB1. Interestingly, a previous study of Sy et al. (128) identified an internal promoter sequence for Stx1 upstream of the *stxB₁* gene (*PstxB₁*) as well. This highlights the importance of studying the separate expression of AB_5 toxin subunit genes. Besides the choice of the promoter, the reporter gene influences the assay. The luciferase catalyzes the enzymatic reaction of the supplemented substrate to emitted light (129). Thus, if the substrate is present in excess, the light corresponds to the luciferase concentration. In the case of the firefly luciferase, cofactors such as the substrate

D-luciferin, adenosine triphosphate (ATP), magnesium ions and oxygen are needed (129, 130). As the reaction was measured in living cells, the energy is taken from the metabolism which can cause bias in the reaction. This is one disadvantage of luciferase as a reporter system compared to fluorescence which is independent from substrates. Another drawback of luciferase reporter systems is that the cells need to be lysed prior to measurement (130). However, luciferase reporter systems display a reduced background interference compared to fluorescence system (131). Moreover, the higher sensitivity of luminescence over fluorescence enables better identification of specific regulation (130, 131).

As the method of the luciferase reporter gene assay itself relies on the functional connection of the proteins to the promoter, only transcriptional effects could be detected. Both Hfq and H-NS can influence transcription by interacting with AT-rich regions in the genome (114, 132). Hfq regulates transcription of different genes either by its subsidiaries sRNAs or by actively binding to the DNA, both influencing the transcription rate (133). By applying quantitative real-time PCR experiments, the effect of the global regulators Hfq and H-NS on toxin gene expression including post-transcriptional effects could be analyzed. Although, this study proved the hypothesis on the impact of global regulatory proteins, those effects may be caused by other secondary factors regulated by Hfq and H-NS. The global regulator RNA polymerase sigma factor (RpoS) is positively affected by Hfq and its subsidiaries RNAs (97, 100), as well as its translation is inhibited by H-NS (106, 134). This fact highlights the complexity of the regulatory network in which the regulation of virulence factors and toxin genes is integrated.

Strikingly, deletion of the genes of global regulators had additional effects to those described in chapter 2 that could be measured. Deletion of genes of global regulatory proteins induced a significant decrease in growth of the STEC strain TS18/08. Moreover, deletion of *hns* caused prophage induction and lysis of the bacterial cells. A decline in the growth of *E. coli* TS18/08 Δ*hns* compared to wild type STEC TS18/08 was observed during standard cultivation. Additionally, diminished recovery rate after transformation and subsequent analysis by plaque assay verified the assumption of phage induction (data not shown). Furthermore, the impact of global regulators on toxin production was investigated, hence the deletion mutant *E. coli* TS18/08 Δ*hns* was characterized by its hemolytic phenotype on blood agar plates. Growth on blood agar plates containing washed sheep erythrocytes revealed over-production of EHEC-hemolysin in *E. coli* TS18/08 Δ*hns*. This hyper-hemolytic phenotype was characteristic in comparison to the wild type TS18/08 strain or the complemented deletion mutant (see experimental part of (39)).

Studies on different pathogenic bacterial species have indicated the importance of H-NS in virulence and fitness gene regulation. H-NS can bind to regions that flank promoters of different genes and alter DNA-topology by introducing looping of the DNA (135, 136). Subsequently,

the protein H-NS affects virulence factors in pathogenic *E. coli* by interacting with horizontally acquired DNA (118, 137, 138). This interaction with AT-rich DNA has been demonstrated for other pathogenic species as well. In *Salmonella* H-NS acts as a selective silencer of AT-rich DNA (139). This repression of foreign DNA by H-NS offers a fitness advantage to wild-type *Salmonella spp*. (139, 140). Similar to that, H-NS acts mainly as a repressor of virulence genes in pathogenic *E. coli* strains (141–143). In contrast, physiological conditions such as temperature increase induce virulence gene expression in *E. coli* and *Shigella spp.* (86, 138). Being involved in regulation of virulence genes, H-NS has an impact on the pathogenicity of different bacteria. In EHEC, a deletion of *hns* gene leads to decreased survival in macrophages but to increased pathogenicity in mice (141). Analogous, deletion or mutation in *hns* lead to increased virulence of *Acinetobacter baumanii* in *Caenorhabditis elegans* (144). Moreover, naturally ocurring mutation in *hns* was shown to lead to hypervirulent *Vibrio cholera* strains (145). Additionally, H-NS is involved in the regulation of production of the cholera toxin (146). As a global regulator H-NS regulates virulence genes such as those of AB_5 in different pathogenic enteric bacteria.

Comparable to *hns*, negative regulation of virulence genes has been reported for the gene *hfq* as well (93, 147). Hfq influences the expression of many genes in pathogenic *E. coli* (93). By understanding the regulatory mechanisms of toxin or virulence gene expression, the pathogenicity of STEC can be analyzed. The importance of Stx gene induction on virulence and pathogenicity of STEC was demonstrated *in vivo* (72). On account of that, factors which cause induction of gene expression of toxin genes should be analyzed in detail due to their potential to promote pathogenicity of STEC strains. The regulatory pathways of *stx* expression have been studied widely (88, 90, 148, 149) and *stx* expression was shown to be induced during phage induction. Moreover, the Stx late phage promoter $P_{R'}$ regulates *stx* expression (70, 89). Besides this regulatory pathway, post-transcriptional regulation that includes Hfq has been identified (149). Based on Hfq binding sites, different regulatory small RNAs were identified between the lysis genes and the late phage promoter $P_{R'}$ in EHEC strain Sakai of which the sRNA StxS was shown to repress stx_1 expression (150) that is expressed from both stx_1 and stx_2 bacteriophages during the lytic cycle (128). Although StxS did not show effects on stx_2 expression, the production of Stx2a could be regulated by other Hfq-dependent sRNAs (reviewed in (149)). The interaction of Hfq and its subsidiaries RNAs on *stx* expression points out the importance of Hfq-dependent regulation on AB_5 toxins. The impact of the global regulators Hfq on virulence and fitness-associated genes in different bacterial species has been demonstrated. Hfq and its subsidiary sRNAs impact the virulence gene expression in various species including *Salmonella, Vibrio*, *Yersinia,* and pathogenic *E. coli* (104). Besides, the production of toxins such as the exotoxin of *Pseudomonas aeruginosa* (151)*, Vibrio parahaemolyticus* hemolysin (152), and the enterotoxin of *Yersinia enterocolitica* is also

regulated by Hfq (153). The RNA chaperone Hfq is involved in many virulence processes in different species, amongst others in EHEC. The exact role how Hfq is involved in regulation of gene expression of AB_5 toxins needs to be studied in more detail. As it was shown in this thesis that Hfq represses the expression of all toxins investigated, follow-up studies are needed to identify the specific Hfq-dependent sRNAs involved in *subAB* expression.

Gene expression in means of transcription and translation, and subsequent protein detection of investigated virulence factors were analyzed in this thesis by applying different methodological approaches. The effect of Hfq and H-NS in all steps of production of virulence factors were demonstrated and moreover, its influence on all investigated toxins was shown. Further research is needed to elucidate the exact pathways of regulation of the toxin genes of Stx and SubAB. Moreover, the sRNAs that play a crucial role in regulation of those factors need to be identified.

In the second part of this thesis, the functionality of AB_5 toxins was questioned. The results gained, showed the cytotoxic effect of the A-subunit of Stx2a in the absence of its B-subunit. Therefore, separate expression of subunits and a His-tag based purification strategies were established. The observed cytotoxic effect was cell-line independent and showed a comparable cytotoxic effect of StxA2a-His alone as in combination with the B-subunit (StxAB2a-His, see chapter 3). This was the first study to investigate the effects of the A-subunit in the absence of the B-subunit, whereby several studies have investigated the issue of the StxB-subunit alone (154, 155). Comparable to the previous studies, the B-subunit did not exhibit any cytotoxic effect in this study (see chapter 3). The paradigm showing that all components of AB_5 toxins are needed for cytotoxicity was initially challenged by Funk et al. (156) indicating a cytotoxic effect of SubA in absence of its B-subunit. This was further characterized by Sessler et al. (157), showing uptake and internalization of SubA to the endoplasmic reticulum following the same subcellular transport and localization as in the presence of SubB. Moreover, Pellino et al. (158) demonstrated that AB_5 preassembly is not needed for cytotoxicity.

Several studies suggested that the binding of StxB-subunit to its receptor is the first step in cytotoxic activity. The binding of StxB to its receptor Gb_3 is a highly affinity-based binding. Each monomer of the B-subunit harbors three distinct binding sites of the trisaccharide moiety of Gb_3 leading to fifteen binding sites in total of the pentamer (159, 160). Cell culture experiments demonstrated that the inhibition of Gb_3-producing ceramide glycosyltransferase protected HeLa and Vero cells from intoxication by Stx1 indicating the importance of Gb_3-mediated

uptake of Stx (161). This was supported by an *in vivo* study of Okuda et al. (162) in which resistance in mice to Stx1 and Stx2 after deletion of the gene responsible for Gb_3 synthesis was demonstrated. Moreover, incorporation of Gb_3 to deficient cell lines resulted in an increased sensitivity towards Stx cytotoxicity (163). Contrary to that, Gobert et al. (164) showed that Stx2 can bind to Gb_3-negative human intestinal epithelial T84 cells and was internalized to the epithelial cells. In the here presented work, it was shown that recombinant StxA2a-His is not able to bind to the receptor Gb_3 with an enzyme-linked immunosorbent assay (ELISA)-based approach in the absence of the B-subunit (see chapter 3). Therefore, the receptor substance on the host cell surface introducing StxA2a-His binding remains undefined. And moreover, the uptake mechanism of the StxA-subunit leading to subsequent cytotoxicity remains unsolved. Further studies need to be performed reducing Gb_3 on the cell surface as for example by using the glucosylceramide synthetase inhibitor D-threo-1-Phenyl-2-palmitoylamino-3-morpholino-1-propanol (PPMP) to define the role of Gb_3 in StxA induced cytotoxicity. On HeLa cells, it has been shown that the application of PPMP on extracellular vesicles reduced the binding of StxB to them (155).

Alternative uptake mechanisms besides the receptor-mediated pathway have been described. A study by Schüller et. al (165) compared the cytotoxic effects of Stx on Gb_3-positive or Gb_3-negative cells. The ability to endocytose and subsequently direct Stx2 to the endoplasmic reticulum was shown by T84-cells lacking Gb_3. Moreover, experiments using *in vitro* organ cultures of human intestinal epithelium showed damage caused by Stx2 in absence of Gb_3 (165). Besides the receptor mediated endocytosis of free soluble Stx by the host cell as described above, several studies have demonstrated an alternative way. They have shown that toxins are not just transported out of *E. coli* O157:H7 cells as soluble toxins, but can be integrated in outer membrane vesicles (OMVs) (166–168). Those OMVs can be formed at the bacterial membrane and contain many different virulence factors such as the EHEC-hemolysin, Cdt or Stx2a. Dynamin-dependent endocytosis of the OMVs is followed by transport to the early endosomes on which the virulence factors are subsequently transported to the other cell compartments (42). In addition, using deletion mutant *E. coli* O157:H7 Δ*stxA* it was shown that OMVs can contain subunits in absence of one subunit of the toxin proteins as well (154). A study by Sessler et al. (157) on SubAB demonstrated that the A-subunit shows similar intracellular uptake and cytotoxicity mechanism to that of the holotoxin in absence of the SubB-subunit. This study offers the first clue, that A-subunits of AB_5 toxins might exert the same extent of cytotoxicity as the holotoxin.

Pellino et al. (158) have described that upon lysogenization of the phage 933W, originating from EHEC O157:H7, Stx2a is not released as an assembled toxin. Moreover, the ratio of A- to B-subunit was determined to be 1:8, which implies that Stx AB_5 conformation is not stable.

The same study demonstrated that AB_5 preassembly is not required for toxicity of Stx2. The authors concluded from assembled and non-assembled AB_5 complexes of Stx2a *in vivo* that assembly occurs at the host cell membrane (158). As it was shown in this thesis that StxA2a can exert cytotoxic activity in the absence of bound B-subunits, this effect could contribute to the measured cytotoxic activity of the non-assembled complex. The unassembled complex might act in the same cytotoxic pathway as the StxA2a-subunit by exerting the activity independent from receptor binding. Besides the higher association with HUS for Stx2 (169), Stx1 was found to be more potent in *in vitro* studies and a stronger binding to receptor occurred. Comparable studies using the StxA1-subunit and comparing the cytotoxic effect of both Stx-variants are needed.

In this thesis, the cytotoxicity caused by StxA2a-His in the absence of its B-subunit was defined as apoptosis in the cell lines Vero B4, HeLa and HCT-116 which did not differ according to different cell type structures (see chapter 3). All cells investigated in this thesis were positive on presence of Gb_3. Besides the action of inhibiting protein synthesis, Stx has been described to induce programmed cell death, or apoptosis. In animal reservoirs of STEC such as cattle, an infection with STEC mostly remain asymptomatic (3, 170). The receptor Gb_3 is mainly absent in bovine endothelium leading to the hypothesis that the missing of Gb_3 is responsible for the asymptomatic course of STEC infection in ruminants meaning that Stx is not able to bind to its receptor und consequently inactive (171). The research presented in this thesis has proven that StxA can be active even in absence of its B-subunit and that an alternative uptake mechanism to Gb_3 might occur. Therefore, the hypothesis on asymptomatic course in cattle stated above would be neglected. If StxA can cause cytotoxic effects in the absence of the Gb_3-mediated pathway, the cause of asymptomatic disease in cattle must be different from the receptor presence. Moreover, different target cells of Stx were identified in cattle showing its immunomodulatory action in ruminants (reviewed in (172)). This indicates different mode of actions for Stx besides the glycosphingolipid-mediated uptake. Stx can interact in different pathways on different cell types. Further research needs to be conducted to compare the receptors presented on human and ruminant cell surfaces. By this, the question of how StxA is taken up inside the cell and can exhibit its cytotoxic activity can be addressed. Moreover, it remains unclear why Stx can lead to a severe disease in humans but not in animals besides the mentioned immunomodulatory actions and needs to be further elucidated.

Likewise, the question of physiological relevance needs to be addressed. If the A-subunits of AB_5 toxins can cause cytotoxicity in the absence of their respective B-subunits, how often does this occur during EHEC infection? What is the ratio of A-subunit to B-subunit production under different environmental conditions? Both stx_{2a} and $subAB_1$ subunit genes are located each on one operon respectively and thus, the subunits are transcribed parallelly. If one of the subunit

genes is deleted, how is the transcription rate of the other present subunit influenced? As described above, additional internal promoters upstream of the respective B-subunit genes were described for both *stxAB* and *subAB* (82, 128). This indicates a separate transcription rate of the B-subunit genes of AB_5 toxins in pathogenic *E. coli*. Additionally, this leads to the question on the protein concentration of each subunit and whether it is changed if the gene of one subunit is deleted or mutated. Additionally, the secretion mechanism of AB_5 toxins in the absence of one subunit needs to be taken aim at. The subunits of Stx are released upon phage induction and lysis (70, 88). This raises the question of whether one subunit is also released in the lytic cycle if the other subunit is missing. To address the open-ended questions, isogenic deletion mutants of the respective subunit genes can be prepared and subsequently analyzed on their gene expression and protein secretion. Furthermore, those deletion mutants can be used in infection assays to investigate the effect of the missing subunit. This was prepared for the STEC strain TS18/08 on the example of SubAB1-subunits (data not shown). The deletion mutant TS18/08 $\Delta subB_1$ showed similar cytotoxicity in infection assays on HeLa and Vero B4 cells compared to the wild type TS18/08. Contrary to that, the deletion mutant TS18/08 $\Delta subA_1$ did not exhibit any cytotoxic effects (data not shown). Resembling the same results as observed with the separately purified toxin subunits. This gives the first hint on the relevance of deletion mutants on AB_5 toxin subunits.

This single-A effect of StxA is important for the pathology of EHEC bacteria as strains lacking the gene for the B-subunit may be found in the environment. In the past PCR detection analysis of the presence of *stx* in environmental isolates was mainly based on the gene for the A-subunit (173) lacking the evidence on the presence of both subunits. As a result, strains which do not encode for the *stxB* could not be detected by traditional methods. Additionally, the rate at which both genes for the subunits are expressed need to be identified. Further research is needed to understand this paradigm and to investigate this effect in *stxB* deletion mutant strains.

The work presented here contributes to the research of understanding AB_5 toxins and the cytotoxicity caused by AB_5 toxins during EHEC infection. The disease caused by Stx poses a threat to human health due to the lack of therapeutic options. Moreover, the administration of antibiotics in STEC infection is counterproductive. The effect of the antibiotics leads to the SOS response and subsequent phage induction in STEC, thus Stx is produced (90). One approach in the recent years was to use Gb_3 mimicking structures to inhibit the activity of Stx by blocking receptor binding (176, 177). Taking the results obtained in this thesis into consideration, this hypothesis might be neglected. The single-A effect of StxA demonstrates that cytotoxicity can occur even in absence of the Gb_3 receptor. This effect needs to be investigated further. One possibility is that AB_5 toxins such as Stx and SubAB have parallel mechanisms of cytotoxicity.

One of them is the B-subunit mediated uptake by receptor binding and the other the single-A effect.

Current knowledge shows that *subAB* is mainly present in *stx*-positive STEC isolates, showing a connection of both toxins. Tozzoli et al. (83) have described the presence of *subAB* genes located near the *tia* genes even in *stx*-negative STEC isolates. As synergistic effects of both AB_5 toxins were suggested (82), this combination was analyzed in this thesis as well. Moreover, a recent study by Álvarez et al. (174) revealed that the co-injection of Stx2 and SubAB in mice diminished the survival of those compared to the ones treated with one toxin. This study highlights the correlation of Stx and SubAB *in vivo* and their synergistic effects in pathogenicity of EHEC (174). Additionally, it has been shown that different recombinant variants of SubAB can form heteromeric complexes between the A- and the B-subunit of different variants (175). This leaves the question if hybrid toxins can be built of Stx and SubAB subunits. In this thesis, the synergistic effects of SubAB1 and Stx2a were analyzed according to the regulation of the gene expression and functionality of the combined purified subunits. The single-A effect of SubA1-His was unaffected by the addition of the StxB2a-His subunit. Even more, the cytotoxic effects of StxA2a-His were diminished in presence of the SubB1-His subunit on HeLa and HCT-116 cells (see chapter 3). Those results indicate a receptor for StxA2a on the host cells which might be utilized by SubB1. Consequently, synergistic effects of both variants could not be verified in this study by cytotoxic activity of hybrid toxins indicating separated mode of actions for both toxins. The question why STEC possess different AB_5 toxins which are integrated in the same regulatory mechanisms remains to be solved.

In the recent years, the paradigm of AB_5 toxins included that the A-subunit exhibits the catalytic activity, and the B-subunit mediates binding to cell receptors. This thesis points out that this paradigm needs to be changed, as StxA2a showed cytotoxic effects in the absence of the B-subunit. Hence, this pathway might be independent of receptor-mediated uptake. The question of which role the receptor Gb_3 plays in Stx-mediated disease needs to be further elucidated. The binding and uptake mechanism of StxA in absence of its B-subunit and in the correlation of the glycosphingolipids presented on the host cell surface must be investigated in detail. The physiological relevance of this single-A effect needs to be studied in detail to elucidate if cytotoxic pathways of the holotoxin and the A-subunit occur at the same conditions.

Conclusion

The heterogenous group of AB_5 toxins consists of the cholera toxin, pertussis toxin, heat labile enterotoxins, Stx, and SubAB. The principal functionality is the binding to receptors of the pentameric B-subunit which is non covalently linked to the catalytic activity of the A-subunit. Studies vary between the definition where the complexes of the AB_5 bacterial toxins are formed but point out that this is the crucial point for cytotoxic activity. Previous studies on the cytotoxic effects of the SubA-subunit (156, 157) and results of this thesis challenge this paradigm. Both AB_5 toxins of *E. coli* demonstrate a single-A effect showing cytotoxic effects of the A-subunit in the absence of its corresponding B-subunit. Research is needed to elucidate the cytotoxic effects of the A-subunits of AB_5 toxins, and their uptake mechanism compared to the mechanisms introduced by the holotoxin. Moreover, this thesis emphasized the effect of global regulatory proteins on toxin gene expression of STEC. Induction of toxin gene expression leads to increased pathogenicity of STEC. It was shown that Stx2a, SubAB1, Cdt-V, and the EHEC-hemolysin were regulated by Hfq and/ or H-NS. In addition, all toxins investigated were integrated in the regulatory pathway of bacterial life cycle. This indicates the expression of virulence factors of STEC is not only regulated by adaptation to environmental stimuli. Further research is needed to investigate the connection of STEC virulence toxins, their regulatory pathways, and the importance on STEC pathogenicity.

References

In the following the references of Chapter 1 and Chapter 4 are listed. The references of Chapter 2 and Chapter 3 are given in the respective sections.

1. Kaper JB, Nataro JP, Mobley HLT. 2004. Pathogenic *Escherichia coli*. Nat Rev Microbiol 2:123–140.

2. Moxley RA. 2004. *Escherichia coli* 0157:H7: an update on intestinal colonization and virulence mechanisms. Anim Heal Res Rev 5:15–33.

3. Gyles CL. 2007. Shiga toxin-producing *Escherichia coli*: An overview. J Anim Sci 85:E45–E62.

4. Kim J-S, Lee M-S, Kim JH. 2020. Recent updates on outbreaks of Shiga toxin-producing *Escherichia coli* and its potential reservoirs. Front Cell Infect Microbiol 10:273.

5. Stevens MP, Marchès O, Campbell J, Huter V, Frankel G, Phillips AD, Oswald E, Wallis TS. 2002. Intimin, Tir, and Shiga toxin 1 do not influence enteropathogenic responses to Shiga toxin-producing *Escherichia coli* in bovine ligated intestinal loops. Infect Immun 70:945–952.

6. Shaw DJ, Jenkins C, Pearce MC, Cheasty T, Gunn GJ, Dougan G, Smith HR, Woolhouse MEJ, Frankel G. 2004. Shedding patterns of Verocytotoxin-producing *Escherichia coli* strains in a cohort of calves and their dams on a Scottish beef farm. Appl Environ Microbiol 70:7456–7465.

7. Nataro JP, Kaper JB. 1998. Diarrheagenic *Escherichia coli*. Clin Microbiol Rev 11:142–201.

8. Karch H, Tarr PI, Bielaszewska M. 2005. Enterohaemorrhagic *Escherichia coli* in human medicine. Int J Med Microbiol 295:405–418.

9. Lee M-S, Tesh V. 2019. Roles of Shiga toxins in immunopathology. Toxins (Basel) 11:212.

10. Lee M-S, Koo S, Jeong D, Tesh V. 2016. Shiga toxins as multi-functional proteins: Induction of host cellular stress responses, role in pathogenesis and therapeutic applications. Toxins (Basel) 8:77.

11. Tuttle J, Gomez T, Doyle MP, Wells JG, Zhao T, Tauxe R V, Griffin PM. 1999. Lessons from a large outbreak of *Escherichia coli* O157:H7 infections: insights into the infectious dose and method of widespread contamination of hamburger patties. Epidemiol Infect

122:185–92.

12. Erickson MC, Doyle MP. 2007. Food as a vehicle for transmission of Shiga toxin-producing *Escherichia coli*. J Food Prot 70:2426–49.

13. Kintz E, Brainard J, Hooper L, Hunter P. 2017. Transmission pathways for sporadic Shiga-toxin producing *E. coli* infections: A systematic review and meta-analysis. Int J Hyg Environ Health 220:57–67.

14. Espinosa L, Gray A, Duffy G, Fanning S, McMahon BJ. 2018. A scoping review on the prevalence of Shiga-toxigenic *Escherichia coli* in wild animal species. Zoonoses Public Health 65:911–920.

15. Mellmann A, Bielaszewska M, Köck R, Friedrich AW, Fruth A, Middendorf B, Harmsen D, Schmidt MA, Karch H. 2008. Analysis of collection of hemolytic uremic syndrome–associated enterohemorrhagic *Escherichia coli*. Emerg Infect Dis 14:1287–1290.

16. O'Brien AD, LaVeck GD, Thompson MR, Formal SB. 1982. Production of *Shigella dysenteriae* Type 1-like cytotoxin by *Escherichia coli*. J Infect Dis 146:763–769.

17. Havelaar AH, Kirk MD, Torgerson PR, Gibb HJ, Hald T, Lake RJ, Praet N, Bellinger DC, de Silva NR, Gargouri N, Speybroeck N, Cawthorne A, Mathers C, Stein C, Angulo FJ, Devleesschauwer B. 2015. World Health Organization global estimates and regional comparisons of the burden of foodborne disease in 2010. PLOS Med 12:e1001923.

18. Robert-Koch-Institut. 2012. Hygienemaßnahmen bei Infektionen oder Besiedlung mit multiresistenten gramnegativen Stäbchen (german). Bundesgesundheitsblatt-Gesundheitsforschung-Gesundheitsschutz 55:1311–54.

19. Johnson TJ, Nolan LK. 2009. Pathogenomics of the virulence plasmids of *Escherichia coli*. Microbiol Mol Biol Rev 73:750–774.

20. Abedon ST, LeJeune JT. 2005. Why bacteriophage encode exotoxins and other virulence factors. Evol Bioinforma 1:117693430500100.

21. Schmidt H, Hensel M. 2004. Pathogenicity islands in bacterial pathogenesis. Clin Microbiol Rev 17:14–56.

22. Torres AG, Zhou X, Kaper JB. 2005. Adherence of diarrheagenic *Escherichia coli* strains to epithelial cells. Infect Immun 73:18–29.

23. Rendon MA, Saldana Z, Erdem AL, Monteiro-Neto V, Vazquez A, Kaper JB, Puente JL, Giron JA. 2007. Commensal and pathogenic *Escherichia coli* use a common pilus adherence factor for epithelial cell colonization. Proc Natl Acad Sci 104:10637–10642.

24. Erdem AL, Avelino F, Xicohtencatl-Cortes J, Girón JA. 2007. Host protein binding and adhesive properties of H6 and H7 flagella of attaching and effacing *Escherichia coli*. J Bacteriol 189:7426–7435.

25. Low AS, Holden N, Rosser T, Roe AJ, Constantinidou C, Hobman JL, Smith DGE, Low JC, Gally DL. 2006. Analysis of fimbrial gene clusters and their expression in enterohaemorrhagic *Escherichia coli* O157:H7. Environ Microbiol 8:1033–1047.

26. Kenny B, DeVinney R, Stein M, Reinscheid DJ, Frey EA, Finlay BB. 1997. Enteropathogenic *E. coli* (EPEC) transfers its receptor for intimate adherence into mammalian cells. Cell 91:511–520.

27. Jerse AE, Yu J, Tall BD, Kaper JB. 1990. A genetic locus of enteropathogenic *Escherichia coli* necessary for the production of attaching and effacing lesions on tissue culture cells. Proc Natl Acad Sci 87:7839–7843.

28. Jaglic Z, Desvaux M, Weiss A, Nesse LL, Meyer RL, Demnerova K, Schmidt H, Giaouris E, Sipailiene A, Teixeira P, Kačániová M, Riedel CU, Knøchel S. 2014. Surface adhesins and exopolymers of selected foodborne pathogens. Microbiology 160:2561–2582.

29. Moon HW, Whipp SC, Argenzio RA, Levine MM, Giannella RA. 1983. Attaching and effacing activities of rabbit and human enteropathogenic *Escherichia coli* in pig and rabbit intestines. Infect Immun 41:1340–1351.

30. McDaniel TK, Jarvis KG, Donnenberg MS, Kaper JB. 1995. A genetic locus of enterocyte effacement conserved among diverse enterobacterial pathogens. Proc Natl Acad Sci U S A 92:1664–1668.

31. O'Brien AD, Newland JW, Holmes RK, Smith HW, Formal SB. 1984. Shiga-like toxin-converting phages from *Escherichia coli* strains that cause hemorrhagic colitis or infantile diarrhea. Science (80) 226:694–696.

32. Fierz L, Cernela N, Hauser E, Nüesch-Inderbinen M, Stephan R. 2017. Characteristics of Shiga toxin-producing *Escherichia coli* strains isolated during 2010-2014 from human infections in Switzerland. Front Microbiol 8:1–7.

33. Rasko DA, Webster DR, Sahl JW, Bashir A, Boisen N, Scheutz F, Paxinos EE, Sebra R, Chin C-S, Iliopoulos D, Klammer A, Peluso P, Lee L, Kislyuk AO, Bullard J, Kasarskis A, Wang S, Eid J, Rank D, Redman JC, Steyert SR, Frimodt-Møller J, Struve C, Petersen AM, Krogfelt KA, Nataro JP, Schadt EE, Waldor MK. 2011. Origins of the *E. coli* strain causing an outbreak of hemolytic–uremic syndrome in Germany. N Engl J

Med 365:709–717.

34. Krause M, Barth H, Schmidt H. 2018. Toxins of locus of enterocyte effacement-negative Shiga toxin-producing *Escherichia coli*. Toxins (Basel) 10:1–19.

35. Williams, Clarke. 1998. Why do microbes have toxins? J Appl Microbiol 84:1S-6S.

36. Lemichez E, Barbieri JT. 2013. General aspects and recent advances on bacterial protein toxins. Cold Spring Harb Perspect Med 3:a013573–a013573.

37. Popoff MR. 2004. Bacterial Exotoxins, p. 28–54. *In* Concepts in Bacterial Virulence.

38. Schmidt H, Karch H, Beutin L. 1994. The large-sized plasmids of enterohemorrhagic *Escherichia coli* O157 strains encode hemolysins which are presumably members of the *E. coli alpha*-hemolysin family. FEMS Microbiol Lett 117:189–96.

39. Schwidder M, Heinisch L, Schmidt H. 2019. Genetics, toxicity, and distribution of enterohemorrhagic *Escherichia coli* hemolysin. Toxins (Basel) 11:502.

40. Schmidt H, Beutin L, Karch H. 1995. Molecular analysis of the plasmid-encoded hemolysin of *Escherichia coli* O157:H7 strain EDL933. Infect Immun 63:1055–1061.

41. Bielaszewska M, Aldick T, Bauwens A, Karch H. 2014. Hemolysin of enterohemorrhagic *Escherichia coli*: Structure, transport, biological activity and putative role in virulence. Int J Med Microbiol 304:521–529.

42. Bielaszewska M, Rüter C, Bauwens A, Greune L, Jarosch K-A, Steil D, Zhang W, He X, Lloubes R, Fruth A, Kim KS, Schmidt MA, Dobrindt U, Mellmann A, Karch H. 2017. Host cell interactions of outer membrane vesicle-associated virulence factors of enterohemorrhagic *Escherichia coli* O157: Intracellular delivery, trafficking and mechanisms of cell injury. PLOS Pathog 13:e1006159.

43. Friedrich AW, Lu S, Bielaszewska M, Prager R, Bruns P, Xu J-G, Tschape H, Karch H. 2006. Cytolethal distending toxin in *Escherichia coli* O157:H7: Spectrum of conservation, structure, and endothelial toxicity. J Clin Microbiol 44:1844–1846.

44. Bielaszewska M, Fell M, Greune L, Prager R, Fruth A, Tschäpe H, Schmidt MA, Karch H. 2004. Characterization of cytolethal distending toxin genes and expression in Shiga toxin-producing *Escherichia coli* strains of non-O157 serogroups. Infect Immun 72:1812–1816.

45. Cortes-Bratti X, Frisan T, Thelestam M. 2001. The cytolethal distending toxins induce DNA damage and cell cycle arrest. Toxicon 39:1729–1736.

46. DiRienzo JM. 2014. Cytolethal distending toxin: A unique variation on the AB toxin

paradigm. New J Sci 2014:1–26.

47. Henkel JS, Baldwin MR, Barbieri JT. 2010. Toxins from bacteria. EXS 100:1–29.

48. Odumosu O, Nicholas D, Yano H, Langridge W. 2010. AB toxins: A paradigm switch from deadly to desirable. Toxins (Basel) 2:1612–1645.

49. Merritt EA, Hol WG. 1995. AB_5 toxins. Curr Opin Struct Biol 5:165–171.

50. Beddoe T, Paton AW, Le Nours J, Rossjohn J, Paton JC. 2010. Structure, biological functions and applications of the AB_5 toxins. Trends Biochem Sci 35:411–418.

51. Trofa AF, Ueno-Olsen H, Oiwa R, Yoshikawa M. 1999. Dr. Kiyoshi Shiga: Discoverer of the dysentery bacillus. Clin Infect Dis 29:1303–1306.

52. Konowalchuk J, Speirs JI, Stavric S. 1977. Vero response to a cytotoxin of *Escherichia coli*. Infect Immun 18:775–779.

53. De Grandis S, Ginsberg J, Toone M, Climie S, Friesen J, Brunton J. 1987. Nucleotide sequence and promoter mapping of the *Escherichia coli* Shiga-like toxin operon of bacteriophage H-19B. J Bacteriol 169:4313–4319.

54. Strockbine NA, Jackson MP, Sung LM, Holmes RK, O'Brien AD. 1988. Cloning and sequencing of the genes for Shiga toxin from *Shigella dysenteriae* type 1. J Bacteriol 170:1116–1122.

55. Jackson MP, Newland JW, Holmes RK, O'Brien AD. 1987. Nucleotide sequence analysis of the structural genes for Shiga-like toxin I encoded by bacteriophage 933J from *Escherichia coli*. Microb Pathog 2:147–153.

56. Calderwood SB, Auclair F, Donohue-Rolfe A, Keusch GT, Mekalanos JJ. 1987. Nucleotide sequence of the Shiga-like toxin genes of *Escherichia coli*. Proc Natl Acad Sci 84:4364–4368.

57. Scheutz F. 2014. Taxonomy meets public health: The case of Shiga toxin-producing *Escherichia coli*. Microbiol Spectr 2.

58. Scheutz F, Teel LD, Beutin L, Piérard D, Buvens G, Karch H, Mellmann A, Caprioli A, Tozzoli R, Morabito S, Strockbine NA, Melton-Celsa AR, Sanchez M, Persson S, O'Brien AD. 2012. Multicenter evaluation of a sequence-based protocol for subtyping Shiga toxins and standardizing Stx nomenclature. J Clin Microbiol 50:2951–2963.

59. Fraser ME, Chernaia MM, Kozlov Y V, James MNG. 1994. Crystal structure of the holotoxin from *Shigella dysenteriae* at 2. 5 A resolution. Struct Biol 1:59–64.

60. Hughes AK, Stricklett PK, Schmid D, Kohan DE. 2000. Cytotoxic effect of Shiga toxin-1 on human glomerular epithelial cells. Kidney Int 57:2350–2359.

61. Shin IS, ishii S, Shin JS, Sung K Il, Park BS, Jang HY, Kim BW. 2009. Globotriaosylceramide (Gb3) content in HeLa cells is correlated to Shiga toxin-induced cytotoxicity and Gb3 synthase expression. BMB Rep 42:310–314.

62. Shimizu T, Sato T, Kawakami S, Ohta T, Noda M, Hamabata T. 2007. Receptor affinity, stability and binding mode of Shiga toxins are determinants of toxicity. Microb Pathog 43:88–95.

63. Menge C. 2020. Molecular biology of *Escherichia coli* Shiga toxins' effects on mammalian cells. Toxins (Basel) 12:345.

64. Plunkett G, Rose DJ, Durfee TJ, Blattner FR. 1999. Sequence of Shiga toxin 2 phage 933W from *Escherichia coli* O157:H7: Shiga toxin as a phage late-gene product. J Bacteriol 181:1767–1778.

65. Endo Y, Tsurugi K, Yutsudo T, Takeda Y, Ogasawara T, Igarashi K. 1988. Site of action of a Vero toxin (VT2) from *Escherichia coli* O157:H7 and of Shiga toxin on eukaryotic ribosomes. Eur J Biochem 171:45–50.

66. Garred Ø, Van Deurs B, Sandvig K. 1995. Furin-induced cleavage and activation of Shiga toxin. J Biol Chem 270:10817–10821.

67. Garred Ø, Dubinina E, Polesskaya A, Olsnes S, Kozlov J, Sandvig K. 1997. Role of the disulfide bond in Shiga toxin A-chain for toxin entry into cells. J Biol Chem 272:11414–11419.

68. Johansen BK, Wasteson Y, Granum PE, Brynestad S. 2001. Mosaic structure of Shiga-toxin-2-encoding phages isolated from *Escherichia coli* O157:H7 indicates frequent gene exchange between lambdoid phage genomes. Microbiology 147:1929–1936.

69. Unkmeir A, Schmidt H. 2000. Structural analysis of phage-borne *stx* genes and their flanking sequences in Shiga toxin-producing *Escherichia coli* and *Shigella dysenteriae* Type 1 strains. Infect Immun 68:4856–4864.

70. Wagner PL, Livny J, Neely MN, Acheson DWK, Friedman DI, Waldor MK. 2002. Bacteriophage control of Shiga toxin 1 production and release by *Escherichia coli*. Mol Microbiol 44:957–970.

71. Boerlin P, McEwen SA, Boerlin-Petzold F, Wilson JB, Johnson RP, Gyles CL. 1999. Associations between virulence factors of Shiga toxin-producing *Escherichia coli* and disease in humans. J Clin Microbiol 37:497–503.

72. Hauser JR, Atitkar RR, Petro CD, Lindsey RL, Strockbine N, O'Brien AD, Melton-Celsa AR. 2020. The virulence of *Escherichia coli* O157:H7 isolates in mice depends on Shiga toxin type 2a (Stx2a)-induction and high levels of Stx2a in Stool. Front Cell Infect Microbiol 10.

73. Paton AW, Woodrow MC, Doyle RM, Lanser JA, Paton JC. 1999. Molecular characterization of a Shiga toxigenic *Escherichia coli* O113:H21 strain lacking *eae* responsible for a cluster of cases of hemolytic-uremic syndrome. J Clin Microbiol 37:3357–3361.

74. Funk J, Stoeber H, Hauser E, Schmidt H. 2013. Molecular analysis of subtilase cytotoxin genes of food-borne Shiga toxin-producing *Escherichia coli* reveals a new allelic *subAB* variant. BMC Microbiol 13:0–7.

75. Tasara T, Fierz L, Klumpp J, Schmidt H, Stephan R. 2017. Draft genome sequences of five Shiga toxin-producing *Escherichia coli* isolates harboring the new and recently described subtilase cytotoxin allelic variant *subAB*$_{2\text{-}3}$. Genome Announc 5:e01582-16.

76. Paton AW, Beddoe T, Thorpe CM, Whisstock JC, Wilce MCJ, Rossjohn J, Talbot UM, Paton JC. 2006. AB_5 subtilase cytotoxin inactivates the endoplasmic reticulum chaperone BiP. Nature 443:548–52.

77. Le Nours J, Paton AW, Byres E, Troy S, Herdman BP, Johnson MD, Paton JC, Rossjohn J, Beddoe T. 2013. Structural basis of subtilase cytotoxin SubAB assembly. J Biol Chem 288:27505–27516.

78. Byres E, Paton AW, Paton JC, Löfling JC, Smith DF, Wilce MCJ, Talbot UM, Chong DC, Yu H, Huang S, Chen X, Varki NM, Varki A, Rossjohn J, Beddoe T. 2008. Incorporation of a non-human glycan mediates human susceptibility to a bacterial toxin. Nature 456:648–652.

79. Yamaji T, Hanamatsu H, Sekizuka T, Kuroda M, Iwasaki N, Ohnishi M, Furukawa J ichi, Yahiro K, Hanada K. 2019. A CRISPR screen using subtilase cytotoxin identifies SLC39A9 as a glycan-regulating factor. iScience 15:407–420.

80. Tangvoranuntakul P, Gagneux P, Diaz S, Bardor M, Varki N, Varki A, Muchmore E. 2003. Human uptake and incorporation of an immunogenic nonhuman dietary sialic acid. Proc Natl Acad Sci U S A 100:12045–12050.

81. Seyahian EA, Oltra G, Ochoa F, Melendi S, Hermes R, Paton JC, Paton AW, Lago N, Castro Parodi M, Damiano A, Ibarra C, Zotta E. 2017. Systemic effects of subtilase cytotoxin produced by *Escherichia coli* O113:H21. Toxicon 127:49–55.

82. Paton AW, Srimanote P, Talbot UM, Wang H, Paton JC. 2004. A new family of potent AB_5 cytotoxins produced by Shiga toxigenic *Escherichia coli*. J Exp Med 200:35–46.

83. Tozzoli R, Caprioli A, Cappannella S, Michelacci V, Marziano ML, Morabito S. 2010. Production of the subtilase AB_5 cytotoxin by Shiga toxin-negative *Escherichia coli*. J Clin Microbiol 48:178–183.

84. Foster DB. 2013. Modulation of the enterohemorrhagic *E. coli* virulence program through the human gastrointestinal tract. Virulence 4:315–323.

85. Polzin S, Huber C, Eylert E, Elsenhans I, Eisenreich W, Schmidt H. 2013. Growth media simulating ileal and colonic environments affect the intracellular proteome and carbon fluxes of enterohemorrhagic *Escherichia coli* O157:H7 strain EDL933. Appl Environ Microbiol 79:3703–3715.

86. Umanski T, Rosenshine I, Friedberg D. 2002. Thermoregulated expression of virulence genes in enteropathogenic *Escherichia coli*. Microbiology 148:2735–2744.

87. Hammer BK, Bassler BL. 2007. Regulatory small RNAs circumvent the conventional quorum sensing pathway in pandemic *Vibrio cholerae*. Proc Natl Acad Sci 104:11145–11149.

88. Tyler JS, Mills MJ, Friedman DI. 2004. The operator and early promoter region of the Shiga toxin type 2-encoding bacteriophage 933W and control of toxin expression. J Bacteriol 186:7670–7679.

89. Wagner PL, Acheson DWK, Matthew K. 2001. Human neutrophils and their products induce Shiga toxin production by enterohemorrhagic *Escherichia coli*. Infect Immun 69:1934–1937.

90. McGannon CM, Fuller CA, Weiss AA. 2010. Different classes of antibiotics differentially influence Shiga toxin production. Antimicrob Agents Chemother 54:3790–3798.

91. Zhang X, McDaniel AD, Wolf LE, Keusch GT, Waldor MK, Acheson DWK. 2000. Quinolone antibiotics induce Shiga toxin–encoding bacteriophages, toxin production, and death in mice. J Infect Dis 181:664–670.

92. Łoś JM, Łoś M, Węgrzyn A, Węgrzyn G. 2010. Hydrogen peroxide-mediated induction of the Shiga toxin-converting lambdoid prophage ST2-8624 in *Escherichia coli* O157:H7. FEMS Immunol Med Microbiol 58:322–329.

93. Kendall MM, Gruber CC, Rasko DA, Hughes DT, Sperandio V. 2011. Hfq virulence regulation in enterohemorrhagic *Escherichia coli* O157:H7 Strain 86-24. J Bacteriol 193:6843–6851.

94. Hansen AM, Kaper JB. 2009. Hfq affects the expression of the LEE pathogenicity island in enterohaemorrhagic *Escherichia coli*. Mol Microbiol 73:446–465.

95. Carmichael GG, Weber K. 1975. The host factor required for RNA phage Qβ RNA replication *in vitro*. J Biol Chem 250:3607–3612.

96. de Fernandez MTF, Hayward WS, August JT. 1972. Bacterial proteins required for replication of phage Qβ ribonucleic acid. J Biol Chem 247:824–831.

97. Zhang A, Wassarman KM, Ortega J, Steven AC, Storz G. 2002. The Sm-like Hfq protein increases OxyS RNA interaction with target mRNAs. Mol Cell 9:11–22.

98. Moll I, Leitsch D, Steinhauser T, Bläsi U. 2003. RNA chaperone activity of the Sm-like Hfq protein. EMBO Rep 4:284–9.

99. Waters LS, Storz G. 2009. Regulatory RNAs in bacteria. Cell 136:615–628.

100. Zhang A, Altuvia S, Tiwari A, Argaman L, Hengge-Aronis R, Storz G. 1998. The OxyS regulatory RNA represses rpoS translation and binds the Hfq (HF-I) protein. EMBO J 17:6061–6068.

101. Jin Y, Watt RM, Danchin A, Huang J. 2009. Small noncoding RNA GcvB is a novel regulator of acid resistance in *Escherichia coli*. BMC Genomics 10:165.

102. Gruber CC, Sperandio V. 2015. Global analysis of posttranscriptional regulation by GlmY and GlmZ in enterohemorrhagic *Escherichia coli* O157:H7. Infect Immun 83:1286–1295.

103. De Lay N, Gottesman S. 2012. A complex network of small non-coding RNAs regulate motility in *Escherichia coli*. Mol Microbiol 86:524–538.

104. Chao Y, Vogel J. 2010. The role of Hfq in bacterial pathogens. Curr Opin Microbiol 13:24–33.

105. Kulesus RR, Diaz-Perez K, Slechta ES, Eto DS, Mulvey MA. 2008. Impact of the RNA chaperone Hfq on the fitness and virulence potential of uropathogenic *Escherichia coli*. Infect Immun 76:3019–3026.

106. Battesti A, Majdalani N, Gottesman S. 2011. The RpoS-mediated general stress response in *Escherichia coli*. Annu Rev Microbiol 65:189–213.

107. Sittka A, Pfeiffer V, Tedin K, Vogel J. 2007. The RNA chaperone Hfq is essential for the virulence of *Salmonella typhimurium*. Mol Microbiol 63:193–217.

108. Bojer MS, Jakobsen H, Struve C, Krogfelt KA, Løbner-Olesen A. 2012. Lack of the RNA

chaperone Hfq attenuates pathogenicity of several *Escherichia coli* pathotypes towards *Caenorhabditis elegans*. Microbes Infect 14:1034–1039.

109. Spassky A, Rimsky S, Garreau H, Buc H. 1984. H1a, an *E. coli* DNA-binding protein which accumulates in stationary phase, strongly compacts DNA in vitro. Nucleic Acids Res 12:5321–5340.

110. Falconi M, Higgins NP, Spurio R, Pon CL, Gualerzi CO. 1993. Expression of the gene encoding the major bacterial nucleoid protein H-NS is subject to transcriptional auto-repression. Mol Microbiol 10:273–282.

111. Dame RT, Noom MC, Wuite GJL. 2006. Bacterial chromatin organization by H-NS protein unravelled using dual DNA manipulation. Nature 444:387–390.

112. Navarre WW, Porwollik S, Wang Y, McClelland M, Rosen H, Libby SJ, Fang FC. 2006. Selective silencing of foreign DNA with low GC content by the H-NS protein in *Salmonella*. Science 313:236–8.

113. Sette M, Spurio R, Trotta E, Brandizi C, Brandi A, Pon CL, Barbato G, Boelens R, Gualerzi CO. 2009. Sequence-specific recognition of DNA by the C-terminal domain of nucleoid-associated protein H-NS. J Biol Chem 284:30453–30462.

114. Tupper A, Owen-Hughes T, Ussery DW, Santos DS, Ferguson DJ, Sidebotham JM, Hinton JC, Higgins CF. 1994. The chromatin-associated protein H-NS alters DNA topology *in vitro*. EMBO J 13:258–68.

115. Hommais F, Krin E, Laurent-Winter C, Soutourina O, Malpertuy A, Le Caer JP, Danchin A, Bertin P. 2001. Large-scale monitoring of pleiotropic regulation of gene expression by the prokaryotic nucleoid-associated protein, H-NS. Mol Microbiol 40:20–36.

116. Ueguchi C, Mizuno T. 1993. The *Escherichia coli* nucleoid protein H-NS functions directly as a transcriptional repressor. EMBO J 12:1039–46.

117. Yoshida T, Ueguchi C, Yamada H, Mizuno T. 1993. Function of the *Escherichia coli* nucleoid protein, H-NS: molecular analysis of a subset of proteins whose expression is enhanced in a *hns* deletion mutant. Mol Gen Genet 237:113–22.

118. Srinivasan R, Scolari VF, Lagomarsino MC, Seshasayee ASN. 2015. The genome-scale interplay amongst xenogene silencing, stress response and chromosome architecture in *Escherichia coli*. Nucleic Acids Res 43:295–308.

119. Brunet YR, Khodr A, Logger L, Aussel L, Mignot T, Rimsky S, Cascales E. 2015. H-NS silencing of the *Salmonella* pathogenicity island 6-encoded type VI secretion system limits *Salmonella enterica* Serovar Typhimurium interbacterial killing. Infect Immun

83:2738–50.

120. Fu Q, Li S, Wang Z, Shan W, Ma J, Cheng Y, Wang H, Yan Y, Sun J. 2017. H-NS mutation-mediated CRISPR-Cas activation inhibits phage release and toxin production of *Escherichia coli* Stx2 phage lysogen. Front Microbiol 8:652.

121. Winardhi RS, Gulvady R, Mellies JL, Yan J. 2014. Locus of enterocyte effacement-encoded regulator (Ler) of pathogenic *Escherichia coli* competes off histone-like nucleoid-structuring protein (H-NS) through noncooperative DNA binding. J Biol Chem 289:13739–50.

122. Li H, Granat A, Stewart V, Gillespie JR. 2008. RpoS, H-NS, and DsrA influence EHEC hemolysin operon (*ehxCABD*) transcription in *Escherichia coli* O157:H7 strain EDL933. FEMS Microbiol Lett 285:257–262.

123. Madrid C, Nieto JM, Paytubi S, Falconi M, Gualerzi CO, Juárez A. 2002. Temperature- and H-NS-dependent regulation of a plasmid-encoded virulence operon expressing *Escherichia coli* hemolysin. J Bacteriol 184:5058–5066.

124. Slanec T, Fruth A, Creuzburg K, Schmidt H. 2009. Molecular analysis of virulence profiles and Shiga toxin genes in food-borne Shiga toxin-producing *Escherichia coli*. Appl Environ Microbiol 75:6187–97.

125. Hauser E, Bruederle M, Reich C, Bruckbauer A, Funk J, Schmidt H. 2016. Subtilase contributes to the cytotoxicity of a Shiga toxin-producing *Escherichia coli* strain encoding three different toxins. Int J Food Microbiol 217:156–61.

126. Konowalchuk J, Dickie N, Stavric S, Speirs JI. 1978. Comparative studies of five heat-labile toxic products of *Escherichia coli*. Infect Immun 22:644–648.

127. Bergholz TM, Wick LM, Qi W, Riordan JT, Ouellette LM, Whittam TS. 2007. Global transcriptional response of *Escherichia coli* O157:H7 to growth transitions in glucose minimal medium. BMC Microbiol 7:97.

128. Sy BM, Lan R, Tree JJ. 2020. Early termination of the Shiga toxin transcript generates a regulatory small RNA. Proc Natl Acad Sci U S A 117:25055–25065.

129. de Wet JR, Wood K V, DeLuca M, Helinski DR, Subramani S. 1987. Firefly luciferase gene: structure and expression in mammalian cells. Mol Cell Biol 7:725–737.

130. Greer LF, Szalay AA. 2002. Imaging of light emission from the expression of luciferases in living cells and organisms: a review. Luminescence 17:43–74.

131. Hakkila K, Maksimow M, Karp M, Virta M. 2002. Reporter genes *lucFF*, *luxCDABE*, *gfp*,

and *dsred* have different characteristics in whole-cell bacterial sensors. Anal Biochem 301:235–42.

132. Cech GM, Szalewska-Pałasz A, Kubiak K, Malabirade A, Grange W, Arluison V, Węgrzyn G. 2016. The *Escherichia coli* Hfq protein: An unattended DNA-transactions regulator. Front Mol Biosci 3:36.

133. De Lay N, Schu DJ, Gottesman S. 2013. Bacterial small RNA-based negative regulation: Hfq and its accomplices. J Biol Chem 288:7996–8003.

134. Battesti A, Tsegaye YM, Packer DG, Majdalani N, Gottesman S. 2012. H-NS regulation of IraD and IraM antiadaptors for control of RpoS degradation. J Bacteriol 194:2470–2478.

135. Dillon SC, Dorman CJ. 2010. Bacterial nucleoid-associated proteins, nucleoid structure and gene expression. Nat Rev Microbiol 8:185–195.

136. Rimsky S. 2004. Structure of the histone-like protein H-NS and its role in regulation and genome superstructure. Curr Opin Microbiol 7:109–114.

137. Mellies JL, Barron AMS. 2006. Virulence gene regulation in *Escherichia coli*. EcoSal Plus 2:ecosalplus.8.9.1.

138. Picker M, Wing H. 2016. H-NS, its family members and their regulation of virulence genes in *Shigella* species. Genes (Basel) 7:112.

139. Lucchini S, Rowley G, Goldberg MD, Hurd D, Harrison M, Hinton JCD. 2006. H-NS mediates the dilencing of laterally acquired genes in bacteria. PLoS Pathog 2:e81.

140. Ali SS, Soo J, Rao C, Leung AS, Ngai DH-M, Ensminger AW, Navarre WW. 2014. Silencing by H-NS potentiated the evolution of *Salmonella*. PLoS Pathog 10:e1004500.

141. Wan B, Zhang Q, Tao J, Zhou A, Yao YF, Ni J. 2016. Global transcriptional regulation by H-NS and its biological influence on the virulence of enterohemorrhagic *Escherichia coli*. Gene 588:115–123.

142. Torres AG, López-Sánchez GN, Milflores-Flores L, Patel SD, Rojas-López M, Martínez De La Peña CF, Arenas-Hernández MMP, Martínez-Laguna Y. 2007. Ler and H-NS, regulators controlling expression of the long polar fimbriae of *Escherichia coli* O157:H7. J Bacteriol 189:5916–5928.

143. Yang J, Tauschek M, Strugnell R, Robins-Browne RM. 2005. The H-NS protein represses transcription of the *eltAB* operon, which encodes heat-labile enterotoxin in enterotoxigenic *Escherichia coli*, by binding to regions downstream of the promoter.

Microbiology 151:1199–1208.

144. Eijkelkamp BA, Stroeher UH, Hassan KA, Elbourne LDH, Paulsen IT, Brown MH. 2013. H-NS plays a role in expression of *Acinetobacter baumannii* virulence features. Infect Immun 81:2574–2583.

145. Russell R, Wang H, Benitez JA, Silva AJ. 2018. Deletion of gene encoding the nucleoid-associated protein H-NS unmasks hidden regulatory connections in El Tor biotype *Vibrio cholerae*. Microbiology 164:998–1003.

146. Stone JB, Withey JH. 2021. H-NS and ToxT inversely control cholera toxin production by binding to overlapping DNA sequences. J Bacteriol 6.

147. Shakhnovich EA, Davis BM, Waldor MK. 2009. Hfq negatively regulates type III secretion in EHEC and several other pathogens. Mol Microbiol 74:347–363.

148. Herold S, Siebert J, Huber A, Schmidt H. 2005. Global expression of prophage genes in *Escherichia coli* O157:H7 strain EDL933 in response to norfloxacin. Antimicrob Agents Chemother 49:931–944.

149. Sy BM, Tree JJ. 2021. Small RNA regulation of virulence in pathogenic *Escherichia coli*. Front Cell Infect Microbiol 10:1–11.

150. Tree JJ, Granneman S, McAteer SP, Tollervey D, Gally DL. 2014. Identification of bacteriophage-encoded anti-sRNAs in pathogenic *Escherichia coli*. Mol Cell 55:199–213.

151. Sonnleitner E, Sorger-Domenigg T, Madej MJ, Findeiss S, Hackermüller J, Hüttenhofer A, Stadler PF, Bläsi U, Moll I. 2008. Detection of small RNAs in *Pseudomonas aeruginosa* by RNomics and structure-based bioinformatic tools. Microbiology 154:3175–3187.

152. Nakano M, Takahashi A, Su Z, Harada N, Mawatari K, Nakaya Y. 2008. Hfq regulates the expression of the thermostable direct hemolysin gene in *Vibrio parahaemolyticus*. BMC Microbiol 8:155.

153. Nakao H, Watanabe H, Nakayama S, Takeda T. 1995. *yst* gene expression in *Yersinia enterocolitica* is positively regulated by a chromosomal region that is highly homologous to *Escherichia coli* host factor 1 gene (*hfq*). Mol Microbiol 18:859–865.

154. Kim S-H, Lee S-R, Kim K-S, Ko A, Kim E, Kim Y-H, Chang K-T. 2010. Shiga toxin A subunit mutant of *Escherichia coli* O157:H7 releases outer membrane vesicles containing the B-pentameric complex. FEMS Immunol Med Microbiol 58:412–420.

155. Willysson A, Ståhl A, Gillet D, Barbier J, Cintrat J-C, Chambon V, Billet A, Johannes L, Karpman D. 2020. Shiga toxin uptake and sequestration in extracellular vesicles is mediated by its B-subunit. Toxins (Basel) 12:449.

156. Funk J, Biber N, Schneider M, Hauser E, Enzenmüller S, Förtsch C, Barth H, Schmidt H. 2015. Cytotoxic and apoptotic effects of recombinant subtilase cytotoxin variants of Shiga toxin-producing *Escherichia coli*. Infect Immun 83:2338–2349.

157. Sessler K, Papatheodorou P, Wondany F, Krause M, Noettger S, Bernhard D, Michaelis J, Schmidt H, Barth H. 2021. The enzyme subunit SubA of Shiga toxin-producing *E. coli* strains demonstrates comparable intracellular transport and cytotoxic activity as the holotoxin SubAB in HeLa and HCT116 cells *in vitro*. Arch Toxicol 95:975–983.

158. Pellino CA, Karve SS, Pradhan S, Weiss AA. 2016. AB_5 preassembly is not required for Shiga toxin activity. J Bacteriol 198:1621–1630.

159. Ling H, Boodhoo A, Hazes B, Cummings MD, Armstrong GD, Brunton JL, Read RJ. 1998. Structure of the Shiga-like toxin I B-pentamer complexed with an analogue of its receptor Gb3. Biochemistry 37:1777–1788.

160. Lingwood CA, Law H, Richardson S, Petric M, Brunton JL, De Grandis S, Karmali M. 2014. Glycolipid binding of purified and recombinant *Escherichia coli* produced Verotoxin *in vitro*. J Biol Chem 262, No. 1:8834–8839.

161. Smith DC, Sillence DJ, Falguières T, Jarvis RM, Johannes L, Lord JM, Platt FM, Roberts LM. 2006. The association of Shiga-like toxin with detergent resistant membranes is modulated by glucosylceramide and is an essential requirement in the endoplasmic reticulum for a cytotoxic effect. Mol Biol Cell 17:1375–1387.

162. Okuda T, Tokuda N, Numata S, Ito M, Ohta M, Kawamura K, Wiels J, Urano T, Tajima O, Furukawa K, Furukawa K. 2006. Targeted disruption of Gb3/CD77 synthase gene resulted in the complete deletion of globo-series glycosphingolipids and loss of sensitivity to Verotoxins. J Biol Chem 281:10230–10235.

163. Waddell T, Cohen A, Lingwood CA. 1990. Induction of verotoxin sensitivity in receptor-deficient cell lines using the receptor glycolipid globotriosylceramide. Proc Natl Acad Sci 87:7898–7901.

164. Gobert AP, Vareille M, Glasser A-L, Hindré T, de Sablet T, Martin C. 2007. Shiga toxin produced by enterohemorrhagic *Escherichia coli* inhibits PI3K/NF-κB signaling pathway in globotriaosylceramide-3-negative human intestinal epithelial cells. J Immunol 178:8168–8174.

165. Schüller S, Frankel G, Phillips AD. 2004. Interaction of Shiga toxin from *Escherichia coli* with human intestinal epithelial cell lines and explants: Stx2 induces epithelial damage in organ culture. Cell Microbiol 6:289–301.

166. Kolling GL, Matthews KR. 1999. Export of virulence genes and Shiga toxin by membrane vesicles of *Escherichia coli* O157:H7. Appl Environ Microbiol 65:1843–1848.

167. Bauwens A, Kunsmann L, Marejková M, Zhang W, Karch H, Bielaszewska M, Mellmann A. 2017. Intrahost milieu modulates production of outer membrane vesicles, vesicle-associated Shiga toxin 2a and cytotoxicity in *Escherichia coli* O157:H7 and O104:H4. Environ Microbiol Rep 9:626–634.

168. Yokoyama K, Horii T, Yamashino T, Hashikawa S, Barua S, Hasegawa T, Watanabe H, Ohta M. 2000. Production of Shiga toxin by *Escherichia coli* measured with reference to the membrane vesicle-associated toxins. FEMS Microbiol Lett 192:139–144.

169. Alonso MZ, Krüger A, Sanz ME, Padola NL, Lucchesi PMA. 2016. Serotypes, virulence profiles and *stx* subtypes of Shigatoxigenic *Escherichia coli* isolated from chicken derived products. Rev Argent Microbiol 48:325–328.

170. Monaghan Á, Byrne B, Fanning S, Sweeney T, McDowell D, Bolton DJ. 2011. Serotypes and virulence profiles of non-O157 Shiga toxin-producing *Escherichia coli* isolates from bovine farms. Appl Environ Microbiol 77:8662–8668.

171. Pruimboom-Brees IM, Morgan TW, Ackermann MR, Nystrom ED, Samuel JE, Cornick NA, Moon HW. 2000. Cattle lack vascular receptors for *Escherichia coli* O157:H7 Shiga toxins. Proc Natl Acad Sci 97:10325–10329.

172. Menge C. 2020. The role of *Escherichia coli* Shiga toxins in STEC colonization of cattle. Toxins (Basel) 12:607.

173. Zheng J, Cui S, Teel LD, Zhao S, Singh R, O'Brien AD, Meng J. 2008. Identification and characterization of Shiga toxin type 2 variants in *Escherichia coli* isolates from animals, food, and humans. Appl Environ Microbiol 74:5645–5652.

174. Álvarez RS, Gómez FD, Zotta E, Paton AW, Paton JC, Ibarra C, Sacerdoti F, Amaral MM. 2021. Combined action of Shiga toxin type 2 and subtilase cytotoxin in the pathogenesis of hemolytic uremic syndrome. Toxins (Basel) 13:536.

175. Krause M, Sessler K, Kaziales A, Grahl R, Noettger S, Barth H, Schmidt H. 2019. Variants of *Escherichia coli* subtilase cytotoxin subunits show differences in complex formation in vitro. Toxins (Basel) 11.

176. Kitov PI, Sadowska JM, Mulvey G, Armstrong GD, Ling H, Pannu NS, Read RJ, Bundle

DR. 2000. Shiga-like toxins are neutralized by tailored multivalent carbohydrate ligands. Nature 403:669–672.

177. Nishikawa K, Matsuoka K, Watanabe M, Igai K, Hino K, Hatano K, Yamada A, Abe N, Terunuma D, Kuzuhara H, Natori Y. 2005. Identification of the optimal structure required for a Shiga toxin neutralizer with oriented carbohydrates to function in the circulation. J Infect Dis 191:2097–2105.